NEW PRECURSORS FOR THE CVD OF HIGH TEMPERATURE SUPERCONDUCTORS

A THESIS SUBMITTED FOR THE DEGREE OF DOCTOR OF PHILOSOPHY

BY
SIMON C. THOMPSON

1991

DECLARATION

I, Simon Carl Thompson hereby certify that this thesis has been composed by myself, that it is a record of my own work and that it has not been accepted in partial or complete fulfilment of any other degree or professional qualification.

Signed . Date 13/9/91...

I was admitted to the Faculty of Science of the University of St. Andrews under Ordinance General No. 12 on 1st September, 1988 and as a candidate for the degree of Ph.D. on 1st October, 1989.

Signed Date 13/9/91.

I hereby certify that the candidate has fulfilled the conditions of the Resolution and the Regulations appropriate to the degree of Ph. D.

Signature of Supervisor Date 20th October 1991

In submitting this thesis to the University of St. Andrews I understand that I am giving permission for use in accordance with the regulations of the University Library for the time being in force, subject to any copyright vested in the work not being affected thereby. I also understand that the title and abstract will be published and that a copy of the work may be made and supplied to any bona fide library or research worker.

ACKNOWLEDGEMENTS

I should like to thank the following people and organisations without whom the preparation of this thesis would not have been possible;

Professor David Cole-Hamilton for project supervision over the last three years.

Douglas Gilliland, my co-worker at Strathclyde for his friendship and advice.

Professor Michael Hitchman, Douglas' supervisor.

Dr Les Wylde, Dr Steve Cook and Dr Barbara Richards of Associated Octel inc. for their enthusiastic assistance during the project. Their suggestions during our technical discussions contributed greatly towards the successful completion of this thesis.

Associated Octel inc. for sponsoring the project and for the STA analyses.

Melanja Smith who ran all of the NMR analyses described in this thesis, always in a helpful and constructive manner.

My fellow researchers in Labs 334-7.

Dr John Barnes and John Paton from the University of Dundee for finding the time at short notice to devote to the solving of the crystal structure of [Cu(TDFND)$_2$(EtOH)].

Finally to my parents who have always taken a keen interest in my education for whom the completion of this thesis will be a deserving reward.

ABSTRACT

A range of β-diketonates and alkoxides of the group 2 metals, copper and yttrium has been prepared.

The first β-diketonates which we prepared were based upon commercially available ligands. These ligands were benzoyl-trifluoroacetone, napthoyltrifluoroacetone, thenoyltrifluoroacetone, dibenzoylmethane and malonyl chloride. We prepared complexes of these ligands with various group 2 metals. Unfortunately, these complexes were insufficiently volatile and thermally stable to be used as CVD precursors.

It was known that although bis(dipivaloylmethane) barium(II) could be volatilised in a CVD rig the accompanying decomposition was too great for the precursor to be re-used. We were able to prepare a monomeric complex which showed enhanced volatility and left only a minimal residue on sublimation by coordinating a molecule of tetraglyme to the complex.

The most successful precursors which were prepared incorporated two new sterically crowded, highly fluorinated β-diketones; 1, 1, 1, 2, 2, 3, 3, 7, 7, 8, 8, 9, 9, 9 - tetradecafluoro-nonane-4,6-dione and 1,1,1,2,2,3,3,7,7,7-decafluoroheptane-4,6-dione. The copper, yttrium and group two metal derivatives of these ligands were prepared and proved to be thermally stable and volatile complexes which exhibited little or no decomposition. They were, therefore, suitable for use as CVD pecursors.

Certain of these new, fluorinated β-diketonates were tested on the CVD rig by our co-workers at the University of Strathclyde. They found that the complexes can produce oriented barium fluoride films of high quality. Initial growth rates are high although there are some problems in maintaining this deposition rate throughout a series of runs. The used compounds were examined and reasons for the the loss of

volatility, which is not caused by decomposition, examined.

Other new complexes synthesised are group two alkoxides and fluoroalkoxides. None of these complexes showed adequate volatility for CVD purposes and they were all clearly oligomeric in nature.

CONTENTS

Section **Page**

CHAPTER 1

INTRODUCTION TO SUPERCONDUCTIVITY AND METHODS OF PRODUCING THIN FILMS

1.1; THE HISTORY OF SUPERCONDUCTIVITY:

1.1.1; Low temperature superconductors;

In the early years of this century Kamerlingh Onnes[1] achieved the liquifaction of helium. Some of his initial work with liquid helium involved the study of the electrical properties of pure metals at temperatures close to absolute zero. In 1911, he discovered that when placed in liquid helium (< 4.2 K) the resistance of mercury wire fell abruptly to zero. Onnes called this new property the superconducting state, the temperature at which resistance falls to zero was termed T_c zero.

This class of superconductor was later to be called a Type 1 superconductor. They have the limitation that they can only stand a small current flow or magnetic field. A more detailed explanation of this will be found under section 1.2 where the critical field and critical current will be discussed. The above limitations prevented the use of these superconductors as materials for large magnets and power applications.

In 1954 Matthias and co-workers[2] discovered that Nb_3Sn had a T_c zero of 18.1 K, at that time the highest recorded temperature. More importantly, however, it was found that Nb_3Sn would remain superconducting in a field of 8.8 Tesla and that it was capable of carrying much larger currents. This breakthrough, and the family of so-called Type 2 superconductors which resulted, made the building of powerful superconducting magnets possible.

Over the next three decades new materials with steadily increasing Tc zero were produced. The culmination of this improvement was the discovery of Nb_3Ge which had a Tc zero above

the temperature of liquid hydrogen (20.3 K). This was technologically important as hydrogen is both a more efficient and a cheaper coolant than helium.

Despite these advances, however, 75 years of research had not produced a superconductor capable of operating more than 23 K above absolute zero. One discovery in 1986 was to change all of this.

1.1.2; High temperature superconductors;

In September, 1986 Bednorz and Muller published a paper entitled 'Possible High Tc superconductivity in the BaLaCuO system'[3]. They reported a resistance drop at about 30 K. Whilst this in itself was not a major improvement on previous superconductors it was achieved with a totally new kind of compound. This group of superconductors raised the T_c zero by over 100 K in just 17 months.

The discovery by Bednorz and Muller sparked off an international research effort to find other similar compounds which would superconduct at even higher temperatures. The key temperature was 77 K, this being the boiling point of liquid nitrogen. Superconductors operating in liquid nitrogen would be a great improvement even on those operating in liquid hydrogen. Liquid helium is still used as a standard coolant but costs about £8 per litre, liquid nitrogen is only 20p for the same volume of liquid. Furthermore, the abundance of nitrogen in the atmosphere means that coolant availability is not a problem.

Within a few months this temperature had been achieved by a team led by C.W. Chu[4]. They prepared yttrium barium copper oxide, $YBa_2Cu_3O_{7-x}$, commonly abbreviated to 'YBCO' or '123' and which

has a T_c zero of 93 K. A whole family of superconductors based upon YBCO now exists, all with critical temperatures in the 90 K region. For the general formula; $MBa_2Cu_3O_{7-x}$, M can be Y, Nd, Sm, Eu, Gd, Dy, Ho, Tm, Yb or Lu.

Two other successful systems have been reported since the discovery of YBCO, in January and February 1988 respectively. These are $Bi_2Sr_2Ca_2Cu_3O_{10-x}$[5] (T_c zero 110 K) and $Tl_2Ba_2Ca_2Cu_3O_{10-x}$[6] (Tc zero 125K). However, these compounds have more phases than YBCO, each phase having a different T_c zero. The effective isolation of the correct phase is problematic , hence the majority of work has been done on the simpler YBCO system which has a single phase. Additionally, YBCO has the further major advantages of a high flux density and a high critical current. In section 1.2 it is explained why these two properties are essential for superconducting devices. Unless a superconductor is developed which markedly improves these properties, or operates at room temperature, YBCO is likely to remain the preferred compound for most applications.

1.2; PROPERTIES OF SUPERCONDUCTORS:

1.2.1; Critical Temperature (T_c), Critical Current (J_c) and Critical Magnetic Field (H_c);

Superconductors have the capability of conducting electricity with no loss of energy. This requires the material to have no resistance, which will occur if the following conditions are met;

(1) The magnetic field should not exceed the critical magnetic field (H_c)

(2) The current should not exceed the critical current (J_c)

(3) The temperature should be below the critical temperature (T_c)

There is an inter-relationship between these parameters such that a lowering of one of them will increase the other two. This results in the raising of H_c and J_c levels as the temperature is lowered, which has a clear effect on the resistance / temperature curve for a superconductor.

1.2.1.1; Critical Temperature;

The temperature at which the resistance starts to decline is the Transition Onset Temperature (T_c on) which is the value often given in publications to substantiate exaggerated claims. The material is only truly superconducting when there is zero resistance. This temperature is referred to as the critical temperature, T_c zero. T_c zero may be a far lower temperature than T_c on so it is important to draw the distinction between these two temperatures.

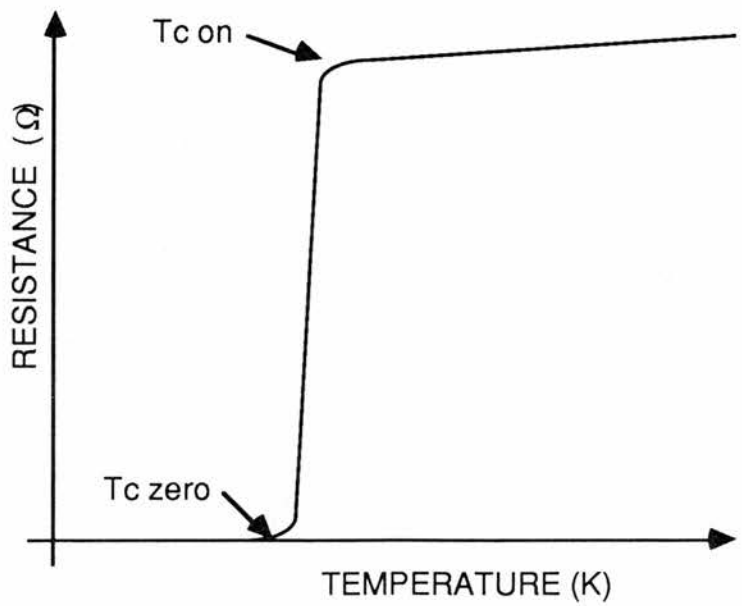

Figure1.1; Resistance versus temperature for a typical superconductor

1.2.1.2; Critical Magnetic Field;

The application of a magnetic field equal to the critical magnetic field (H_c) will prevent superconductivity. Type 1 superconductors are only able to withstand a field of 0.1 Tesla. When the magnetic field exceeds this value (the lower critical field, H_{c1}) the material ceases to superconduct.

Type 2 superconductors can withstand a field of 8.8 Tesla because they have an upper critical field (H_{c2}). Below H_{c1} Type 2 superconductors behave in the same way as Type 1 superconductors. However, between H_{c1} and H_{c2} is the 'mixed' state which allows penetration of a magnetic field without loss of superconductivity. This accounts for the ability of Type 2 superconductors to withstand higher magnetic field strengths.

Although the behaviour and properties of High T_c superconductors are not yet fully understood, they have been seen to behave in the same manner as Type 2 superconductors. Watanabe et al[7] have shown that YBCO has an upper critical field of 27 Tesla at 81 K and they estimate the H_{c2} to be 35 Tesla at 77 K. The critical current density which they achieved is of the same order of magnitude as would be seen in Type 2 superconductors and is as high as 6.5×10^4 Acm^{-2} at 81K and 27 Tesla.

1.2.1.3; Critical Currents;

For relatively thick samples this equals the current which would create a magnetic field equal to H_c.

1.2.2; Meissner Effect;

This was first discovered by Meissner and Ocherfeld in 1933[8]. It is dependent upon the fact that superconductors can be perfect diamagnetic* materials, and thus exclude any magnetic field which approaches them. In practical terms a superconductor is able to repel a magnet.

1.2.3; Josephson Effect;

This was first described, and later experimentally verified, by Brian Josephson[9]. The effect is observed if two pieces of superconductor are separated by a thin layer of insulator (100-200nm). This insulating barrier can then be penetrated by macroscopic wave functions, producing overlap or electron pair tunnelling. When a phase difference exists between these two wave functions a current will flow in the absence of a potential difference. Furthermore, as the current increases to a critical value a voltage appears and the junction behaves resistively. This so-called d.c. Josephson effect has found applications in switching devices.

The 'a.c.' Josephson Effect occurs when a voltage is applied over the barrier. Oscillating currents are produced with the frequency of oscillation being proportional to the applied voltage.

* Paramagnetism produces a positive magnetic moment parallel to the field.
In diamagnetism the magnetic field always sets up an induced current with its magnetic field directed opposite to that of the applied field.
All materials have a diamagnetic effect which is usually obscured by the paramagnetic effect.

1.3; APPLICATIONS OF SUPERCONDUCTORS:

One of the ultimate aims for superconductors must be to use them in power cables, allowing electricity to be transported with no loss of energy. However, the High T_c materials are unsuitable for cables in their present form and the T_c zero is still far too low. Furthermore, the production cost would have to be reduced to a level only slightly above that for existing cables as electricity losses are presently only 10% of that produced.

It is far more likely that superconductors will be used in coils for iron core electromagnets. The desired characteristics of the material for such electromagnets are a high transition temperature and a high upper critical field. These properties will increase the critical current density which must be above 10^5 Acm^{-2} to be effective. The replacement of low temperature superconductor-based magnets by high temperature derived versions is advantageous for two reasons. Firstly, the cooling system for liquid nitrogen is much cheaper, as was outlined earlier and secondly the field a superconducting magnet can produce is directly related to temperature, so higher fields should be possible.

The earliest applications for high temperature superconductors are likely to be in the production of sensitive devices and in the field of computer technology. Sensitive instruments based upon the Josephson Effect have already been produced using high temperature superconductors. The most notable of these are SQUIDS (Superconducting Quantum Interference Devices). These have the greatest sensitivity of all devices available for measuring magnetic fields, magnetic susceptibilities and voltages and are able to detect changes as small as 10^{-11} Tesla. Vasilev[10] has used an YBCO based SQUID to measure the magnetic field produced by a human heart.

The development of a superconductor computer is a particularly important challenge. In computer circles speed is everything. As it takes a finite time for a signal to travel any distance, computer components must be tightly packed. With semiconductor elements this produces a great deal of heat which limits the size, and therefore the speed, of the computer. This problem does not apply to superconducting materials as no heat is produced, hence the elements can be packed much more closely together.

In the long term computers might contain Josephson switching elements but more rapid applications are likely to be semi / superconductor hybrids incorporating active semiconductor chips connected by superconductor transmission lines[11].

Unfortunately, to be of use for instuments or computers, methods of producing thin films of the superconductors must be found. A number of different processes are being investigated for this purpose, which are described below. Not only have such techniques been used to produce working SQUIDS they have also been employed to produce logic cicuits using high temperature superconductors. Simon et al[12] have prepared logic circuits using YBCO with AgPbIn junctions. Furthermore, they have succeeded in developing working AND and OR gates. These achievements prove the feasibility of superconductor computers.

1.4; PROCESSES TO PRODUCE THIN FILM SUPERCONDUCTORS:

The three main processes which have been used to prepare thin film superconductors are; (1) sputtering, (2) laser ablation and (3) chemical vapour deposition (CVD).

1.4.1; Sputtering;

This involves the attack of an ion beam on the constituent metals or metal oxides. A rotating shutter controls the composition of the deposited films. Wasa et al[13] report that BiSCCO can be layed down with a target temperature of 650°C and that the film requires annealing under oxygen at 750°C.

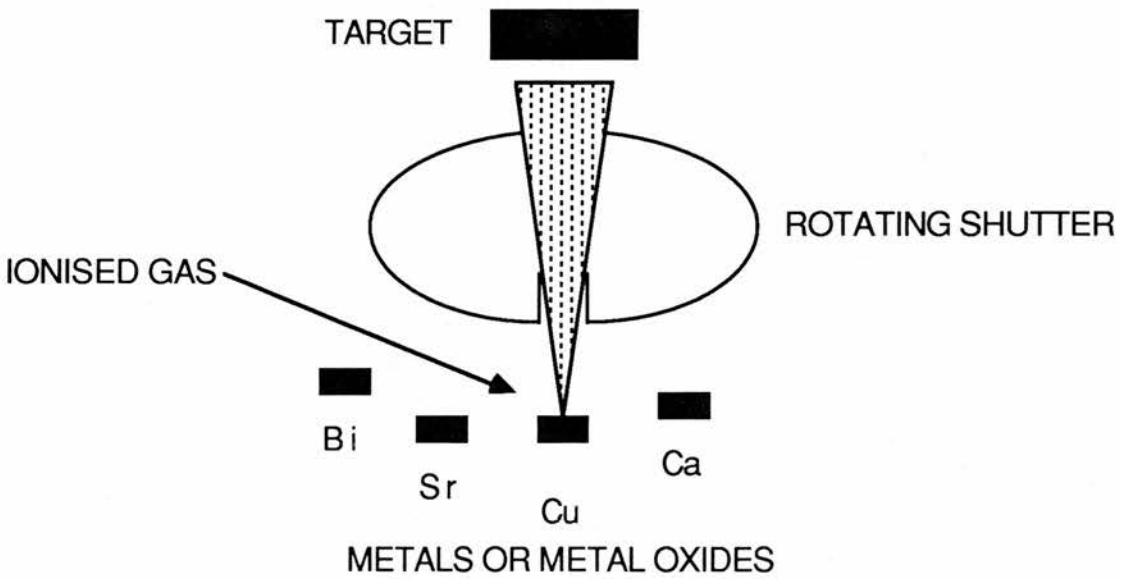

Figure 1.2; Schematic diagram of a BiSCCO sputtering apparatus

1.4.2; Laser Ablation;

A pellet of the superconductor is used as a target and a laser is then fired at this pellet. A thin film is then produced on the heated substrate in the reactor vessel. A typical substrate temperature for YBCO is 730°C[14] and there is a necessity for post annealing to attain optimum superconductor properties.

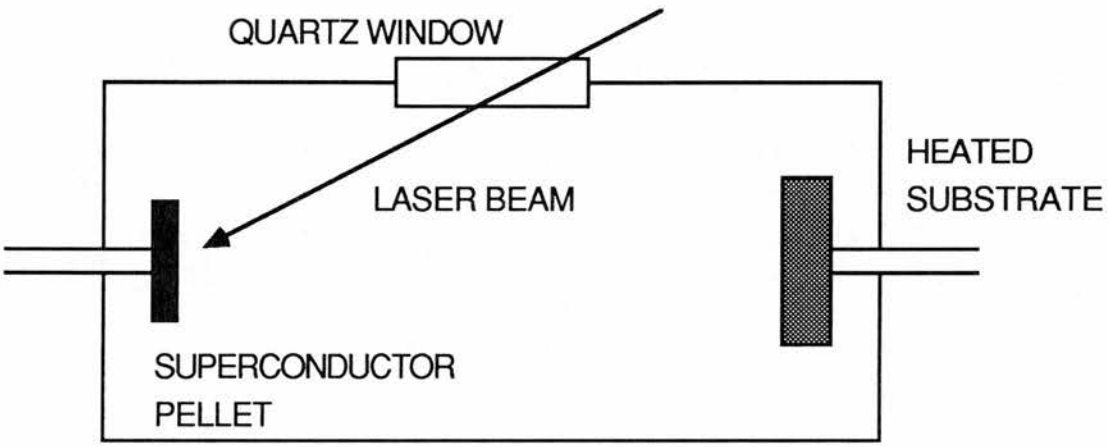

Figure 1.3; A schematic diagram of a laser ablation apparatus

1.4.3; CVD and Plasma-enhanced CVD;

The source material is heated at around 150-200°C under vacuum conditions. A carrier gas, usually inert, flows over the sources to carry them over to the substrate. Source materials for this process are usually β-diketonates. Following deposition, the substrate is heated to around 800°C then cooled under oxygen[15,16,17,18]. Given the correct conditions it has been shown that post-annealing is unneccessary[19]. The

ion chemical technique of plasma-enhanced CVD requires a lower substrate temperature of around 570°C[20].

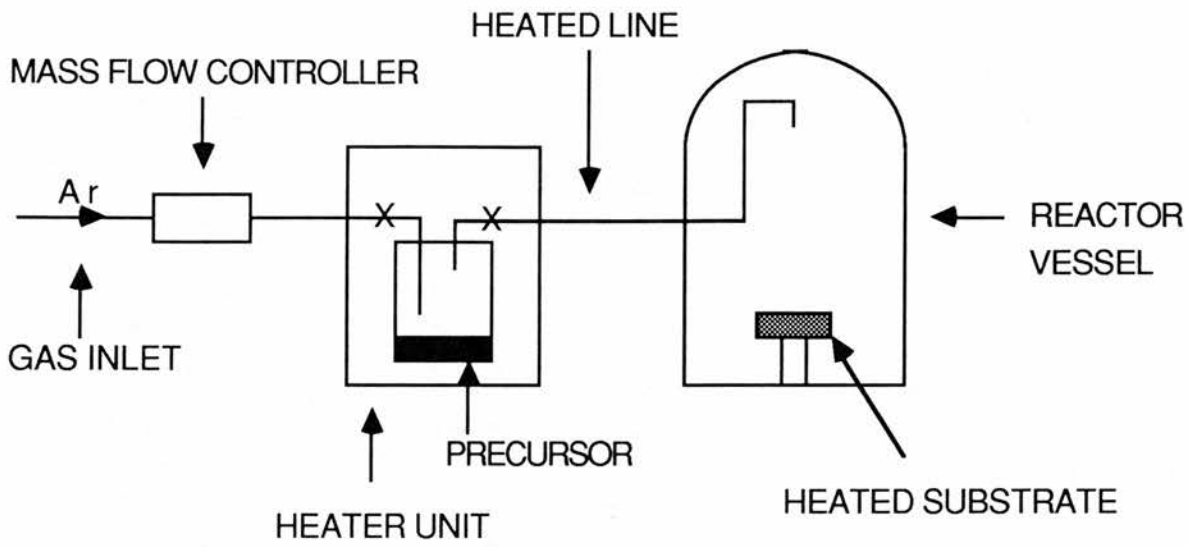

Figure 1.4; CVD apparatus showing a single precursor line

In collaboration with Michael Hitchman and Douglas Gilliland of the Department of Pure and Applied Chemistry, Strathclyde University, we decided to use CVD as the method of preparing thin films of superconductors. Their results using this process are described in chapter 6. The remainder of this thesis is dedicated to the preparation and analysis of precursors for use in this process. Chapter 2 is a review of the work of others in this field whilst chapters 3, 4, 5 and 7 describe a variety of precursors which we have prepared.

CHAPTER 2

THE PREPARATION OF VOLATILE PRECURSORS FOR USE IN THE CVD OF HIGH TEMPERATURE SUPERCONDUCTORS; A REVIEW

2.1; REQUIREMENTS FOR A CVD PRECURSOR:

The ideal precursor will be volatile at a temperature of well under 200°C at reduced pressure, be thermally stable at this temperature and be insensitive to both air and moisture. The first requirement is necessary for ease of use of the precursors, temperatures much above 200°C cause problems with the sample pot heaters and with maintaining the sublimation lines at an adequate temperature. Thermal stability is to some extent linked with the sublimation temperature as the higher the sublimation temperature the higher will be the chances of thermal degradation occuring.

Thermal degradation must be avoided for two main reasons. Firstly, it is preferable if the heaters can be turned on and off when required without the need to fill the pot with fresh precursor for each run. This is essential to keep down costs and to boost the efficiency of operation. Secondly, a steady vapour pressure is needed during the deposition process to ensure that the thin film is of suitable quality and can be grown reproducibly. If the precursor is thermally degrading during the deposition run, it is most unlikely that a steady vapour pressure can be maintained.

Insensitivity to both air and moisture is useful if not essential. This greatly simplifies precursor handling and reactor operation as the absolute exclusion of air and moisture is then not a requirement for successful deposition to be achieved.

The precursors of elements present in High T_c superconductors which have been found by other workers most closely to match the aforementioned criteria have been, almost exclusively, β–diketonates. Some researchers have produced alkoxides which they claim have adequate volatility for this application. However, decomposition is

frequently a problem with many of these compounds so they have been less widely used.

A detailed assessment of the use of alkoxides and β–diketonates will now be given.

2.2; AN ASSESSMENT OF THE RELATIVE MERITS OF ALKOXIDES AND β–DIKETONATES AS PRECURSORS:

What is required for the successful growth of thin films of High T_c superconductors are volatile oxygen containing compounds which will decompose at high temperatures to produce metal oxide layers. Many of the compounds which have been used for direct metal oxide deposition are metal alkoxides[21]. It is believed that the mechanism of their decomposition is as shown in Figure 2.1 for a tertiary alkoxide. This involves the transfer of a hydrogen atom from the carbon β to the oxygen to give a hydroxy species, followed by the loss of water and / or alcohol. These compounds may not require an extrinsic oxygen source (H_2O or O_2) to deposit the required oxide films.

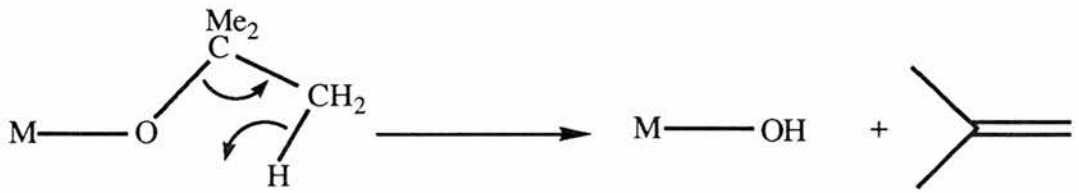

Figure 2.1; Probable mechanism for alkoxide breakdown

In contrast to the alkoxides, β–diketonates do need an extrinsic oxygen source. Although some diketonates do contain hydrogen atoms

on the carbon β to the oxygen, transfer of this hydrogen to the oxygen with consequent C-O bond rupture cannot readily occur. This is because the product would be a high energy allene type molecule (Figure 2.2).

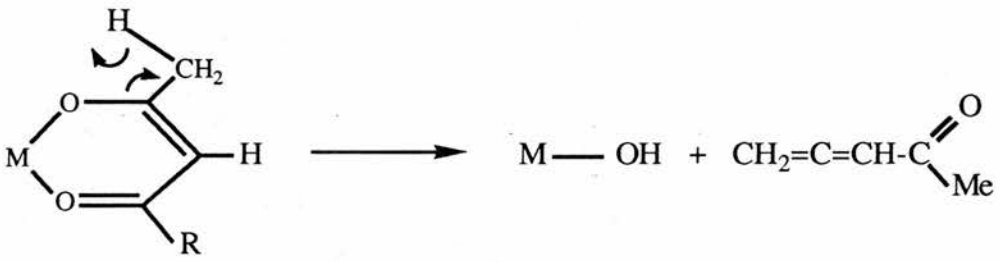

Figure 2.2; β-H transfer breakdown mechanism for a β–diketonate

It can be seen that, in theory, the use of alkoxides has certain advantages over using β–diketonates. Unfortunately, however, alkoxides are, in most cases, unsuitable for CVD use. The problem with these alkoxides is their tendency to form oligomers. This occurs when the ligand bonds through its oxygen atom to two or three metal atoms. Such bonding is by conventional two electron covalent bonds as is illustrated in Figure 2.3.

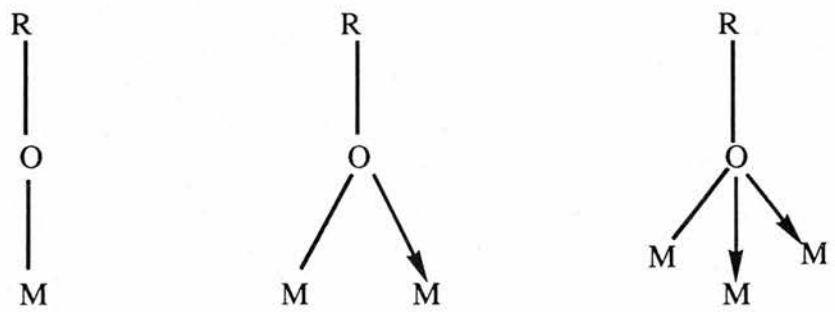

Figure 2.3; Bonding in alkoxides[21]

For most alkoxides the strength of the bridge is sufficient to preclude the alternative mechanism which reduces oligomerisation by coordination expansion, that being the addition of another ligand containing a donor atom. Many alkoxides retain their oligomeric structure in the vapour phase and, obviously, more energy is required to vaporise an oligomer than a monomer.

2.2.1; Why β–diketonates ?

In contrast to the alkoxides, it has been known for some time that lanthanide β-diketonates can be volatilised at low temperatures[22]. For this reason such compounds have commonly been used as CVD precursors for High T_c thin films. It has already been explained that a major problem with the single oxygen (alkoxide) ligands is that they can donate a lone pair of electrons to adjacent metal centres to form a bridge. This oligomerises the alkoxide and reduces its volatility. To prevent this oligomerisation double oxygen (β–diketone) ligands have usually been employed. These ligands may be considered as being special forms of alkoxides containing a β–γ unsaturated ketone substituent (Figure 2.4).

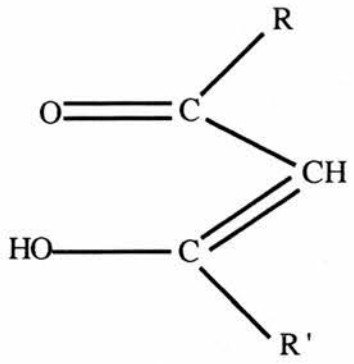

Figure 2.4; β–diketone (enol form)

Coordination of this ligand to the metal via both oxygen atoms blocks some of the sites which might otherwise be used for bridging. In reality the structure is delocalised as in Figure 2.5.

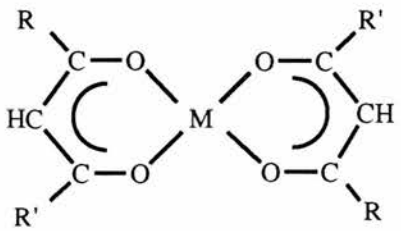

Figure 2.5; β–diketonate of a divalent metal

These compounds are insensitive to both air and moisture which makes them easy to handle and use. Table 2.1 indicates some of the diketone ligands which have been used to prepare volatile compounds of the lanthanides and other elements. Table 2.2 gives a detailed list of the compounds which have been used for the CVD of thin film superconductors.

Table 2.1; Common diketone ligands and the usual abbreviations of the deprotonated ligands

TRIVIAL NAME + STRUCTURAL FORMULA	SYSTEMATIC NAME	ABBREVIATION
Acetylacetone $CH_3C(O)CH_2C(O)CH_3$	2,4 - Pentanedione	ACAC
Trifluoroacetylacetone $CF_3C(O)CH_2C(O)CH_3$	1,1,1- Trifluoro-2,4-pentanedione	TFA
Hexafluoroacetylacetone $CF_3C(O)CH_2C(O)\ CF_3$	1,1,1,5,5,5-Hexafluoro-2,4-pentanedione	HFA
Dipivaloylmethane $(CH_3)_3CC(O)CH_2C(O)C(CH_3)_3$	2,2,6,6-Tetramethyl-3,5-heptanedione	DPM
Trifluoroacetylpivaloylmethane $CF_3C(O)CH_2C(O)C(CH_3)_3$	1,1,1-Trifluoro-5,5-dimethylhexane-2,4-dione	TPM
Pentafluoropropanoyl-pivaloylmethane $CF_3CF_2C(O)CH_2C(O)C(CH_3)_3$	1,1,1,2,2-Pentafluoro-6,6-dimethyl heptane-3,5-dione	PPM
Heptafluorobutanoyl pivaloylmethane $CF_3CF_2CF_2C(O)CH_2C(O)C(CH_3)_3$	1,1,1,2,2,3,3-Heptafluoro-7,7-dimethyloctane-4,6-dione	HPM (HFOD)
Dibenzoylmethane $C_6H_5C(O)CH_2C(O)C_6H_5$	1,3-Diphenylpropane-1,3-dione	DBM
Naphthoyl trifluoroacetone $(C_{10}H_7)C(O)CH_2C(O)CF_3$	1-Naphthyl-4,4,4-trifluoro-butane-1,3-dione	NPTFA
Thenoyl trifluoroacetone $(C_4H_3S)C(O)CH_2C(O)CF_3$	1-Thiophenyl-4,4,4-trifluoro-butane-1,3-dione	THTFA
Benzoyl trifluroacetone $(C_6H_5)C(O)CH_2C(O)CF_3$	1-Phenyl-4,4,4-trifluoro-butane-1,3-dione	BZTFA
Decafluoroheptanedione $CF_3CF_2C(O)CH_2C(O)CF_2CF_3$	1,1,1,2,2,6,6,7,7,7-decafluro-heptane-3,5-dione	DFD

Table 2.2; Compounds used for CVD of superconductor constituents

METAL	PRECURSOR	SUBLIMATION TEMPERATURE	REFERENCE
Copper	$[Cu(ACAC)_2]$	140-170°C	15
Copper	$[Cu(DPM)_2]$	140-155°C	31
Copper	$[Cu(HFA)_2]$	90°C	16
Copper	$[Cu(t\text{-}BuO)]_4$	100°C	36
Copper	$[Cu(NONA\text{-}F)_2]$	85°C	37,38
Copper	$[\varepsilon^5\text{-}C_5H_5CuPR_3]$ (R= Me, Et, t-Bu)	c.70°C	39
Copper	[t-BuOCuPMe$_3$]	65°C	40
Copper	$[(HFA)Cu(PMe_3)]$	45°C	41
Yttrium	$[Y(DPM)_3]$	120-160°C	15
Yttrium	$[Y(HFA)_3]$	130°C	29
Yttrium	$[Y(HFOD)_3]$	...	17
Barium	$[Ba(DPM)_2]$	230-240°C	15
Barium	$[Ba(DPM)_2]$ (+ NEt_3 vapour)	130°C	48
Barium	$[Ba(DPM)_2]$ (+ THF vapour)	210°C	49
Barium	$[Ba(HFA)_2]$	230°C	29
Barium	$[Ba(HFA)_2$(tetraglyme)]	150°C	46
Barium	$[Ba(HFA)_2$(18-crown-6)]	150-200°C	47
Barium	$[Ba(HFOD)_2]$	185°C	18
Barium	$[Ba(DFD)_2]$	140°C	45
Calcium	$[Ca(HFA)_2]$	80-120°C	51
Calcium	$[Ca(HFA)_2]$	180-185°C[A]	51
Calcium	$[Ca(HFA)_2$(triglyme)]	90°C	52
Calcium	$[Ca(DPM)_2]$	<230°C	50

Strontium	$[Sr(HFA)_2]$	220-225°C[A]	51
Strontium	$[Sr(HFA)_2(tetraglyme)]$	120°C	52
Strontium	$[Sr(DPM)_2]$	<230°C	50
Bismuth	$[BiPh_3]$	<230°C	50
Bismuth	$[Bi(t\text{-}BuO)_3]$	80°C	53
Bismuth	$[Bi(OEt)_3]$	130°C	53
Bismuth	$[Bi(DPM)_3]$	110°C	53
Thallium	$[Tl(C_5H_5)]$	50-80°C[A]	54
Thallium	[Tl(DPM)]	165°C[B]	55
Thallium	$[Me_2Tl(ACAC)]$	135-140°C[A]	56
Thallium	[Tl(ACAC)]	140-145°C[A]	56

All measurements taken under vacuum conditions, except those marked 'A' or 'B' which were carried out at atmospheric pressure and 50 Torr respectively.

2.2.2; β-diketonates in CVD;

As has already been stated, it has long been known that the β–diketonates of the YBCO precursors are relatively volatile. For copper, the acetylacetonate (ACAC) which has methyl substituents has adequate volatility, although the ditertiarybutyl substituted dipivaloylmethane (DPM) is probably more suitable. However, for reasons which are described in Section 2.2.3., more bulky diketones than ACAC are required for yttrium and barium precursors. In the case of yttrium the DPM has been used effectively whilst barium has required sterically crowded fluorinated diketones. Calcium and strontium, which are required for BiSCCO (calcium is also a constituent of TBaCCO) utilise the same precursors as barium but these show greater volatility than the comparable barium precursors. There are a broad range of suitable

volatile precusors available for both thallium and bismuth. A more detailed description of the precursors employed for each metal is given in Section 2.3. Alternative precursors to the diketonates, where available, are also discussed.

2.2.3; The requirement for bulky alkyl and fluoroalkyl side chains on diketones;

It has just been explained that large alkyl or fluoroalkyl groups are required to produce adequate volatility for certain metal complexes. It is neccessary to offer some explanation of this peculiar phenomenon whereby an increase in the molecular weight can lead to a marked reduction in the sublimation temperature. Of all the precursors, volatile barium compounds are the most difficult to come by. Hence this element will be used as an example to explain the aforementioned observation.

It has been reported by Williams[23] that barium has a tendency to expand its coordination number to as large as 10 (in $[Ba(HFA)_2]$). In order to prevent this expansion it is necessary to introduce steric crowding which physically prevents bridges from forming. This has been successfully achieved with both fluoroalkyl and tertiarybutyl side groups. In addition to increasing precursor volatility by steric crowding, the use of fluoroalkyl groups may have other beneficial effects. By replacing hydrogen with fluorine intermolecular hydrogen bonds are removed, however this may be offset by agostic interactions between fluorines and adjacent barium centres (Section 2.3.1.1). Notwithstanding this the greater electronegativity of fluorine relative to hydrogen is certainally advantageous as it produces much lower van der Waal's interactions[24]. It can, therefore, be seen that the increase in weight of the ligands is more than offset by the reduction in

oligomerisation.

2.3; SUITABLE PRECURSORS FOR THE CVD OF HIGH T_c SUPERCONDUCTOR CONSTITUENTS:

2.3.1; Copper;

It has already been stated that simple diketonates of copper are sufficiently volatile for CVD use. The crystal structure of $[Cu(ACAC)_2]$ has been identified by both Starikova[25] (Figure 2.6) and Lebrun[26]. They showed that the the shortest intermolecular distances were of the order 3.0 Å. The length of these bonds is sufficiently great for them to be described as semi-coordinate. These bonds are too weak to lead to involatility but are sufficiently strong to increase significantly the sublimation temperature.

If the acetylacetonate is replaced by a branched diketonate a monomeric complex can result. Cotton and Wise[27,28] investigated the crystal structure of the $[Ni(DPM_2]$ complex which they stated to be isostructural with its Cu(II) analogue. $[Ni(DPM)_2]$ was seen to be monomeric and planar in the crystal and in the vapour phase. This can be attributed to the steric hindrance which results from adjacent $[Ni(DPM)_2]$ units arranging so as to minimise intermolecular contacts between methyl groups on opposite ligands. The consequent reduction in intramolecular bonding greatly increases the volatility of the DPM complex when compared with the ACAC.

The compounds so far used for CVD include $[Cu(ACAC)_2]$[15,17,18,29], $[Cu(DPM)_2]$[30] and $[Cu(HFA)_2]$[16]. Oda and co-workers[29] preferred to use the simple ACAC as the operating temperature (onset of vaporisation 200°C) is similar to that of their other precursors (in this

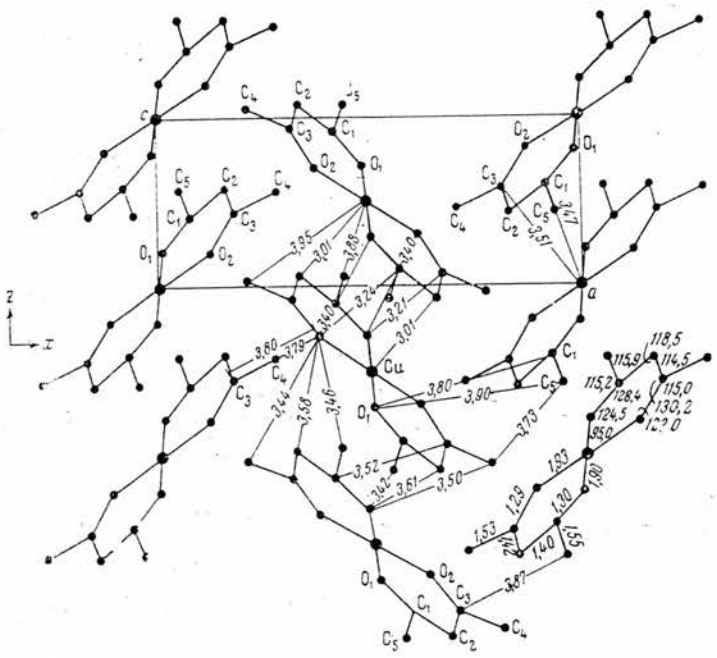

Figure 2.6; Crystal structure of $[Cu(ACAC)_2]$[25]

case the $[Ba(HFA)_2]$ and $[Y(HFA)_3]$ complexes). The $[Cu(DPM)_2]$ has been probably the widest used precursor[30, 31, 32, 33]. Yamane et al[30] found that $[Cu(DPM)_2]$ could be sublimed at 120°C under reduced pressure. No problems with decomposition were reported. For those who seek to minimise the volatilisation temperature, $[Cu(HFA)_2]$ would seem to be an ideal precursor, it having been volatilised at the much lower temperature of 90°C[16].

We have stated that many alkoxides undergo thermal decomposition and are thus rendered unsuitable for CVD use. In the case of copper, however there is a volatile alkoxide which might be suitable for this application. This is copper tertiary butoxide, $[Cu(t\text{-}BuO)]_4$, and it owes its volatility to its tetrameric structure (Figure 2.7). Its preparation and volatility were first reported by Tsuda

et al[34] who found that it was readily sublimable at 100°C under a pressure of 10^{-4} Torr. Greiser and Weiss[35] identified the structure of the alkoxide finding it to be a planar ring containing four copper and four oxygen atoms. They also found that the tetrameric structure was maintained in the vapour phase.

Jeffries and Girolami[36] have used $[Cu(t\text{-}BuO)]_4$ for CVD. They report that the white, air sensitive solid undergoes slow sublimation at 100°C and 10^{-5} Torr. By varying the conditions it was possible to deposit Cu or Cu_2O. Copper metal was produced when the precursor was heated to 100°C with a pressure of 10^{-5} Torr under dry conditions. The deposition zone was maintained at a constant temperature of 400°C. Under the same conditions, except that the reactor walls had been dosed with small amounts of water, Cu_2O was deposited.

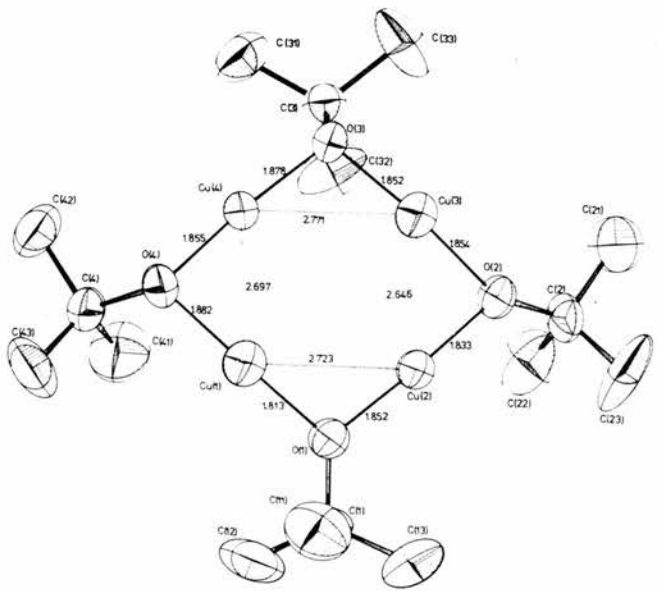

Figure 2.7; Crystal structure of $[Cu(Ot\text{-}Bu)]_4$[35]

A new group of complexes which have been developed by Norman et al[37, 38], and which are closely related to the β-diketonates, are highly fluorinated β–ketoimine complexes. The general formula for these complexes is provided in Figure 2.8.

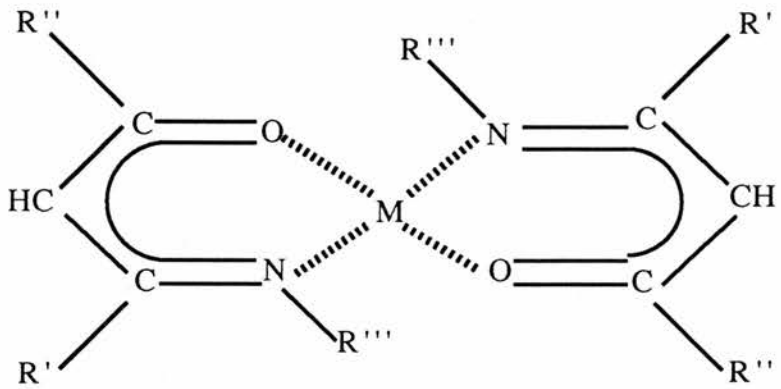

Figure 2.8; General formula for a M^{2+} β–ketoimine complex

Thus far the only such complex which has been employed in CVD work is bis[4-(2,2,2-trifluoroethyl) imino-1,1,1,5,5,5-hexafluor-2-pentanonato] copper(II), [Cu(NONA-F)$_2$]. The crystal structure of this complex is shown in Figure 2.9. [Cu(NONA-F)$_2$] has been sublimed at the relatively low temperature of 85°C under a pressure of 10 Torr. Unlike [Cu(HFA)$_2$], with which it was compared by Norman, it is non hygroscopic. The existence of this complex as an anhydrous species may be due to two factors. The presence of the additional fluoroalkyl groups attatched to the nitrogen atoms may produce steric hindrance making it more difficult for water to bind. Alternatively, the water may be unable to bind because the dihedral angle of the complex is 40° as opposed to, essentially, 0° in [Cu(HFA)$_2$]. The geometry of the molecule thus increases the steric hindrance at the axial sites.

Whilst it may be of little benefit to use this complex for the CVD of copper, the preparation of related complexes of barium might

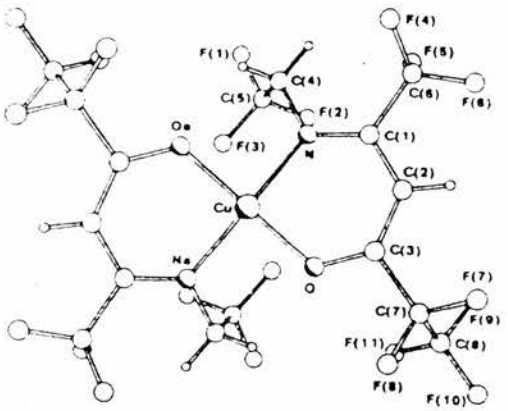

Figure 2.9; The crystal structure of $[Cu(NONA\text{-}F)_2]$[37]

yield particularly volatile species. The presence of alkyl groups on the nitrogens would increase steric crowding around the barium centre and might greatly reduce the capacity for oligomerisation.

Another recent development of some interest is the group of complexes incorporating trialkylphosphine ligands which have been reported by Beach[39], Hampden-Smith[40] and Shin[41].

Beach[39] investigated the use of (trialkylphosphine) cyclopentadienyl copper(I) complexes $[(C_5H_5)CuL]$ which were chosen because of their low molecular weight. Being monomeric, they are relatively volatile (sublimable at ca. 70°C in vacuo) and the ligands impart sufficient stability to allow the complex to transport without decomposition. The volatility, decomposition temperatures and deposition characteristics of the chosen compounds (L= PMe_3, PEt_3, PBu_3) were said to be similar. Most of the reported growths concentrated upon the use of the PEt_3 derivative which was volatilised at 70°C under vacuum conditions.

Hampden-Smith[40] prepared only the methyl derivative of the aforementioned organocopper complexes. This is said to be readily

sublimable at 65°C under a pressure of 10^{-3} Torr. A tertiary butoxy derivative of (trimethylphosphine) copper(I) was also produced, [t-BuOCuPMe$_3$]. This had similar volatility to that of the equivalent cyclopentadienyl complex.

Shin[41] et al have developed complexes based upon diketones consisting of one diketone ligand and one trimethylphosphine ligand per copper atom (Figure 2.10). The three diketone derivatives chosen contained the ACAC, TFA and HFA ligands and were sublimable in the range 40-45°C under a pressure of 10^{-5} Torr. All three complexes are monomeric both in the solid and solution phases and their high volatilities indicate that they are also monomeric in the gas phase.

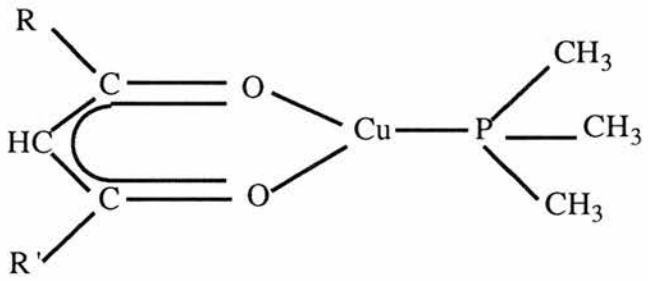

Figure 2.10; The general formula of [(β–diketonate)Cu(PMe$_3$)] complexes

All of these alkyl phosphine complexes are considered to be suitable for laying down copper metal which could be used as packages for electronic chips or for the metallization of chips. They may be less useful for superconductor applications because of contamination with phosphorus and are yet to be used in the preparation of thin film superconductors.

2.3.2; Yttrium;

It is not possible to use [$Y(ACAC)_3$] as a CVD precursor because it is an involatile complex. Berg and Acosta[22] identified it as a trihydrated species of formula [$Y(ACAC)_3(H_2O)_3$]. They claimed that the hydrate was too polar to sublime and that it was not possible to dehydrate the species without causing it to decompose. When the complex was heated either in air or in vacuo thermal decomposition accompanied by the loss of water and acetylacetone resulted. This produced a basic compound which immediately polymerised to an involatile polynuclear species.

As a result of this involatility it was necessary to find alternative β–diketonates. Early High T_c CVD workers were able to draw on the aforementioned and later studies carried out by Berg[22,42] and Eisentraut[43] who studied various β–diketonates of yttrium in the 1960's. Berg[22] and his co-workers prepared the ACAC, DPM, TFA and HFA cmplexes of yttrium, all of which were white solids. Eisentraut prepared the DPM and reported that it was possible to purify it by vacuum sublimation at less than 200°C, this property being attributed to the monomeric nature of [$Y(DPM)_3$].

As Table 2.2 shows, both the HFA and DPM have been used for the CVD of thin film superconductors. Oda et al[29] reported that [$Y(HFA)_3$] can be sublimed at 130°C under 10 torr of pressure. Furthermore, the use of the HFOD derivative has been reported by Panson and co-workers[17]. Whilst they do not state a sublimation temperature, the heated line temperature is given as 225°C and no deposition problems are reported. A more detailed discussion of this ligand appears in the barium section.

2.3.3; Barium;

2.3.3.1; β–diketonate precursors;

Early work, for example that carried out by Berry[15], concentrated upon [$Ba(DPM)_2$]. However, it soon became clear that this precursor produced an inadequate carry-over to the reactor. Further reference to this compound will be made in the thermal analysis comparison in Chapter 4. To overcome the problems with the DPM it was necessary to use the fluorinated compounds. The work of Belcher[44] has shown that the group of diketones with one fluoroalkyl group and one tertiary butyl group could produce sublimable products (Table 2.3). It is clear from the retention times that the volatility increases substantially as the length of the fluoroalkyl chain increases. This precursor has been used because it volatilises at a relatively low temperature, undergoes less decomposition than most precursors and is prepared simply from relatively cheap, freely available starting materials. Its abbreviated name is [$Ba(HFOD)_2$] (also called [$Ba(HPM)_2$]) and it has been used extensively by both Panson[17] and Zhao[18] (Figure 2.11).

The GC results of Belcher were supported by their own thermogravimetric analyses of the metal complexes. These clearly showed that the volatility increased as one progressed from Ba to Ca and from CF_3 to C_3F_7. Furthermore, in the case of the barium precursors, the increase in thermal stability is demonstrated by the increase in percentage mass lost as one passes from CF_3 to C_3F_7. A more detailed explanation of this will be given in Chapter 4.

Table 2.3; Gas chromatographic data for fluorinated β-diketones with R= $C(CH_3)_3$ and R'= CF_3, C_2F_5 or C_3F_7[44]

Acetylacetonate	Thermogravimetric data (% mass loss)	Gas chromatographic data (Retention time)
$Ca(TPM)_2.2H_2O$	100	8 min 34 sec
$Ca(PPM)_2.2H_2O$	100	4 min 45 sec
$Ca(HPM)_2.2H_2O$	100	1 min 24 sec
$Sr(TPM)_2.2H_2O$	98	8 min 55 sec
$Sr(PPM)_2.2H_2O$*	100	6 min 10 sec
$Sr(HPM)_2.2H_2O$	96	1 min 50 sec
$Ba(TPM)_2.2H_2O$	76	9 min 12 sec
$Ba(PPM)_2.2H_2O$	94	5 min 15 sec
$Ba(HPM)_2.2H_2O$	95	2 min 24 sec

* thought to be anhydrous

GC DETAILS; Philips PV4000 (Pye R) Chromatograph with hydrogen flame ionisation detection. Teflon column (3/16" o.d. and 2' in length) packed with E.301 silicone rubber on universal B (60-85) mesh operated at 230°C. Injection port and detector temperatures at 260°C and nitrogen flow of 46 $mlmin^{-1}$. Injections of ca. 1% w/v solutions in Sodium dried ether were made.

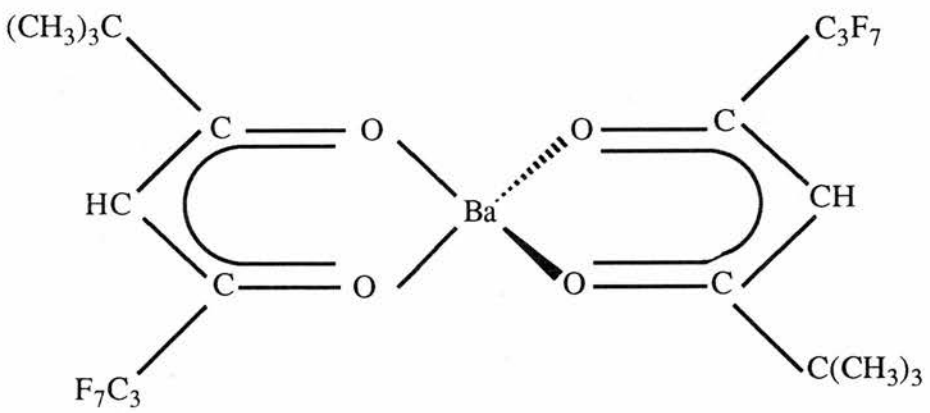

Figure 2.11; $[Ba(HFOD)_2]$

Zhao found that it was possible to sublime the [$Ba(HFOD)_2$] at temperatures as low as 170°C. His group reported that a steady vapour pressure could be maintained during the course of a deposition run and that transport took place at a low temperature and with far less decomposition than if the DPM had been used. However, our own work has shown that there is still a decomposition problem with the HFOD derivative although it is possible to use a single batch of the precursor for a second deposition run.

A still more successful precursor was developed by Marks and Shekleton[45], associates of Zhao. They attempted to improve the volatility of the barium precursor by increasing the level of fluorination of the diketone. This involved the use of two pentafluoroethyl groups on the diketone, one isomer of decafluoroheptanedione (named DFD by these workers). They found that this was a particularly volatile precursor which was sublimable at 140°C under a pressure of 10^{-2} Torr. As the precursor is reported in a patent application, little detail is provided about the thermal stability or the reusability of this ligand. However, the low temperature of sublimation should mean that the ligand is unlikely to undergo much decomposition prior to, or during, sublimation (these comments are supported by the thermal analysis discussions in Chapters 4 and 5).

Other precursors which have been used are of the HFA/TFA type. Berg et al[22] carried out a detailed study of lanthanide and yttrium HFA and TFA compounds and showed that the HFA typically had the greater thermal stability and volatility. It was, therefore, logical that Oda et al[29] used the HFA derivative as their precursor. They reported that the [$Ba(HFA)_2$] was sublimable at 230°C when a pressure of 10 torr was used.

The crystal structure of [$Ba(HFA)_2$] has been elucidated by

Williams[23] (Figure 2.12) and shows that the barium centres are 10-coordinate.

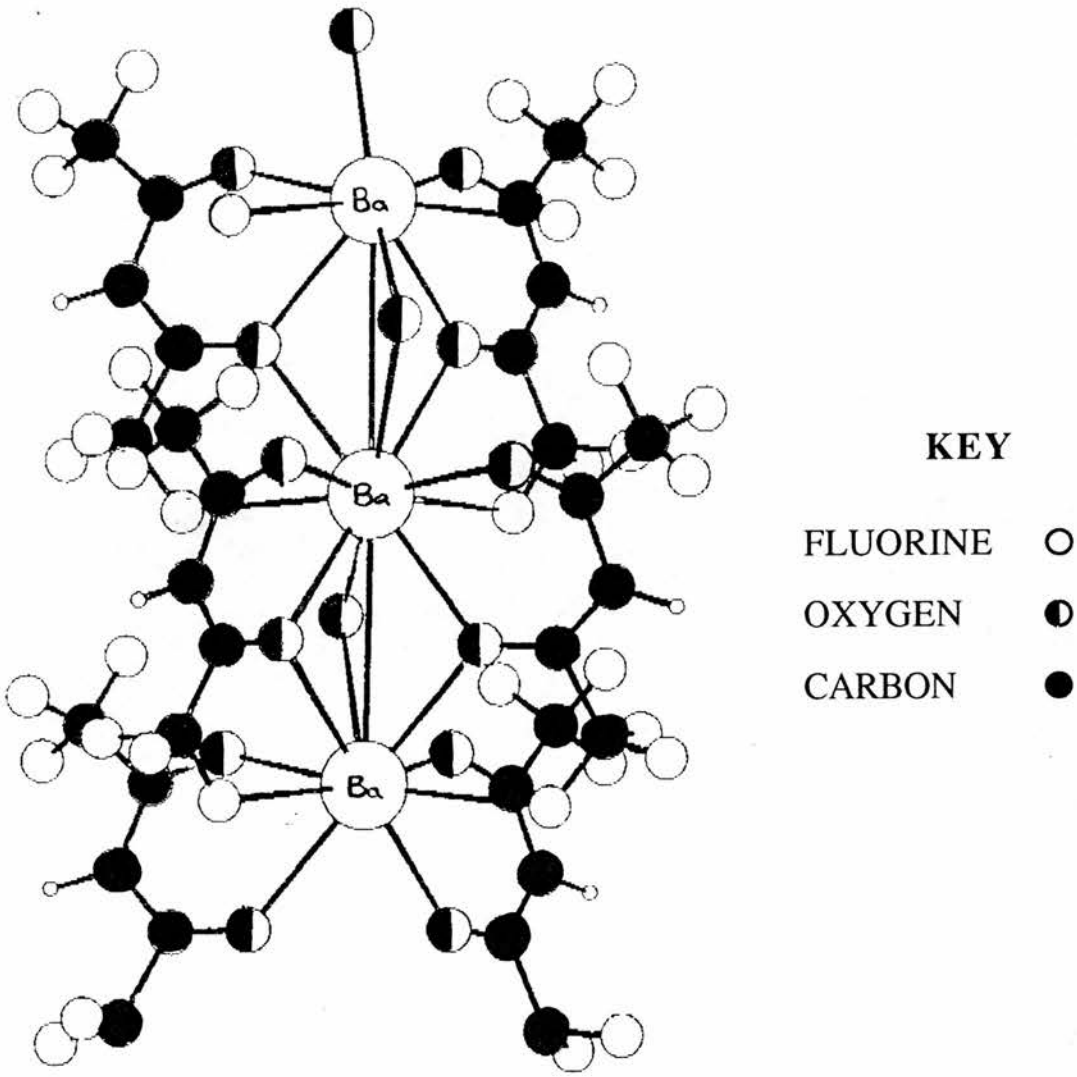

Figure 2.12; The crystal structure of $[Ba(HFA)_2]$[23]

In addition to the normally bound, bidentate diketones there are three types of bridging bond which clearly affect the volatility of the complex. These are;

(i) Bridging water molecules with the two lone pairs on the oxygen bonding to two adjacent metal centres.

(ii) Bridging diketones, whereby a lone pair on one diketone oxygen is donated to an adjacent barium centre to form a bond.

(iii) Agostic fluorine bonds. One of the fluorines of the trifluoromethyl groups forms a bond with an adjacent barium centre.
All three types of bond can be clearly identified from Figure 2.12.

2.3.3.2; Methods of increasing the volatilities of β–diketonates;

Efforts have been made to improve the volatilities of some of these diketonates. The successful approaches taken by (1) Timmer and Meinema[46], (2) Norman and Pez[47], (3) Barron[48] and (4) Matsuno et al[49] are now described;

2.3.3.2.1; The preparation of $[Ba(HFA)_2(tetraglyme)]$;

Timmer and Meinema[46] achieved increased volatility by reacting $[Ba(HFA)_2]$ with one equivalent of tetraglyme (2,5,8,11,14-pentaoxodecane).The complex they prepared is claimed to be a sublimable, non-hygroscopic, thermally stable solid. It clearly overcomes the normal intermolecular interactions by having the polyether ligand wrapped around the barium in a plane. Figure 2.13 shows the bonds in the complex and clearly identifies the 9-coordinate structure. Figure 2.14 is a space filling diagram which demonstrates how enclosed the barium centre is and how this level of steric crowding can prevent intermolecular interactions.

A closer examination of the properties of this compound does reveal one drawback. Whilst it is clearly volatile at the relatively low temperature of 150°C (0.03 mmHg), thermal analyses indicates that there is a 20% decomposition rate, thus hindering precursor reusability. Our preparation of the DPM derivative of this complex, $[Ba(DPM)_2(tetraglyme)]$, which we believe to be the most volatile non-

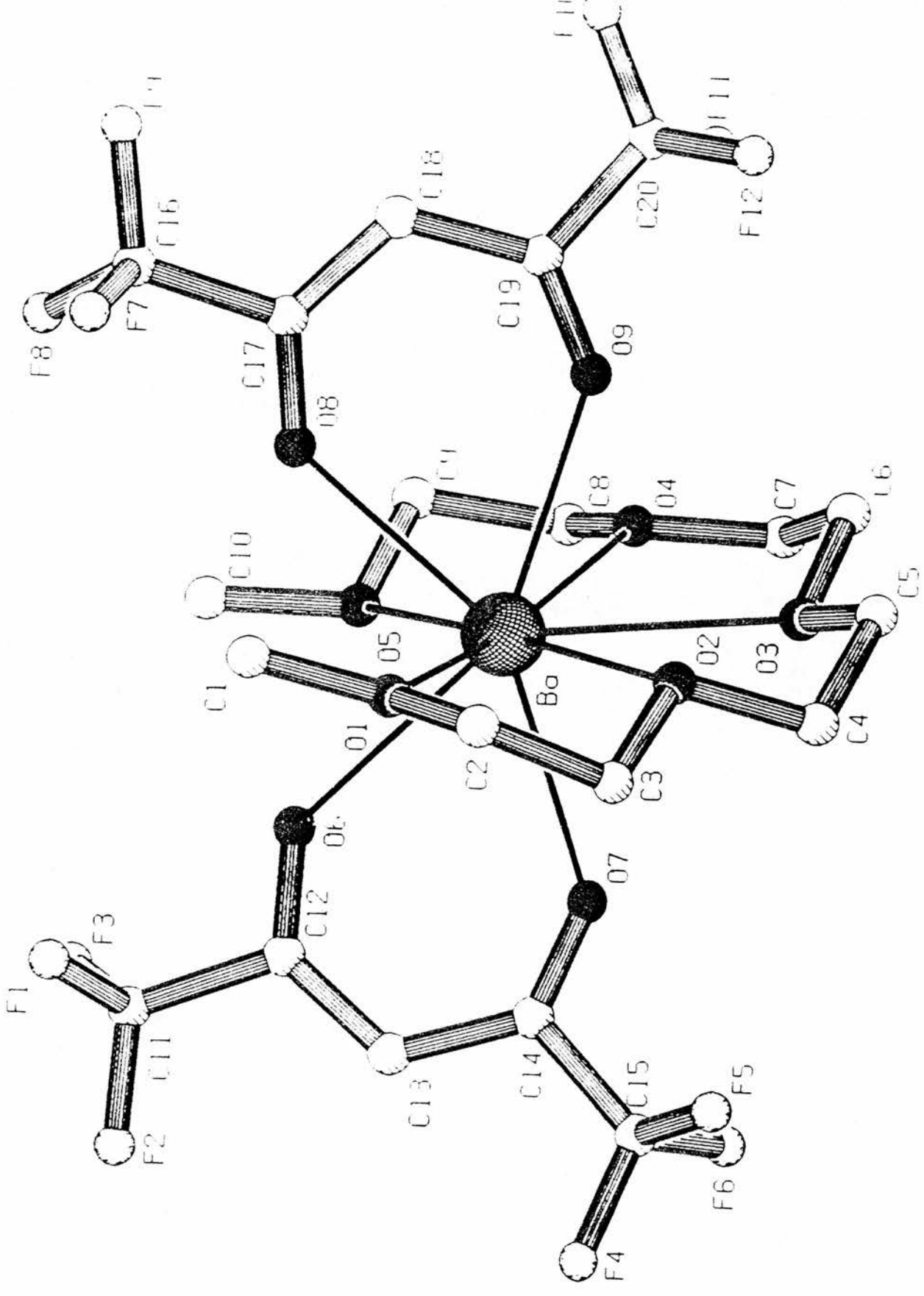

Figure 2.13; The crystal structure of [Ba(HFA)$_2$(tetraglyme)][46]

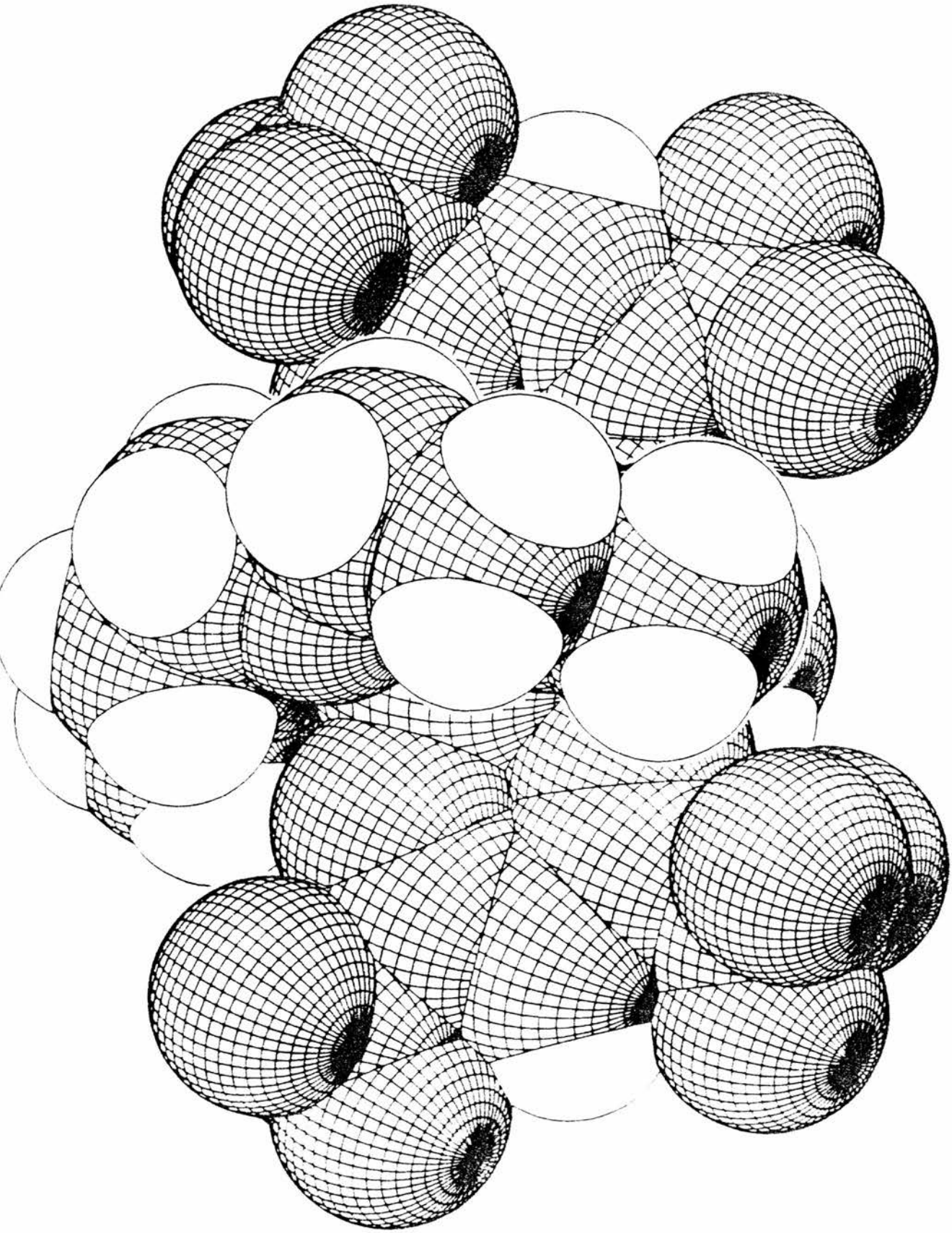

Figure 2.14; Space filling diagram of [Ba(HFA)$_2$(tetraglyme)][46]

fluorinated barium complex, is described in Chapter 3.

2.3.3.2.2; The preparation of $[Ba(HFA)_2(18\text{-crown-6})]$;

Timmer and Meinema made a brief reference to the preparation of this related 18-crown-6 complex. However, a more detailed investigation and structural assessment was undertaken by Norman and Pez[47]. The structure of this complex, Figure 2.15, is clearly similar to that of the tetraglyme complex, with the 6-coordinate polyether wrapping around the barium atom in a plane.

The exact sublimation temperature of the complex is not provided, but purification of the sample by repeated sublimation between 150 and 200°C at 10^{-3} Torr is reported. Assessment of this complex, and the related strontium and calcium derivatives, for CVD use is said to be in progress.

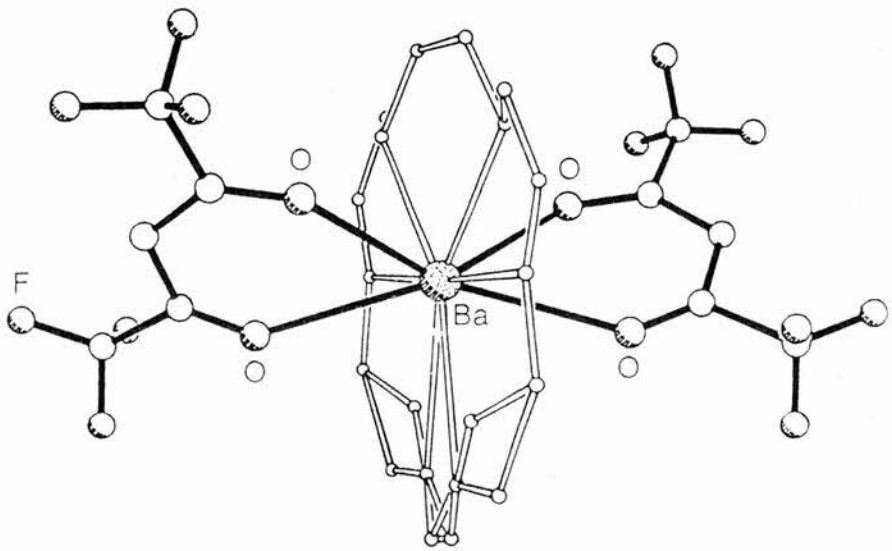

Figure 2.15; The crystal structure of $[Ba(HFA)_2(18\text{-crown-6})]$[47]

2.3.3.2.3; Sublimation studies of [$Ba(DPM)_2$] using a nitrogen base in the carrier gas;

An alternative approach was taken by Barron[48] who reported that the volatility of [$Ba(DPM)_2$] was enhanced by the addition of a nitrogen base to the carrier gas. Barron reports that whilst the addition of an oxygen donor ligand leads to stable, isolatable complexes no such species are isolated for amines or ammonia. The nitrogen donor is, therefore acting as a transport agent without apparently forming a distinct complex. It is this fact that seems to account for the marked volatility enhancement of these ligands.

Barron prepared compounds which could be volatilised at temperatures between 130°C and 230°C depending upon the amine used, with no visible decomposition. No comments are made as to the possibility of reuse of the precursors. The lowest temperature required to make thin films (130°C at atmospheric pressure) was using NEt_3 vapour in the nitrogen / oxygen carrier gas.

2.3.3.2.4; Sublimation studies of [$Ba(DPM)_2$] using THF in the carrier gas;

A less successful technique which nevertheless enhanced the volatility of [$Ba(DPM)_2$] was adopted by Matsuno and co-workers[49]. They introduced THF vapour into the carrier gas by bubbling the argon through THF prior to its introduction into the precursor container. This lowered the reduced pressure sublimation temperature to 210°C which compares favourably with the 230°C reported by Oda[29]. Stable vaporisation of the precursor was reported but no comments on precursor reusability were made.

2.3.4; STRONTIUM AND CALCIUM;

There are obviously great similarities between the volatilities of the diketonates of the group two elements. In general, the order of volatility is calcium > strontium > barium. This trend is confirmed in Table 2.3 and can be attributed to two factors. Firstly the lower mass of earlier members of the group is likely to produce more volatile products and secondly the smaller size of the metal makes oligomerisation less likely because of steric crowding. The choice of precursor is naturally going to be very much the same as for barium and this is reflected in the work of researchers in this field.

Zhang and co-workers[50] used the DPM derivatives of both calcium and strontium as their precursors. They reported that adequate deposition took place and commented that the maximum transport temperature was 230°C (presumably for the strontium precursor). Purdy et al[51] attempted to use the TFA and HFA complexes as precursors. They found that $[Sr(TFA)_2]$ was unsuitable for CVD use as it was not possible to sublime the compound. This, and their other results, clearly confirmed that the volatility of a particular ligand falls as one progresses down the group from calcium to barium. Most of their work was carried out at atmospheric pressure with inlet temperatures in the range 180°C for $[Ca(HFA)_2]$ to 250°C for $[Ca(TFA)_2]$. The calcium complex was transported in the range 80-120°C under vacuum conditions.

Following the work of Timmer[46], Zhang et al[52] adapted their polyether complexes of barium to strontium and calcium. The strontium precursor which they used was $[Sr(HFA)_2(tetraglyme)]$. This sublimed at 120°C under a pressure of 1.5 Torr and was reported to be thermally stable even after prolonged heating. For calcium, the triglyme

derivative, [$Ca(HFA)_2$(triglyme)] was found to have adequate volatility. It sublimed at 90°C under the same pressure as the strontium precursor and had similar stability to that precursor.

2.3.5; BISMUTH;

It was never considered to be a great problem to find suitable precursors for the CVD of bismuth. A number of volatile alkyl compounds of bismuth were known which have since proved to be suitable for this work. Zhang and co-workers[50] used triphenyl bismuth [$BiPh_3$] which they described as being both volatile and easy to handle. They reported that all their precursors for BiSCCO could be volatilised in the range 145-230°C at 2 Torr but do not specify the bismuth temperature. Whilst the superconductor was successfully deposited there was clear evidence of the mixed phase problem which we alluded to earlier and the T_c zero is as low as 75 K.

Recently Hubert-Pfalzgraf et al[53] have reported the investigation of a wide range of bismuth precursors. Three of these, the tertiary butoxide ([$Bi(t\text{-}BuO)_3$]), triethoxide ([$Bi(OEt)_3$]) and DPM ([$Bi(DPM)_3$]) were found to be volatile at relatively low temperatures. [$Bi(t\text{-}BuO)_3$] was sublimable at 80°C under a pressure of 10^{-2} Torr whilst [$Bi(OEt)_3$] required a higher temperature of 130°C and the same pressure. The DPM complex is described as being less volatile than the tertiary butoxide and requires the more severe conditions of 110°C and a pressure of $4x10^{-4}$ Torr.

2.3.6; THALLIUM;

The situation for thallium is very similar to that for bismuth in that adequate thallium precursors were never going to be too problematic. In the case of thallium its toxicity is of far greater concern. Richeson et al[54] used the volatile thallium precursor, cyclopentadienyl thallium (I), [$Tl(C_5H_5)$]. They reported that deposition was possible at atmospheric pressure at temperatures in the range 50-80°C. The T_c zero for the resultant TBaCCO superconductor was 100 K, again well below theoretical values. The explanation for this is the reported existence of multiple phases in the deposited film.

Zhang and co-workers[55] utalised [Tl(DPM)] as their precursor at a temperature of 165°C under a pressure of 50 Torr. They report the preparation of the $Tl_2CaBa_2Cu_2O_y$ phase with, again, a low T_c zero of 94 K. Berry et al[56] used a variety of precursors in their studies, all of which were undertaken at atmospheric pressure. [$Tl(C_5H_5)$] was transported at 125-130°C (note that this is rather higher than the temperature reported by Richeson above), [$Me_2Tl(acac)$] was transported at 135-140°C and [Tl(acac)] was transported at 140-145°C. Tl_2O_3 was found to be the major component of the film produced in all cases. No decomposition was reported for [$Tl(C_5H_5)$] or [$Me_2Tl(acac)$] but a dark brown residue was observed in the precursor container for [Tl(acac)].

CHAPTER 3

THE PREPARATION AND ANALYSIS OF PRECURSORS EITHER BASED UPON COMMERCIALLY AVAILABLE LIGANDS OR INCORPORATING TETRAGLYME

3.1; INTRODUCTION:

We have already explained in Chapter 2 that the established β−diketonates of calcium, strontium and barium are not ideal precursors for High T_c superconductors. Our early attempts to improve upon these compounds were directed at preparing the barium β−diketonates of several commercially available ligands. The molecular formulae of these ligands are shown in Figure 3.1.

The ligands fall into three distinct catogeries; those which have previously been used with barium, those which have previously been used with other metals and those for which we have not found any reference to previous use as chelating agents.

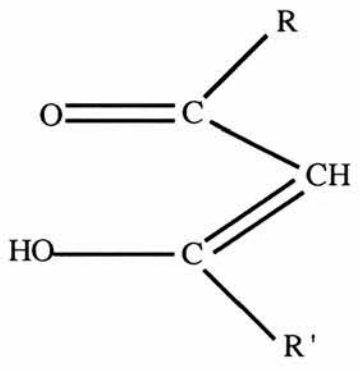

$R=C_4H_3S$, $R=CF_3$; thenoyltrifluoroacetone

$R=C_6H_5$, $R'=CF_3$; benzoyltrifluoroacetone

$R=C_{10}H_7$, $R'=CF_3$; naphthoyltrifluoroacetone

$R=R'=C_6H_5$; dibenzoylmethane

R=R'=Cl; malonyl dichloride

Figure 3.1; The molecular formulae of chelating ligands discussed in this chapter

Thenoyltrifluoroacetone (H(THTFA))[57] and dibenzoylmethane (H(DBM))[56] had been used to form complexes with barium but had not been tested for CVD suitability. Naphthoyltrifluoroacetone[58] (H(NPTFA)) and benzoyltrifluoroacetone[59, 60] (H(BZTFA)) had been used to prepare complexes with other elements but not with barium. We also attempted the prepare the barium derivative of malonyl dichloride

(H(MDC)). We expanded our work to other superconductor constituents by preparing the calcium derivative of H(BZTFA) and the strontium derivatives of H(BZTFA) and H(THTFA).

Additionally, the preparation of [$Ba(DPM)_2$.tetraglyme] was undertaken. This is the DPM analogue of the tetraglyme complexes prepared by Timmer and Meinema[46] which were described in Chapter 2.

3.1.1; [$Ba(THTFA)_2$] and [$Ba(DBM)_2$] previously prepared by Jablonski[56];

Both of these complexes were prepared for stability studies in water-dioxane solutions and their volatilities were not tested. We felt that they had potential as precursors for CVD for the following reasons. The thenoyltrifluoroacetone combined the advantages of a sterically hindering group and a short fluoroalkyl chain. The H(DBM) is clearly not a fluorinated diketone and is most closely related to (H(DPM)). Our hope was that the steric hindrance produced by the phenyl groups would be at least as large as that from the tertiarybutyl groups on the DPM and might thus produce a volatile complex.

3.1.2; β–diketonates of metals other than barium previously prepared by other workers;

Benzoyl trifluoroacetone has been widely used in complexes of a variety of metals. The most closely related metal to barium which has been used to prepare a complex with this diketone is probably zinc[59]. Our purpose in using this ligand was to prepare a sterically hindered, fluorinated diketone along the same lines as HFOD which had been

reported as having greater volatility than non-fluorinated diketones.

The copper derivative of naphthoyltrifluororoacetone had been reported by Reichert[57]. This ligand was, like the benzoyltrifluroacetone, chosen as it is a sterically hindered fluorinated diketone.

3.1.3; β–diketonates not previously prepared by other workers;

The malonyl dichloride was chosen to ascertain whether the inclusion of even bulkier substituents than fluorine might enhance the volatility of these complexes.

3.1.4; β–diketonates of strontium and calcium;

We considered that complexes with H(BZTFA) and H(THTFA) would produce the most likely precursors as they are both fluorinated, of relatively low molecular weight and sterically hindered. Additionally, as there is a tendency to greater volatility as one moves up Group 2, there was an increased probability of seeing volatility in strontium and calcium derivatives than in barium derivatives.

3.15; [$Ba(DPM)_2$(tetraglyme)];

The preparation of a number of volatile barium complexes is described elsewhere in this thesis. Whilst several of these are suitable for CVD use, they are all fluorine containing species. This does not create a major problem as, although the deposited film is usually the metal fluoride, this can be converted to the oxide by annealing.

However, the simplest and best quality result would come from a precursor which lays the oxide down directly. Hence a volatile, thermally stable and fluorine-free precursor might be considered as the ideal.

In an effort to prepare a suitable precursor which contained no fluorine, we decided to prepare the DPM analogue of [$Ba(HFA)_2$.tetraglyme]. We considered that this complex might have good volatility because of the steric crowding of the tertiary butyl groups coupled with the high coordination number resulting from the addition of the tetraglyme. The preparation and analysis of this precursor are described in Section 3.3.

3.2; PREPARATION AND ANALYSIS OF THE β–DIKETONATES:

3.2.1; Preparation of the β-diketonates;

This was carried out by direct reaction of the ligand with barium (II) bromide dihydrate, [$BaBr_2.2H_2O$], in the presence of a base (sodium hydroxide). All reactions were undertaken in aqueous ethanol, with the product being retrieved by precipitation resulting from the addition of water followed by volume reduction under vacuum conditions. All complexes were prepared in air except the H(DBM) derivative. In this case the reaction was carried out in a nitrogen atmosphere in an effort to arrest the decomposition which is described later.

The reactions for calcium and strontium were undertaken using the same conditions as for barium. The metal salts used for these reactions were calcium (II) chloride hexahydrate, [$CaCl_2.6H_2O$], and strontium (II) chloride hexahydrate, [$SrCl_2.6H_2O$].

3.2.2; Analysis of the β-diketonates;

Prior to the discussion of the analysis of these complexes, it is necessary to point out that that it is unlikely that any of them have a simple, monomeric structure. The involatility of the complexes is a clear sign that they exist as oligomers and, as such, have a complicated structure. This makes assignment more difficult and can lead to apparently contradictory data. Whilst it is possible in most cases to assign the data adequately, certain microanalyses are in error to an extent that precludes satisfactory assignment.

The situation might have been resolved by undertaking extensive purification and repeated analysis. This was not done because the complexes were clearly involatile and were, therefore, of no practical use for our purposes.

3.2.2.1; ^{1}H NMR

A summary of the key ^{1}H NMR peaks and their assignments is provided in Table 3.1.

It can be seen in all cases that there is a peak (between δ5.6 and δ6.35) representing the single hydrogen in the methyne group between the two carbonyl groups. The fact that complete reaction has occured can be confirmed by the absence of a second single hydrogen peak at around δ12. The spectrum of the β–diketones, which exist in the enol form, have a peak in this position from the terminal OH group.

The majority of the other peaks in these spectra can be assigned to the side groups which were introduced to increase steric hindrance. The position of these peaks closely match those in the parent β–diketone, so it is not proposed to discuss their assignment at length.

Table 3.1; Key ^1H NMR peaks and their assignments;

β-diketonate	Peak (δ) (s-singlet; m-multiplet)	Assignment
[Ba(BZTFA)2]	4.8(s)	water/solvent
	6.3(s)	methyne hydrogen
	7.5(m)	aromatic hydrogens
	8.0(m)	aromatic hydrogens
[Ba(NPTFA)2]	4.8(s)	water/ethanol/solvent
	6.4(s)	methyne hydrogen
	7.5-8.5(m)	aromatic hydrogens
[Ba(THTFA)2]	4.8(s)	water/solvent
	6.3(s)	methyne hydrogen
	7.2(m)	thienyl hydrogen
	7.8(m)	thienyl hydrogen
[Ba(DBM)2]	4.8(s)	water/ethanol/solvent
	5.6(s)	methyne hydrogen
	7.55(m)	aromatic hydrogens
	8.05(m)	aromatic hydrogens
[Ca(BZTFA)2]	4.85(s)	water/solvent
	6.3(s)	methyne hydrogen
	7.45(m)	aromatic hydrogens
	7.95(m)	aromatic hydrogens
[Sr(THTFA)2]	4.8(s)	water/ethanol/solvent
	6.2(s)	methyne hydrogen
	7.2(m)	thienyl hydrogen
	7.7(m)	thienyl hydrogen
[Sr(BZTFA)2]	4.85(s)	water/ethanol/solvent
	6.35(s)	methyne hydrogen
	7.55(m)	aromatic hydrogens
	8.05(m)	aromatic hydrogens

The barium complex of malonyl dichloride was found to be insoluble in methylene chloride, toluene, ethanol, petrol and other common solvents. As a result of this insolubility we were unable to take the ^1H NMR of this complex.

3.2.2.2; IR;

The most notable features of these spectra are related to M-O vibrations, C-F vibrations, chelated carbonyls, delocalised carbon-carbon double bonds and the presence of water. The bands representing

these groups for all of the complexes are listed in Table 3.2.

The assignment of these peaks was aided by reference to Holtzclaw[61] who had carried out a detailed assignment of the peaks in the IR spectra of β–diketonates and to Nakamoto[62].

Taking first the M-O vibration bands, we would expect to find strong bands below 600cm^{-1}. Table 3.2 shows that these bands are present in all of the complexes. C-F vibrations are also expected for the majority of complexes which we investigated. These strong bands appear in the range 1100-1300cm^{-1} in the complexes.

A key region of the spectrum is that between 1500-1625cm^{-1}. Whilst one observes no intense bands in the 1500cm^{-1} region of β–diketones, metal chelates of β–diketones do absorb strongly in this region. The upper band found here (1620cm^{-1} in [Ba(BZTFA)$_2$]) is assigned to a perturbed (or chelated) carbonyl whilst the lower one (1520cm^{-1} in [Ba(BZTFA)$_2$]) is assigned to a perturbed carbon-carbon double bond. The large frequency shifts are accounted for by the carbonyl and carbon-carbon double bond having less double bond and more single bond character following chelation.

The broad band in the region 3100 to 3700cm^{-1} is a good indication that there is water in the complex, but investigation by other analytical methods is required to confirm whether this is bound water or residue solvent.

3.2.2.2.1; [Ba(BZTFA)$_2$], [Ca(BZTFA)$_2$] and [Sr(BZTFA)$_2$];

A comparison between the spectra of these complexes reveals marked similarities. It can be seen that the spectra are essentially identical, save for the expected differences below 570cm^{-1}, the M-O vibration region.

Table 3.2; Key IR bands of the β-diketonate complexes

COMPLEX	ν(M-O)	ν(C-F)	ν(C-C)	ν(C-O)	H_2O
[Ba(BZTFA)2]	355-500	1115-1295	1520	1620	3100-3700
[Ba(THTFA)2]	310-515	1125-1250	1530	1600	3150-3650
[Ba(NPTFA)2]	215-555	1120-1280	1560	1605	3200-3450
[Ba(BDM)2]	210-510	-	1520	1590	3100-3550
[Ba(MDC)2]	210-415	620-720(C-Cl)	1545	1575	3050-3550
[Ca(BZTFA)2]	230-570	1130-1275	1520	1610	3100-3600
[Sr(BZTFA)2]	250-570	1130-1275	1520	1610	-
[Sr(THTFA)2]	220-575	1120-1290	1525	1570-1600	3050-3600

3.2.2.2.2; [Ba(THTFA)2] and [Sr(THTFA)2];

These complexes again have a close match in the key regions outlined in Table 3.2. There are also the anticipated differences in the region below 575 cm^{-1}.

3.2.2.3; Microanalysis;

The carbon / hydrogen microanalyses have been obtained for all of the complexes. In each case the expected carbon and hydrogen contents are listed for the anhydrous complex and this is supplemented where appropriate with the expected contents for the monohydrated and dihydrated species. A discussion of the probable molecular formulae of the complexes is given in Section 3.2.2.5. This takes account of the results of microanalysis and other analytical techniques.

[$Ba(BZTFA)_2$] Found C 37.53%, H 2.59%

$C_{20}H_{12}BaF_6O_4$ requires C 42.33%, H 2.12%

$C_{20}H_{14}BaF_6O_5$ requires C 41.17%, H 2.40%

$C_{20}H_{16}BaF_6O_6$ requires C 40.07%, H 2.67%*

[$Ba(NPTFA)_2$] Found C 50.03%, H 2.88%

$C_{28}H_{16}BaF_6O_4$ requires C 50.37%, H 2.40%

$C_{28}H_{18}BaF_6O_5$ requires C 49.19%, H 2.63%

[$Ba(THTFA)_2$] Found C 35.29%, H 1.66%

$C_{16}H_8BaF_6O_4S_2$ requires C33.17%, H 1.38%

$C_{16}H_{10}BaF_6O_5S_2$ requires C 32.7%, H 1.7%*

[$Ba(MDC)_2$] Found C 13.27%, H 1.26%

$C_6H_2BaCl_4O_4$ requires C 17.27%, H 0.48%

$C_6H_4BaCl_4O_5$ requires C 16.55%, H 0.92%

$C_6H_6BaCl_4O_6$ requires C 15.89%, H 1.32%*

[$Ba(BDM)_2$] Found C 52.04%, H 3.08%

$C_{30}H_{22}BaO_4$ requires C 61.75%, H 3.77%+

[$Ca(BZTFA)_2$] Found C 48.01%, H 2.64%

$C_{20}H_{12}CaF_6O_4$ requires C 51.06%, H 2.55%

$C_{20}H_{14}BaF_6O_5$ requires C 49.18%, H 2.87%

[$Sr(BZTFA)_2$] Found C 46.37%, H 2.32%

$C_{20}H_{12}SrF_6O_4$ requires C 46.33%, H 2.12%

[$Sr(THTFA)_2$] Found C 34.91%, H 1.75%

$C_{16}H_8F_6O_4S_2Sr$ requires C 36.25%, H 1.51%

$C_{16}H_{10}F_6O_5S_2Sr$ requires C 35.06%, H 1.83%

*These analyses produce too poor a fit to any of the proposed structures for any worthwhile conclusion to be drawn.

+This complex is clearly decomposing, so it would be expected that the microanalysis would be highly inaccurate.

3.2.2.4; Simultaneous Thermal Analysis (STA);

3.2.2.4.1; Introduction;

An STA consists of three separate traces, these are the Differential Thermal Analysis (DTA), the Weight Loss (WL) and the first derivative of the Weight Loss (FD). In the analyses described in this thesis, the sample was usually heated at a rate of 20°C per minute and the flow rate of nitrogen over the sample was $50cm^3$ per minute.

The DTA gives an indication of whether events recorded in the other traces are exothermic or endothermic. This is an important tool for determining when sublimation, melting, solvent loss or decomposition have occured. Exothermic events are observed as peaks in the DTA. Endothermic events are observed as troughs in the DTA. Melts and volatility are endothermic events whilst decomposition can be either an exothermic or an endothermic event. Because of this latter fact it is also necessary to study the Weight Loss curve before coming to a definite conclusion about the nature of the event which has occured.

The Weight Loss curve is to some extent self explanatory. The key features which should be noted are now described. A small (ca. 2%)

weight loss accompanied by an endotherm on the DTA indicates solvent or water loss. A steep drop in the weight loss curve accompanied by an endotherm in the DTA indicates sublimation (the presence of an an exotherm in the DTA would indicate decomposition). Any residue left after sublimation is shown by the level of the weight loss curve after sublimation or decomposition.

The First Derivative is shown only rarely and indicates the rate at which the loss of weight varies with time.

The STA traces are provided in the appendix to this chapter. A discussion of these thermal analyses now follows.

3.2.2.4.2; [$Ba(BZTFA)_2$];

The first two events in the differential thermal analysis are both endotherms. They occur at 31°C and 115°C and are likely to represent the loss of solvent and water respectively. This possibility is reinforced by the small weight losses observed at these temperatures. The next DTA trough at 254°C is likely to be the melt temperature.There is no weight loss here so there is no sublimation taking place. A large exothermic event then commences almost immediately and is accompanied by a rapid weight loss of around 45%. This is clearly the product decomposing. As the temperature increases further decomposition takes place (between 777°C and 990°C) to leave a residue of 26.69%.

In order to determine the minimum percentage of residue which could remain after the complete decomposition of the complex, we must identify the likely composition of this residue. Our CVD work has shown that highly fluorinated precursors usually decompose to the fluoride whilst those with no, or little, fluorine may leave an oxide

residue. If the oxide were produced, the percentage of residue which remained would be 26.9% whilst the fluoride would leave a 30.18% residue. If either the fluoride or the oxide were produced, it is reasonable to assume that near total decomposition has taken place with no volatilisation.

3.2.2.4.3; [$Ba(THTFA)_2$];

There is again evidence of solvent loss in the large trough culminating at 77°C and possibly some water loss above 100°C. The former event is accompanied by a large weight loss supporting the DTA but the latter loses only a small amount of weight so there is unlikely to be much water present. At 270°C there is a trough thus indicating that a melt is occuring. However, there is, once again, a large exotherm immediately after the melt accompanied by a 55% weight loss. This event is clearly the decomposition of the complex. Steady decomposition then follows to leave a residue of around 17% at 1000°C. If the amount of solvent in the complex is accounted for we would expect a residue of around 24.5%. The actual residue is lower than this which may be because there was some limited sublimation along with the decomposition.

3.2.2.4.4; [$Ca(BZTFA)_2$];

Below 88°C there is an endotherm and limited weight loss which would seem to show that solvent is being lost. The large endotherm at around 105°C which is accompanied by a weight loss of around 5% is likely to represent the loss of water from the complex and is the equivalent of slightly more than one mole of water per molecule.

The trough at 280°C is not accompanied by any major weight loss and is, therefore, likely to represent the melting point. The large peak commencing at around 290°C is accompanied by a 60% weight loss and is indicative of decomposition. The residue for the oxide is around 21%, which is greater than that which would be expected for calcium oxide, 12%, or calcium fluoride, 17%, so it can be assumed that it is most unlikely that there was any sublimation.

3.2.2.4.5; [$Sr(BZTFA)_2$];

The trough in the STA below 70°C which is accompanied by a weight loss of around 7% probably represents the loss of solvent. There is no evidence of water loss at 100°C, an indication that this might be an anhydrous complex. There is a slight dip in the STA at around 280°C which shows the onset of melting. However, this is followed immediately by a large exotherm (accompanied by a 50% weight loss) which indicates that the sample is decomposing before a complete melt is achieved. The final residue is of the order 30%, which is a far higher weight than the 20% which one would observe for a residue of barium oxide or 23% which would be observed with a barium fluoride residue. It is, therefore reasonable to conclude that the sample has decomposed completely without showing any signs of volatilisation.

3.2.2.5; Proposed molecular formulae;

3.2.2.5.1; [$Ba(BZTFA)_2$];

There is a clear indication from the ^1H NMR that water is present in this complex and both the STA and the IR are supportive of

this assertion. The microanalysis is too inconclusive to be used to draw any definite conclusions.

Proposed molecular formula; [$Ba(BZTFA)_2.2H_2O$]

3.2.2.5.2; [$Ba(THTFA)_2$];

The ^1H NMR and IR clearly show that water is present in the complex, although the STA seems to show that there is only a limited quantity present. The microanalysis is particularly inaccurate for carbon and is too inconclusive be used to draw any definite conclusions.

Proposed molecular formula; [$Ba(THTFA)_2.H_2O$]

3.2.2.5.3; [$Ba(NPTFA)_2$];

Because of the presence of solvent it is not possible to conclude whether the complex is hydrated from the ^1H NMR spectrum. The IR spectrum does, however, show the presence of water. The microanalysis has a satisfacory match to the monohydrated species.

Proposed molecular formula; [$Ba(NPTFA)_2.H_2O$]

3.2.2.5.4; [$Ba(DBM)_2$];

The tendency of this complex to turn yellow indicates that decomposition is taking place. The fact that sample decomposition has taken place is reflected in the microanalysis which gives low values for both carbon and hydrogen. The formation of a barium oxo species might best explain this result.

3.2.2.5.5; [$Ba(MDC)_2$];

The IR spectrum indicates that water is present in this complex. The microanalysis is highly innacurate, the closest match is to the dihydrate but this is sufficiently in error to prevent a firm conclusion from being drawn. However, the insolubility of this complex in most solvents and its total lack of volatility mean that the species is probably polymeric.

3.2.2.5.6; [$Ca(BZTFA)_2$];

Both the ^1H NMR and the IR spectra show that water is present in this complex. The microanalysis has a carbon content closest to that of the monohydrated species but a hydrogen content closer to that of the anhydrous species and is therefore, inconclusive. The STA indicates the presence of slightly more than one mole of water.

Proposed molecular formula; [$Ca(BZTFA)_2.H_2O$].

3.2.2.5.7; [$Sr(BZTFA)_2$];

The IR spectrum shows that this complex is anhydrous and there is a good match with the formula of the anhydrous species in the microanalysis. Whilst there is evidence of ethanol in the ^1H NMR spectrum, the water/ethanol/solvent peak integral is very small so it does support the findings of the other analytical techniques. The STA also shows no evidence of the presence of water in the complex.

Proposed molecular formula; [$Sr(BZTFA)_2$].

3.2.2.5.8; [$Sr(THTFA)_2$];

The IR spectrum indicates that water is present in this complex and there is a close match between the microanalysis result and the formula of the monohydrated species.

Proposed molecular formula; [$Sr(THTFA)_2.H_2O$].

3.3: PREPARATION AND ANALYSIS OF [$Ba(DPM)_2$(tetraglyme)]:

3.3.1; Preparation of[$Ba(DPM)_2$(tetraglyme)];

This was carried out using the method described by Timmer and Meinema[46]. [$Ba(DPM)_2$] was first prepared using the method described in Section 7.3, then suspended in dry toluene. The tetraglyme was then added to this stirrred suspension dropwise. The resulting slightly turbid solution was filtered and evaporated almost to dryness. The white solid remaining was slightly moist probably due to the presence of unreacted tetraglyme. The sample was recrystallised from a minimum volume of warm petrol to produce clear crystals.

3.3.2; Analysis of [$Ba(DPM)_2$(tetraglyme)];

3.3.2.1; ^1H NMR;

The ^1H NMR of the complex was taken in D_8-toluene. The spectrum is shown in Figure 3.2 whilst the key peaks and their assignments are provided in Table 3.3. The ratio of tetraglyme to DPM is 1:1.591 which is close to the 1:1.636 which one would expect for this complex if there was one mole of tetraglyme per [$Ba(DPM)_2$] molecule.

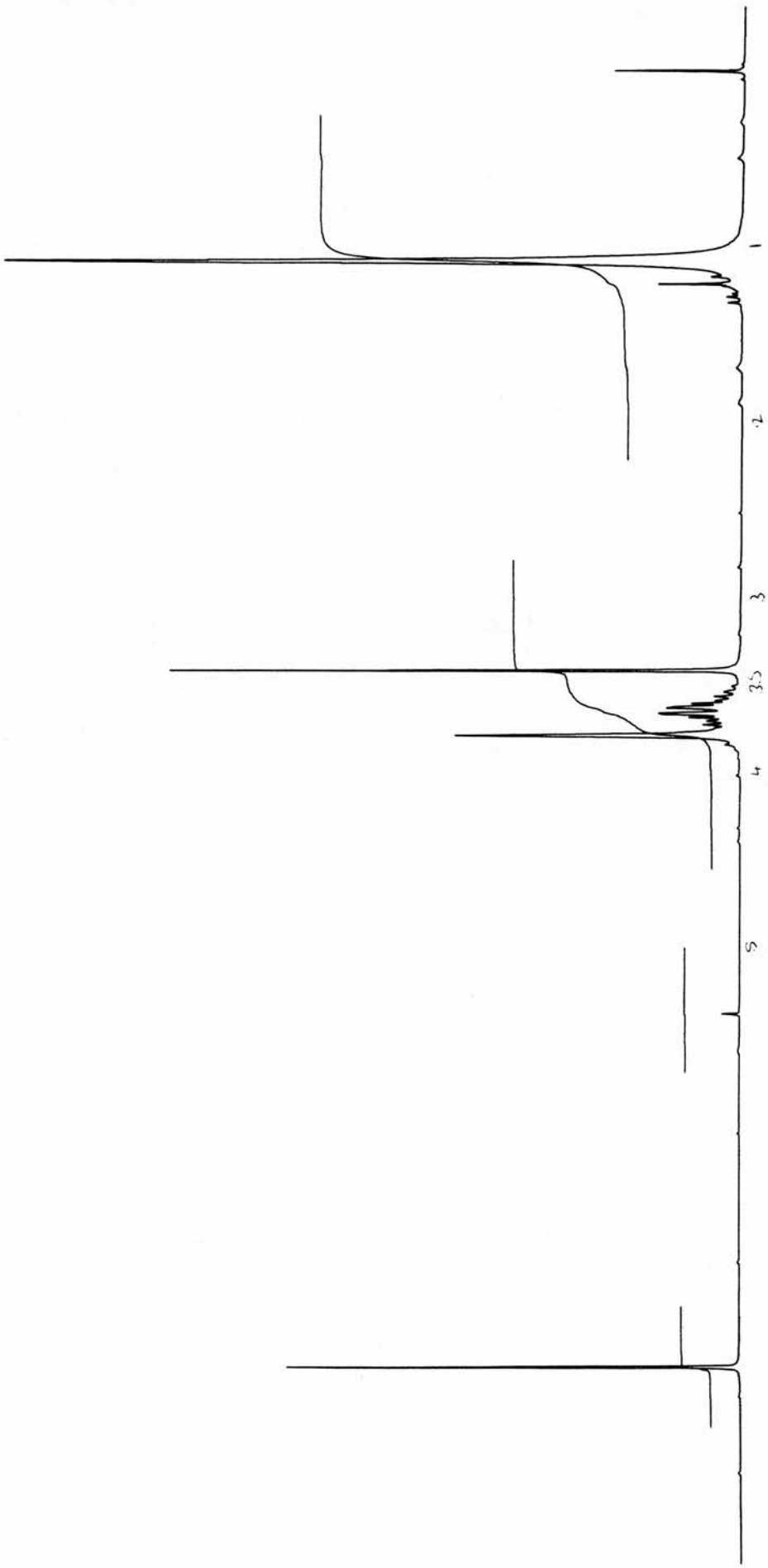

Figure 3.2; The ^{1}H NMR spectrum of [$Ba(DPM)_2$(tetraglyme)]

Table 3.3; Key peaks and assignments of the ^1H NMR of [$Ba(DPM)_2$(tetraglyme)]

δ	MULTIPLICITY	INTEGRAL	ASSIGNMENT
1.35	S	70	CH_3
3.40-3.80	M	44	tetraglyme
5.35	S	1	CH

3.3.2.2; Crystal sructure determination;

Whilst it was not possible to obtain a full data set within the timescale of this thesis, initial X-Ray photographic studies indicated that the crystal was triclinic.

3.3.2.3; Microanalysis;

The microanalysis result, shown below, supports the result of the ^1H NMR spectrum.

Found 52.36% C, 8.33 % H
$C_{36}H_{60}BaO_9$ requires 52.93% C, 9.02 % H

3.3.2.4; Simultaneous Thermal Analysis;

Prior to the discussion of the STA of this complex we will first examine that of the [$Ba(DPM)_2$] in order that a comparison can be made.

The STA of [$Ba(DPM)_2$] does not show a great improvement

over those described earlier in this chapter. Not only is there little evidence of sublimation but there is much evidence of decomposition and a high percentage of residue remaining after the analysis. A detailed assignment of this STA now follows.

The first DTA trough at 60°C is accompanied by a weight loss of 3.5%, this is likely to be due to the loss of solvent (ethanol). There is a small plateau at 100°C at which point there is a weight loss of 8% which would seem to be the loss of 2.5 moles of water. This water is unlikely to be all bound to the metal and the fact that the ^1H NMR indicates that there is ethanol present shows that at least some of this water is residual solvent. Any sublimation that there is takes place between 300 and 350°C there being a weight loss of 46% and a small trough in the DTA. However there are also two DTA peaks in this region so the sublimation may be accompanied by decomposition. Above this temperature there is a large exotherm at 470°C and any further weight loss is clearly decomposition. The final residue is 37.6% (BaO-34.1%) which is extremely high and indicates that little or no sublimation has taken place.

The reason for this lack of volatility is clearly the fact that the sample is oligomeric. Turnispeed et al[62a] identified the crystal structure of the DPM complex prepared from barium hydroxide and found it to be $[Ba_5(DPM)_9(H_2O)(OH)]$. Whilst our complex, prepared from the nitrate, would not contain the OH group it is highly probable that it was also a hydrated oligomeric complex.

In contrast to the STA of $[Ba(DPM)_2]$, that of $[Ba(DPM)_2(tetraglyme)]$ shows a near total volatilisation and a minimal residue. The major features of the STA of $[Ba(DPM)_2(tetraglyme)]$ are now discussed.

The STA of this complex includes a very sharp melt at 100°C

which is indicated by a trough in the DTA and no associated weight loss. The first weight loss of the complex comes over the range 150-250°C and is accompanied by a large trough in the DTA. The total weight lost in this stage is 34 % which corresponds quite closely to the 30.5 % of the complex which is made up of tetraglyme. Above 340°C a further weight loss occurs to leave a residue of approximately 4%. It is thought likely that the first weight loss does represent the loss of the tetraglyme but that the arrangement of the DPM does not revert to the normal oligomeric structure and is therefore more volatile and thermally stable. Time constraints limited further studies of the thermal properties of this complex. However, we do believe that the introduction of tetraglyme vapour into the carrier gas stream in our test rig (Section 4.2.4.8) would have produced greater volatility in this complex.

3.4: EXPERIMENTAL:

3.4.1; [$Ba(BZTFA)_2$];

The H(BZTFA) (2.16 g, 0.01 mol) was dissolved in aqueous ethanol (20 cm^3, 50%) and was reacted with sodium hydroxide (0.40 g, 0.01 mol) dissolved in aqueous ethanol (30 cm^3, 50%). To this stirred solution was added barium (II) bromide dihydrate (1.67 g, 0.005 mol) dissolved in aqueous ethanol (25 cm^3, 50%). The solution was stirred for an hour and was reduced to 66% of its volume under vacuum. Water (30 cm^3) was then added to the solution to ensure the precipitation of all of the product. The precipitate was then collected and dried in vacuo.

All of the NMR spectra were taken using deuterated methanol as the solvent.

IR; 355(w), 400(w), 430(w), 500(m), 570(m), 630(s), 765(s), 790(m), 810(m), 935(m), 995(w), 1020(m), 1050(m), 1070(m), 1115(s), 1140(m), 1185(m), 1235(m), 1275(s), 1295(m), 1315(m), 1490(s), 1510(s), 1570(m), 1620(s), 3100-3700(m) cm^{-1}.

^1H NMR; δ4.85 (s) 54, δ6.275 (s) 5.5, δ7.525 (m) 23, δ8.05 (m) 16.

3.4.2; [$Ba(THTFA)_2$];

This was prepared in the same way as the [$Ba(BZTFA)_2$] complex.

IR; 310(w), 345(w), 380(m), 515(w), 580(m), 650(m), 685(m), 750(w), 770(m), 790(m), 845(w), 855(m), 930(m), 1005(w), 1060(w), 1125(s), 1145(s), 1190(s), 1230(m), 1250(m), 1305(s), 1350(m), 1410(s), 1505(m), 1530(m), 1580(m), 1600(s), 3150-3650(m) cm^{-1}.

^1H NMR; δ4.80 (s) 82, δ5.55 (s) 14, δ6.3 (s) 4.5, δ7.2 (m) 5, δ7.8 (m) 10.

3.4.3; [$Ba(NPTFA)_2$];

The preparation of this complex was undertaken using the same method as that for [$Ba(BZTFA)_2$]. However, it was necessary to increase the volume of aqueous ethanol used to dissolve the β–diketone to 250cm^3 because of the relatively low solubility of H(NPTFA) in this solvent.

IR; 215(w), 235(w), 340(w), 435(w), 465(w), 475(w), 515(w), 555(m), 680(m), 745(w), 760(w), 785(s), 860(w), 905(w), 930(w), 945(w),

1040(m), 1060(m), 1120(s), 1140(s), 1190(s), 1280(s), 1505(s), 1520(s), 1560(s), 1580(s), 1605(s), 3200-3450(w) cm^{-1}.

^1H NMR; δ1.20 (t) 28, δ3.65 (qrt) 19, δ4.775 (s) 45, δ6.375 (s) 7, δ7.6 (m) 44, δ8.0 (m) 44, δ8.5 (s) 12.

3.4.4; $[Ba(MDC)_2]$;

The preparation of this sample was attempted using the general method already employed for the other complexes. As has already been described this complex was insoluble in most solvents, thus precluding analysis by ^1H NMR. We believe that this preparation was unsuccessful and that the product underwent hydrolysis in the aqueous solution used for the reaction.

IR; 210(m), 265(m), 415(w), 440(w), 590(m), 620(m), 690(m), 825(m), 925(m), 965(w), 1165(m), 1250(m), 1350(s), 1400(m), 1545(s), 1560(s), 1575(s), 3050-3550(m) cm^{-1}.

3.4.5; $[Ba(DBM)_2]$;

As was intimated earlier in this chapter this complex undergoes a marked discolouration from off white to bright yellow when the same conditions as for $[Ba(BZTFA)_2]$ are used. Excluding air from the reaction mixture did not solve this problem, however excluding light led to a marked improvement. The complex is, therefore, clearly light sensitive.

IR; 210(w), 340(w), 420(w), 495(w), 510(m), 605(m), 685(s), 775(m),

805(w), 935(w), 995(w), 1015(m), 1050(w), 1065(w), 1150(w), 1170(w), 1220(m), 1275(m), 1300(m), 1400(s), 1520(s,br), 1540(s), 1590(s), 3100-3550(s) cm^{-1}.

^1H NMR; δ1.25 (t) 44, δ3.70 (qrt) 29.5, δ4.80 (s) 43, δ5.60 (s) 3, δ7.55 (m) 11, δ8.05 (m) 8.

3.4.6; [Ca(BZTFA)2];

The H(BZTFA) (2.16g, 0.01 mol) was dissolved in aqueous ethanol (20 cm^3, 50%) and was reacted with sodium hydroxide (0.40 g, 0.01 mol) dissolved in aqueous ethanol (30cm^3, 50%). To this stirred solution was added calcium (II) chloride hexahydrate (1.10g, 0.005 mol) dissolved in aqueous ethanol (25 cm^3, 50%). The solution was stirred for an hour and was reduced to 66% of its volume under vacuum. Water (30 cm^3) was then added to the solution to ensure the precipitation of all of the product. The precipitate was then collected and dried in vacuo.

IR; 230(w), 260(w), 305(w), 385(w), 495(w), 510(w), 570(m), 630(m), 695(m), 745(m), 760(m), 790(m), 805(w), 920(w), 935(m), 995(w), 1020(m), 1060(m), 1130(s), 1175(s), 1240(m), 1275(s), 1485(m), 1520(s), 1570(s), 1610(s), 3100-3600(m) cm^{-1}.

^1H NMR; δ4.85 (s), δ6.30 (s) 28, δ7.45 (m) 100, δ7.95 (m) 67.

3.4.7; [Sr(BZTFA)2];

The H(BZTFA) (2.16g, 0.01 mol) was dissolved in aqueous

ethanol (20 cm^3, 50%) and was reacted with sodium hydroxide (0.40 g, 0.01 mol) dissolved in aqueous ethanol (30 cm^3, 50%). To this stirred solution was added strontium (II) chloride hexahydrate (1.33 g, 0.005 mol) dissolved in aqueous ethanol (25 cm^3, 50%). The solution was stirred for an hour and was reduced to 66% of its volume under vacuum. Water (30 cm^3) was then added to the solution to ensure the precipitation of all of the product. The precipitate was then collected and dried in vacuo.

IR; 250(w), 290(w), 315(w), 365(m), 440(w), 500(m), 570(s), 625(s), 695(s), 755(s), 790(m), 805(m), 840(w), 870(w), 935(m), 995(w), 1015(m), 1045(m), 1070(m), 1130(s), 1175(s), 1235(s), 1275(s), 1485(s), 1520(s), 1570(s), 1610(s), 3100-3600(m) cm^{-1}.

^1H NMR; δ1.2(t) 18.5, δ3.7 (qrt) 12.5, δ4.85 (s) 18, δ6.35 (s) 16, δ7.55 (m) 56, δ8.05 (m) 39.

3.4.8 $[Sr(THTFA)_2]$;

This preparation was carried out in the same way as that of the $[Sr(BZTFA)_2]$.

IR; 220(s), 250(m), 295(m), 360(m), 445(m), 480(s), 515(m), 575(s), 600(m), 640(s), 680(s), 695(m), 750(m), 770(m), 780(s), 860(m), 930(s), 1005(m), 1030(m), 1055(m), 1060(s), 1080(m), 1120-1150(s), 1180(s), 1220(s), 1245(s), 1290(s), 1350(s), 1410(s), 1470(m), 1510(s), 1525(s), 1540(s), 1570-1600(s), 3050-3600(m) cm^{-1}.

^1H NMR; δ1.2 (t) 12, δ3.65 (qrt) 7, δ4.8 (s) 54, δ6.2 (s) 23, δ7.2 (m)

24, δ7.7 (m) 52.

3.4.9; [$Ba(DPM)_2$(tetraglyme)]

A sample of [$Ba(DPM)_2$] was first prepared using the method described in Section 7.3.

[$Ba(DPM)_2$] (5.03 g, 0.01 mol) was suspended in dry toluene (60 cm^3). To this stirred suspension was added tetraglyme (2.22 g, 0.01 mol) dropwise over 15 minutes. The slightly turbid solution was then filtered and the toluene was removed in vacuo. The residue appeared to be slightly moist after the removal of solvent, a fact we attribute to the presence of unreacted tetraglyme. The solid was then dissolved in warm, dry petrol (25 cm^3) and placed in the refrigerator.at 5°C for recrystallisation. A good crop of clear crystals up to 3mm in length was produced.

APPENDIX 3;

STA ANALYSES

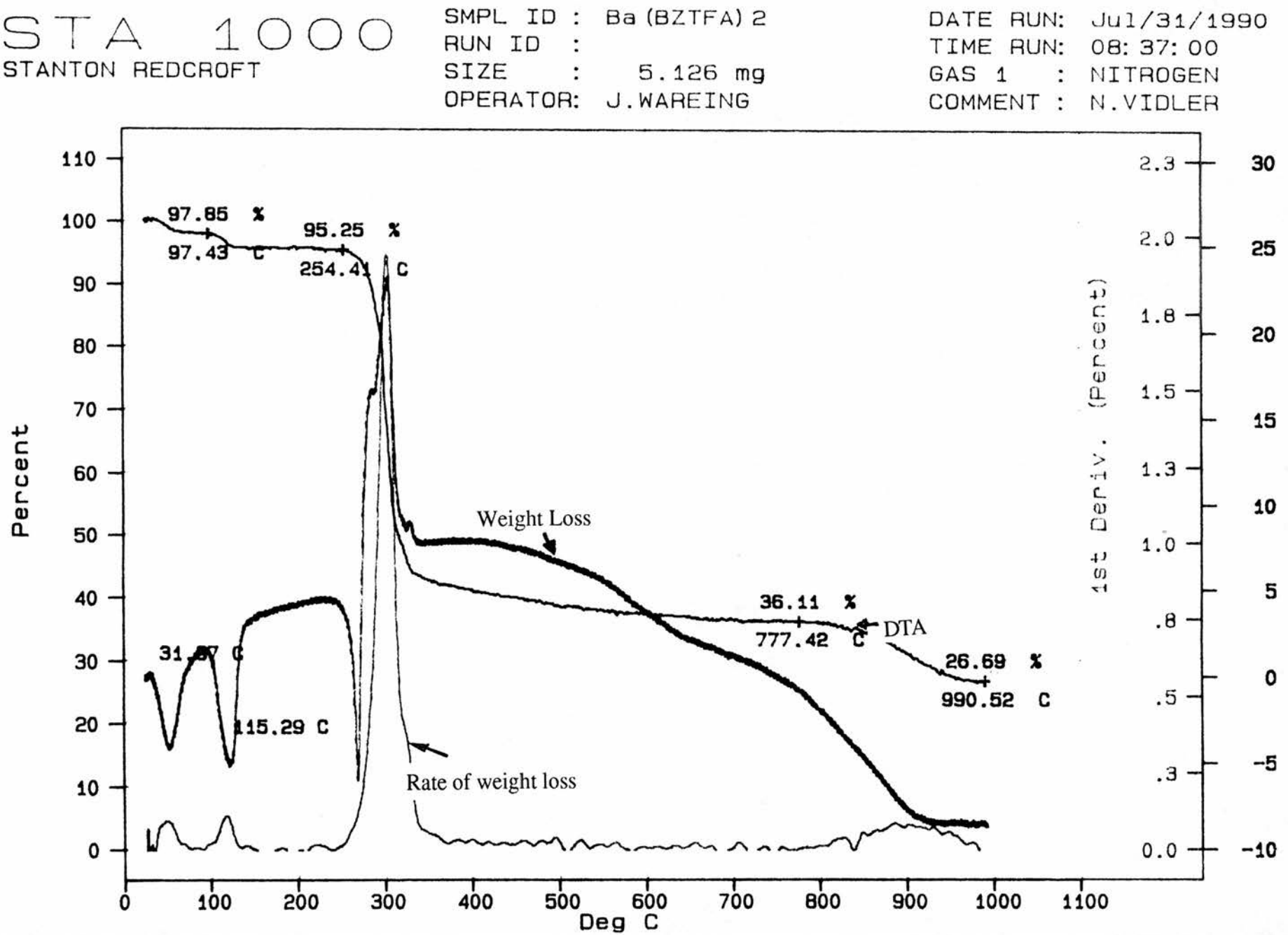

Figure A.3.1; [Ba(BZTFA)2]

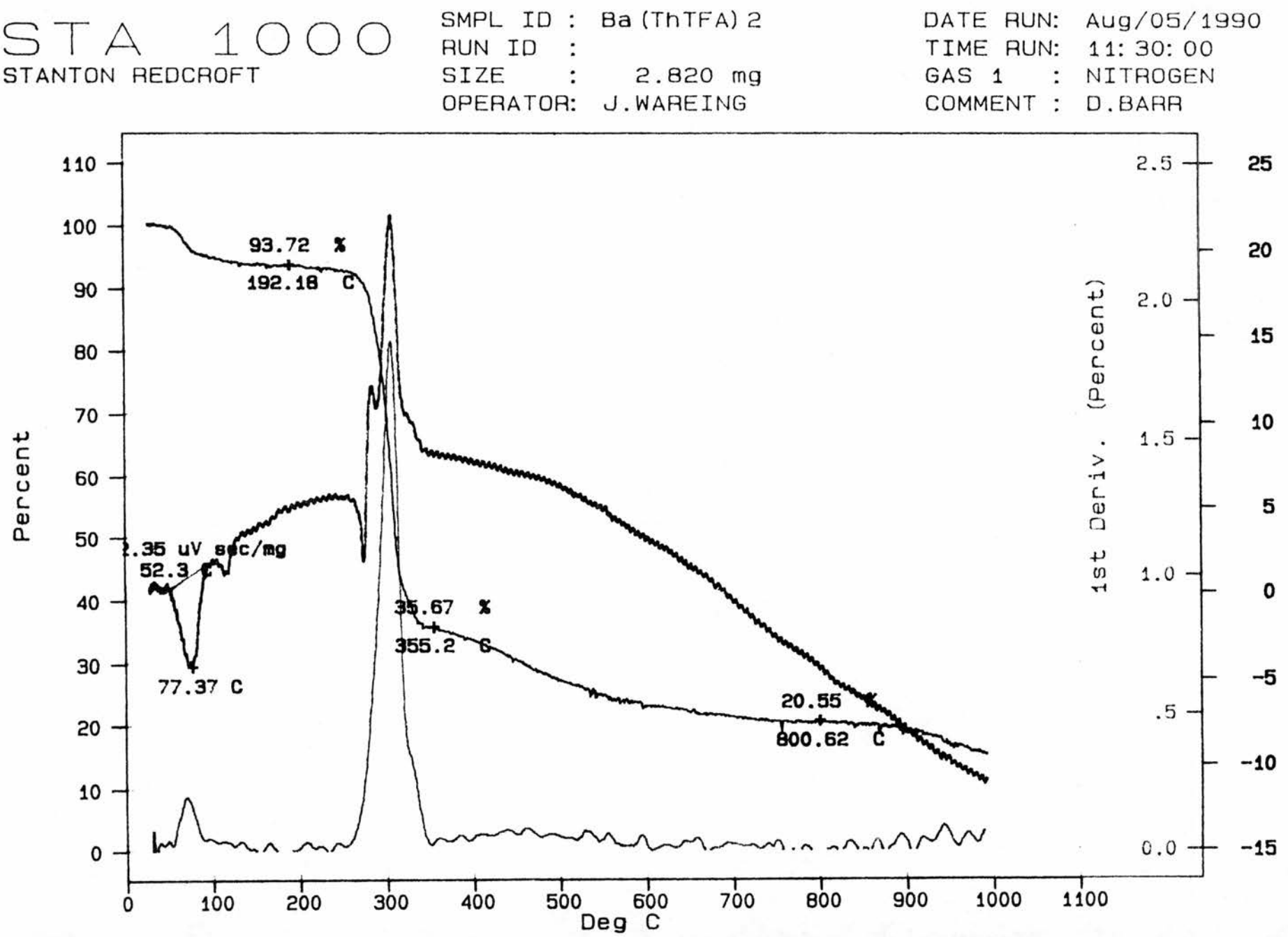

Figure A.3.2; [Ba(THTFA)2]

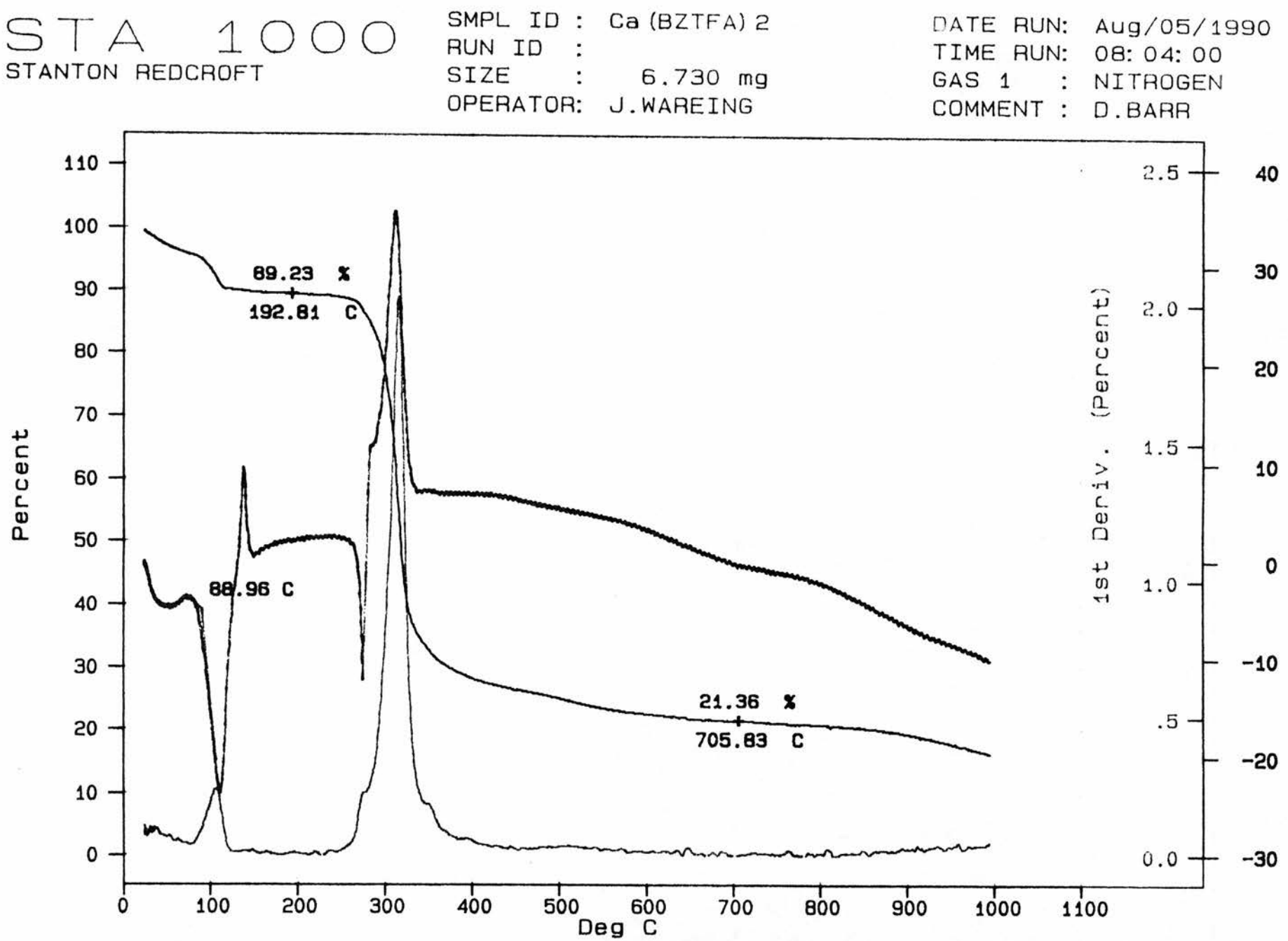

Figure A.3.3; [Ca(BZTFA)$_2$]

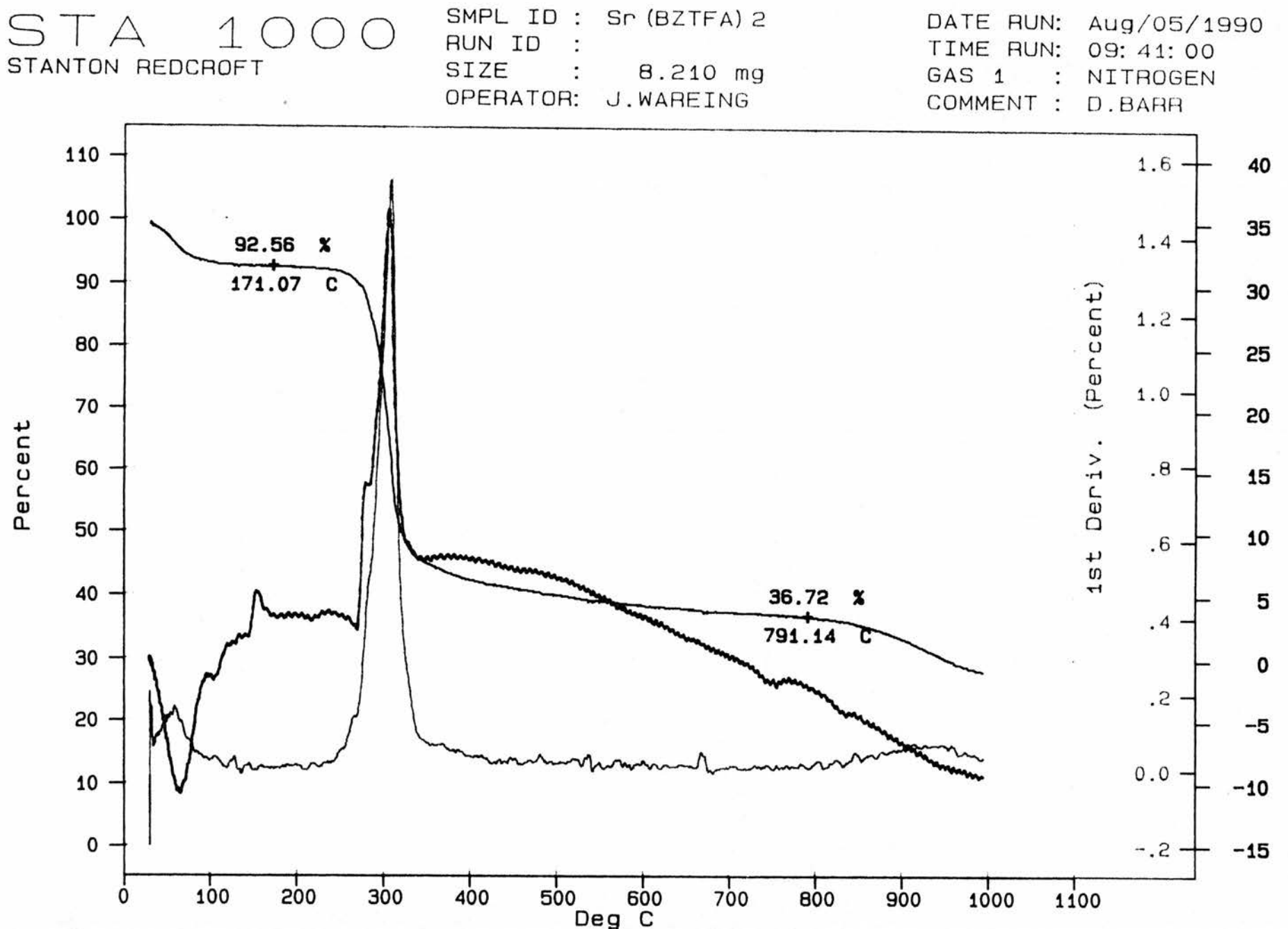

Figure A.3.4; $[Sr(BZTFA)_2]$

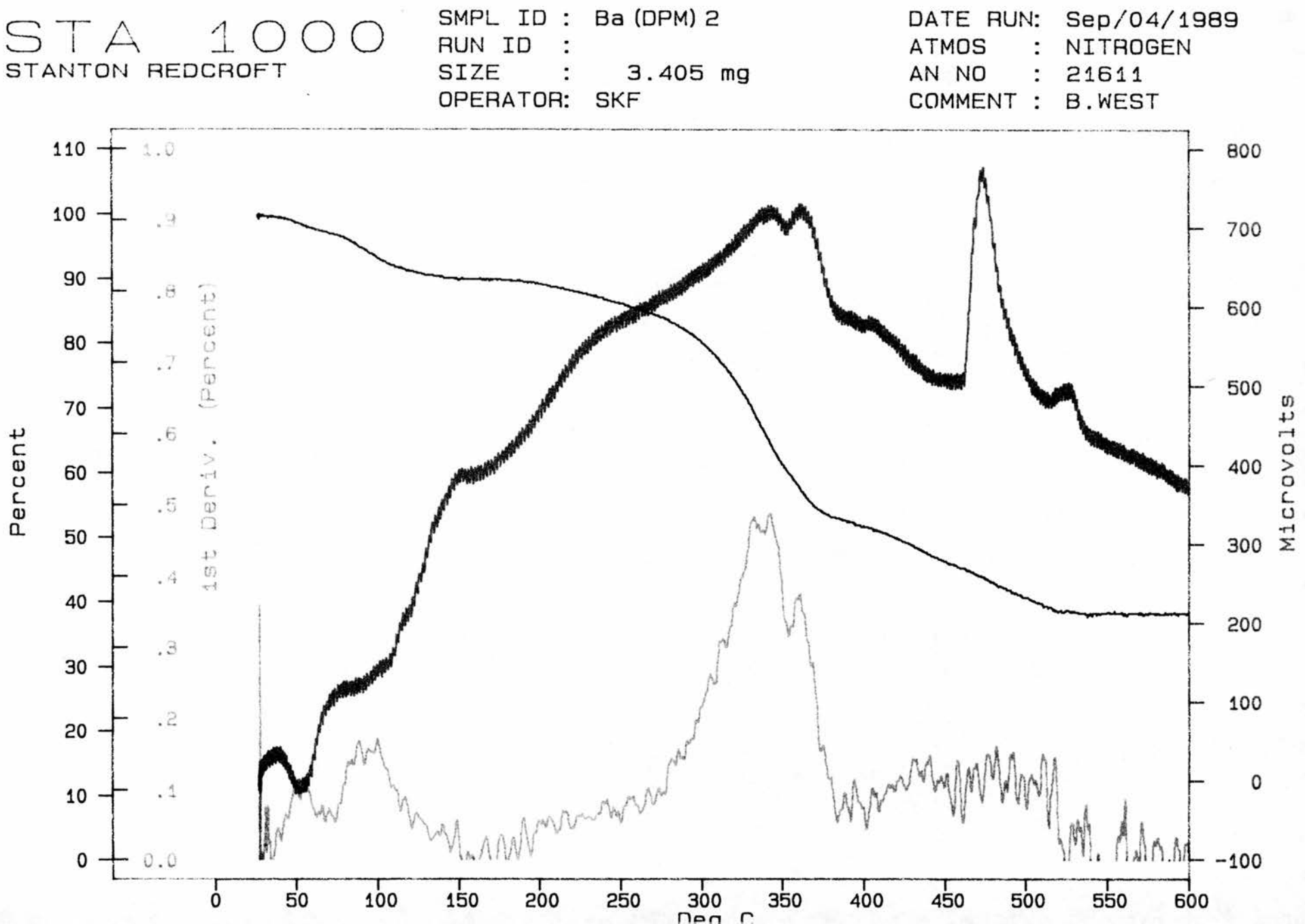

Figure A.3.5; [Ba(DPM)$_2$]

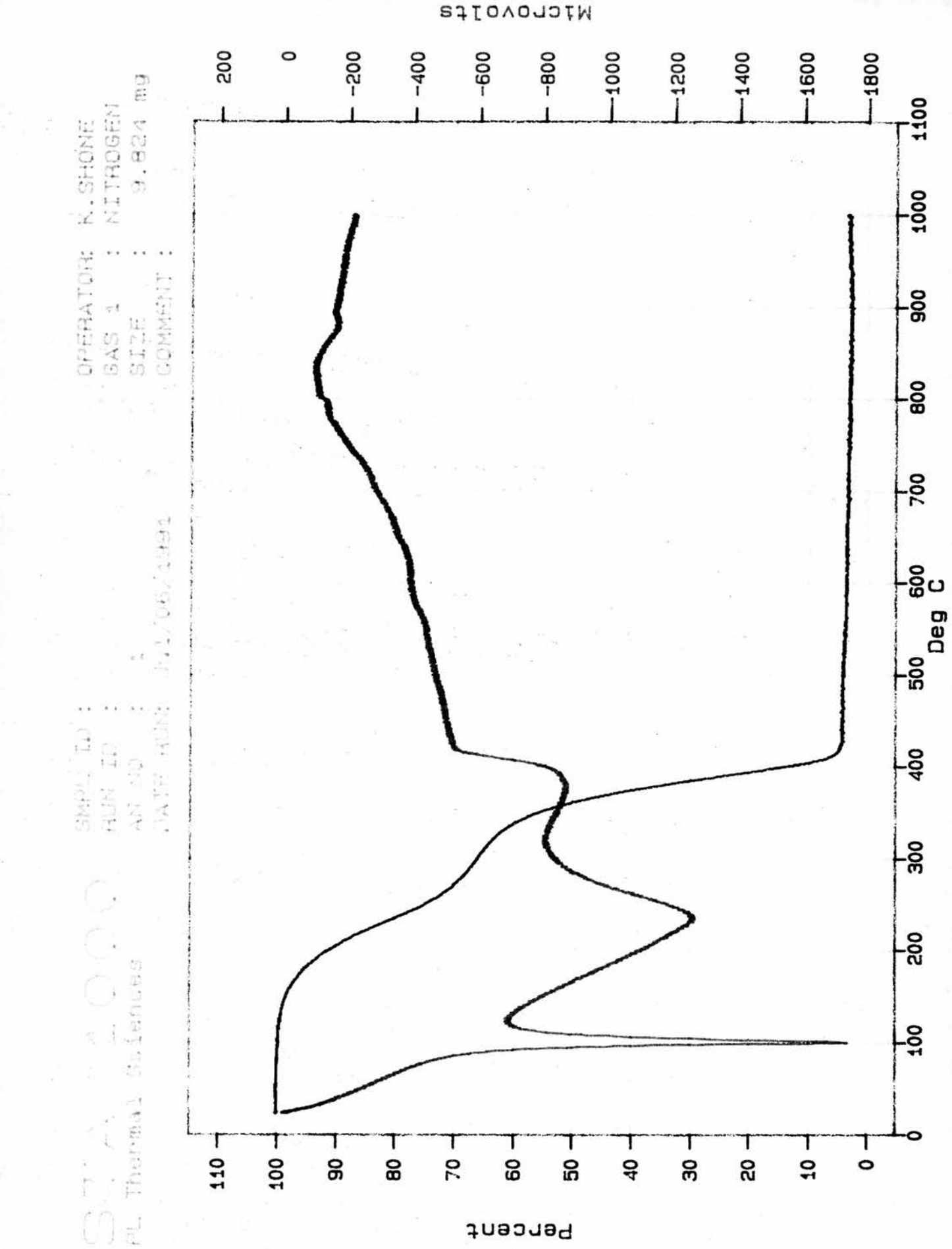

Figure A.3.6; [Ba(DPM)$_2$(tetraglyme)]

CHAPTER 4

THE PREPARATION AND ANALYSIS OF METAL COMPLEXES OF HIGHLY FLUORINATED β-DIKETONATES

4.1; INTRODUCTION:

In Chapter 3 we described the preparation, analysis and thermal properties of some β–diketonates of Group 2 elements prepared from commercially available ligands or incorporating tetraglyme. None of the complexes using commercially available ligands was sufficiently volatile for CVD use. Whilst the [$Ba(DPM)_2$(tetraglyme)] complex showed more volatility and less decomposition than these other complexes it did dissociate prior to sublimation.

It was, therefore, clear that we would have to develop our own new ligands. Before selecting the type of ligand to develop, it was necessary to study the existing compounds and to identify any trends which were present.

As we explained in Chapter 2, an obvious way to increase the volatility of precursors is to increase the level of fluorination of the ligand. Two different series of compounds will now be described to show how increasing the fluorination increases the volatility of the complex and that, at least for barium, the longer the fluorocarbon chain the more volatile will be the complex.

The first case is the series of ligands H(ACAC), H(TFA) and H(HFA) in which the methyl group of the diketone is progressively fluorinated. By assessing the work of Farona[63], who prepared both single and mixed copper diketonates based upon the above ligands we were able to confirm that an increased degree of fluorination leads to an increase in volatility.

In this work, Farona measured the melting points of these copper complexes. The melting points of these complexes are of interest as it provides an indication of the degree of association and the strength of intermolecular bonds. In Sections 2.3.1 and 4.2.4.3 the

intermolecular interactions of $[Cu(ACAC)_2]$ and $[Cu(DPM)_2]$ are discussed. These discussions show that the higher melting complex, $[Cu(ACAC)_2]$, is also the one with the greatest intermolecular interactions. As the volatility of the complex is also related to the size of the intermolecular interactions, we can see that for these complexes there is a direct link between the melting point and the sublimation temperature.

This table shows clearly that as we progress from ACAC to TFA to HFA, the melting point falls drastically. Additionally, with the mixed β-diketonates it is clear that the more fluorinated complexes have the lower melting points and are, therefore, the more volatile complexes.

Table 4.1; The melting points of selected copper β-diketonates;

β–DIKETONATE	MELTING POINT (°C)
$Cu(ACAC)_2$	236
$Cu(TFA)_2$	189
$Cu(HFA)_2$	95-98
Cu(ACAC)(TFA)	230-232
Cu(ACAC)(HFA)	170-173
Cu(TFA)(HFA)	110-112

A further pair of compounds worthy of discussion is $[Ba(DPM)_2]$ and $[Ba(HFOD)_2]$. We have already explained that the $[Ba(HFOD)_2]$ shows far greater volatility than the $[Ba(DPM)_2]$. This can be attributed to the replacement of one of the tertiary butyl groups of the $[Ba(DPM)_2]$ comples with a heptafluoropropyl group.

Having established that the incorporation of fluoroalkyl groups

was likely to increase the volatility of the complex, it was then necessary to ascertain the optimium length of these fluorinated chains. A valuable insight into this was provided by the GC studies of Belcher et al[44]. As we reported in Chapter 2 they investigated the series of compounds with one tertiary butyl group and one fluoralkyl group for barium, strontium and calcium (Figure 4.1).

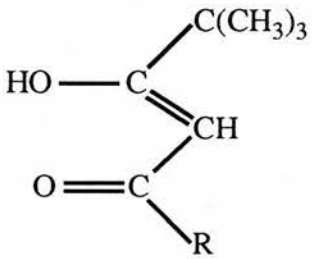

R= CF_3: H(TPM)
R= C_2F_5: H(PPM)
R= C_3F_7: H(HPM)/H(HFOD)

Figure 4.1; β-diketone ligands used by Belcher[44]

Table 2.3, which summarised their work, indicated that volatility increases with the length of the fluoroalkyl chain.

4.2; PRECURSOR DESIGN, PROPERTIES AND ANALYSIS:

4.2.1; Precursor design;

Two principles had, therefore, been firmly established. Firstly, replacement of alkyl by fluoroalkyl side chains increases volatility and secondly, longer fluorocarbon chains produce more volatile complexes. It was clear to us that the ideal precursor would be a fully fluorinated β–diketonate (except for the hydrogen intermediate to the carbonyl group) with long fluorocarbon chains.

Our first choice of ligand based upon this evidence was the previously prepared β–diketone, 1,1,1,2,2,3,3,7,7,7,-decafluoro-

heptane-4,6-dione (H(DFHD))[64]. The copper complex of this β−diketone was prepared during the purification of the parent diketone[64] and this complex was further studied by Volkov et al[65]. This complex had not, however, been used in CVD applications and none of the barium, strontium, calcium or yttrium derivatives had been prepared . Figure 4.2 shows the enol form of this diketone.

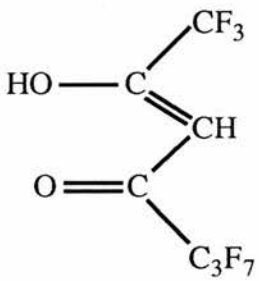

Figure 4.2; H(DFHD)

Having successfully prepared the H(DFHD) we then turned to the one which we considered to be the ideal ligand for our purposes based upon the previously described information. In this case we included two heptafluoroprpyl groups in the diketone to produce 1, 1, 1, 2, 2, 3, 3, 7, 7, 8, 8, 9, 9, 9 -tetradecafluorononane-4, 6-dione, H(TDFND). Figure 4.3 shows the enol form of this ligand. H(TDFND) had not been prepared previously but was synthesised by adapting the synthetic method for H(DFHD) referred to above.

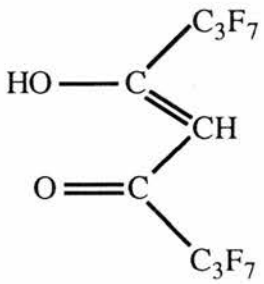

Figure 4.3 H(TDFND)

4.2.2; Ligand Preparation;

Both H(DFHD) and H(TDFND) were prepared by a Claisen condensation reaction based upon the synthesis described by Scribner et al[64]. Figure 4.4 shows the reaction mechanism which holds in both cases (R=CF_3 or C_3F_7).

A dry apparatus was used for the reaction which was carried out under dry nitrogen to prevent hydrolysis of the base, sodium methoxide. The sodium methoxide was freshly prepared and handled under dry nitrogen at all times. Product purification was achieved by preparing the copper complex then regenerating the β–diketone by the addition of concentrated sulphuric acid. Distillation then produced a product of high purity in a yield of approximately 30%.

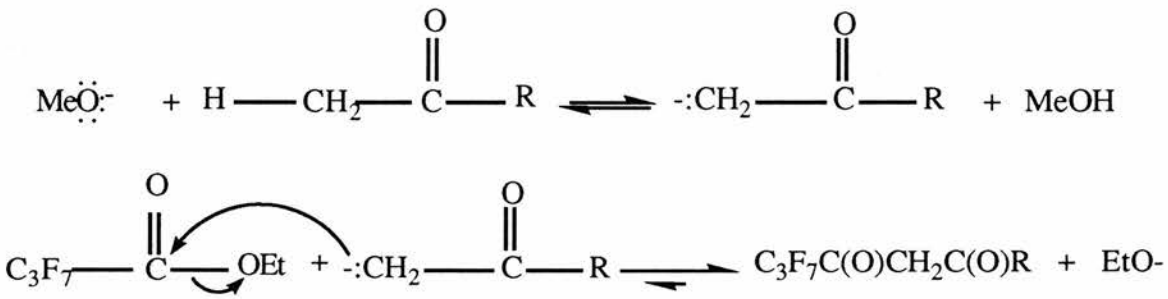

Figure 4.4; Reaction mechanism for the Claisen condensation of heptafluorobutyrate with a fluoroketone;

4.2.3; Ligand analysis;

As is the case with other β–diketones we found that the H(DFHD) and the H(TDFND) existed in the enol form (the structures were shown in Figures 4.2 and 4.3 respectively). Evidence for this was

clear in the ^1H NMR spectra of the diketones which gave 2 peaks in each case in a 1:1 ratio at δ6.4 and δ12.4 for H(DFHD) and at δ6.6 and δ12.9 for H(TDFND). Figure 4.5 shows the ^1H NMR of H(TDFND) in $CDCl_3$. The peaks with the high shift represent the OH group and those with the low shift the CH group. Sample purity is confirmed by the absence of other peaks in the spectrum.

4.2.4; Preparation and analysis of the β–diketonates;

For all but one of the metals studied the complexes were prepared by direct reaction of the ligand with a metal salt in the presence of sodium hydroxide. The exceptions were the copper complexes of both H(TDFND) and H(DFHD) which were prepared during the purification of the respective β–diketones (Section 4.3). The metal salts used were barium (II) bromide dihydrate, strontium (II) chloride hexahydrate, calcium (II) chloride hexahydrate and yttrium (III) nitrate pentahydrate.

All of the reactions were carried out in air using aqueous ethanol as the solvent. Product recrystallisation was achieved for $[Cu(DFHD)_2]$, $[Cu(TDFND)_2]$ and $[Ba(TDFND)_2]$. Recrystallisation of $[Cu(TDFND)_2]$ produced plate-like crystals for which it was possible to determine the crystal structure. This structural determination is described in Section 4.2.4.3. The $[Ba(TDFND)_2]$ complex, however, was found to consist of bundles of long (up to 2cm), fine needles. Hence, it was not possible to obtain a crystal structure of this complex. We will discuss later the relevance of the crystal appearance to our proposed structure of $[Ba(TDFND)_2]$.

Analysis was undertaken by the following techniques to achieve a broad picture of the thermal properties and structures of the

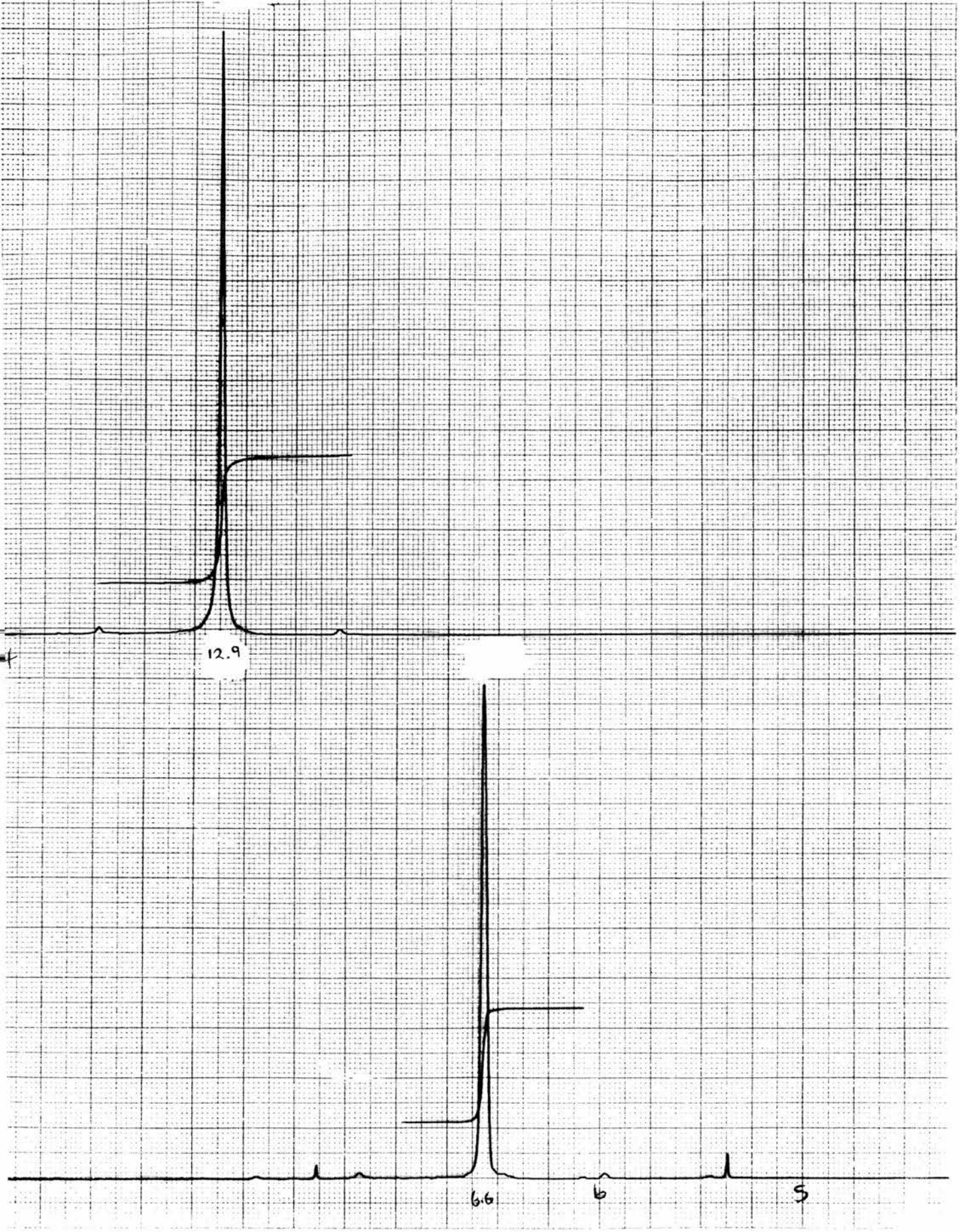

Figure 4.5; ^{1}H NMR of H(TDFND)

complexes; ^{1}H NMR, ^{19}F NMR, IR, Electron Impact Mass Spectrometry, Fast Atom Bombardment Mass Spectrometry, Solution phase molecular weight determination, Microanalysis and Simultaneous Thermal Analysis.

4.2.4.1; ^{1}H NMR;

As there is only one hydrogen present in these β–diketonates, the ^{1}H NMR spectra of these complexes are relatively straightforward. Other peaks in the spectra are related to water content, D_4-methanol and residue ethanol. The key peaks and their assignments are given in Table 4.2 whilst the ^{1}H NMR spectrum of $[Ba(TDFND)_2]$ is shown in Figure 4.6 .

TABLE 4.2; ^{1}H NMR ASSIGNMENTS;

β-DIKETONATE	CHEMICAL SHIFT (δ)	MULTIPLICITY	INTEGRAL	ASSIGNMENT
$[Ba(TDFND)_2]$	5.9	s		C-H
$[Ca(TDFND)_2]$	6.00	s		C-H
$[Sr(TDFND)_2]$	5.95	s		C-H
$[Y(TDFND)_3]$	6.30	s		C-H
$[Ba(DFHD)_2]$	5.85	s		C-H
$[Ca(DFHD)_2]$	5.85	s		C-H
$[Sr(DFHD)_2]$	5.90	s		C-H
$[Y(DFHD)_3]$	6.25	s		C-H

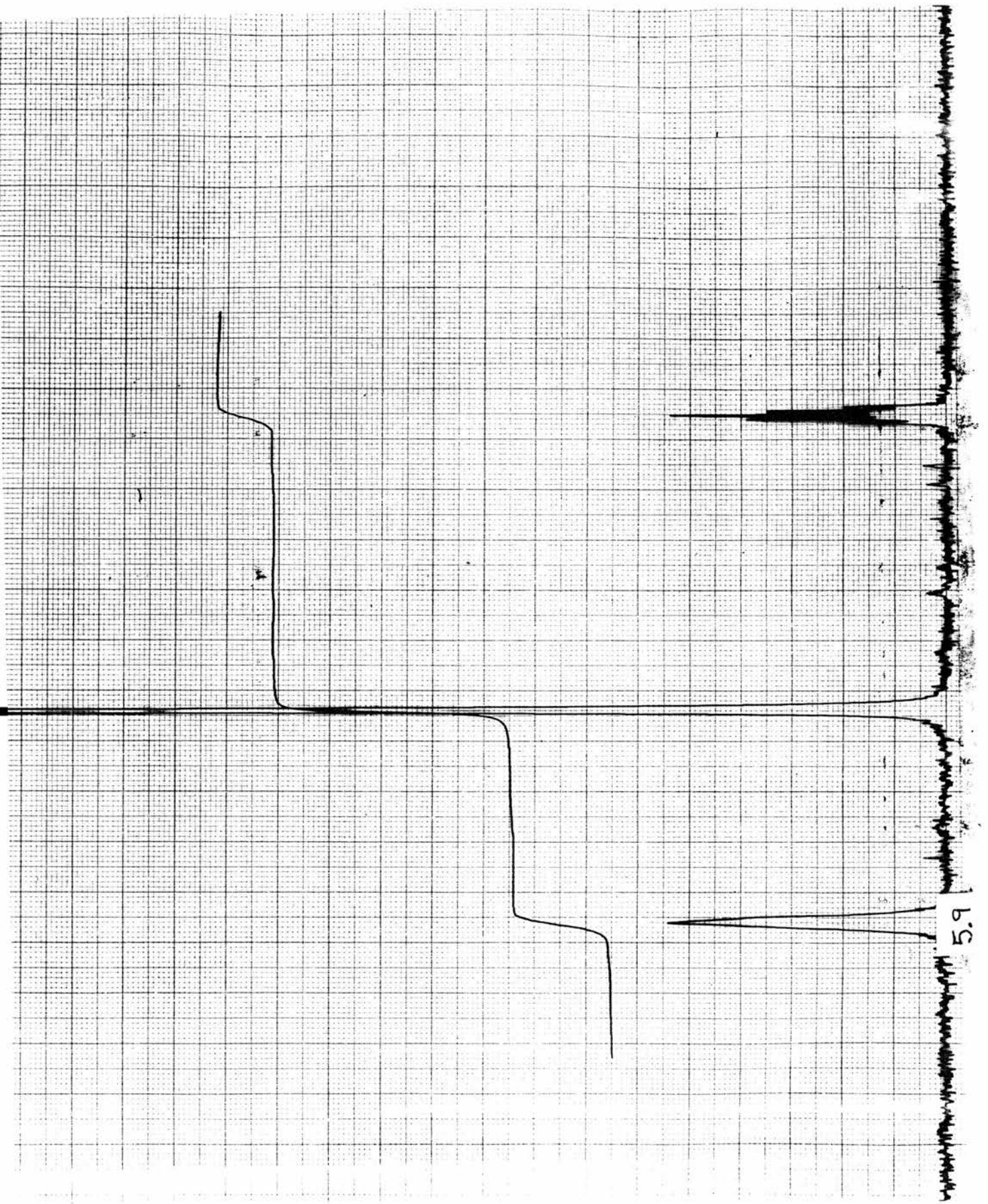

Figure 4.6; ^{1}H NMR of $[Ba(TDFND)_2]$

The peak normally positioned at δ4.8 in these spectra is due to an exchange betwen up to three separate OH groups. These are CD_3OH impurities in the solvent (CD_3OD), water and, in some cases, ethanol. In the [$Ba(TDFND)_2$] complex the ethanol had been totally driven off. This enabled us to estimate the quantity of water present by comparing the relative sizes of the OH and CD_3 peaks in the solvent and product spectra. We were, therefore, able to conclude that there was approximately one mole of water present. Further details of this water determination are provided in Section 4.3.4. The solvent ^1H NMR spectrum is shown in Figure 4.7.

4.2.4.2; ^{19}F NMR

Our main purpose in examining the ^{19}F NMR spectra of these complexes was to see whether the fluorine atoms were involved in either inter or intra molecular bonding. Any such bonding would take the form of agostic* interactions which were mentioned briefly in Section 2.2.3. For the TDFND complexes intermolecular bonding was thought to be less likely to happen due to the increased length of the fluorocarbon chains making such bonds less sterically favourable. Furthermore, the near total removal of hydrogen from the complex leads to the virtual elimination of intermolecular hydrogen bonding and the greater electronegativity of fluorine relative to hydrogen reduces the size of Van der Waal's interactions. However, intramolecular bonds might well be possible with TDFND complexes, thus enabling vacant sites to be filled and helping to explain the increased volatility and

* Agostic is taken from the Greek word αγοστω meaning to clasp or to hold oneself.

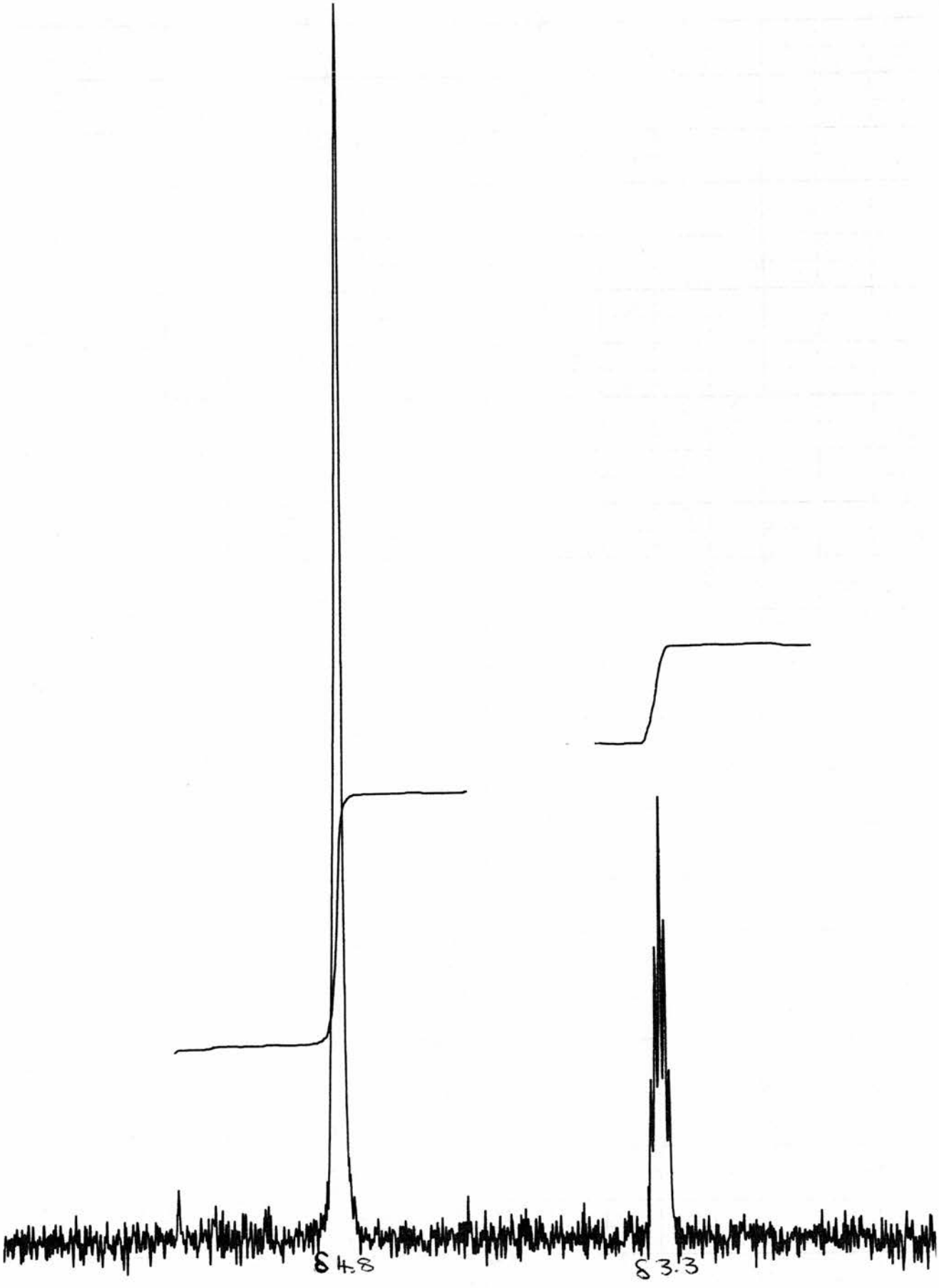

Figure 4.7; The ^{1}H NMR spectrum of CD_3OD

thermal stability of the complexes. Figure 4.8 shows the proposed agostic interaction for [Ba(TDFND)$_2$]. Additional comments upon the affect of the fluoroalkyl chains are made in Section 4.2.4.3.

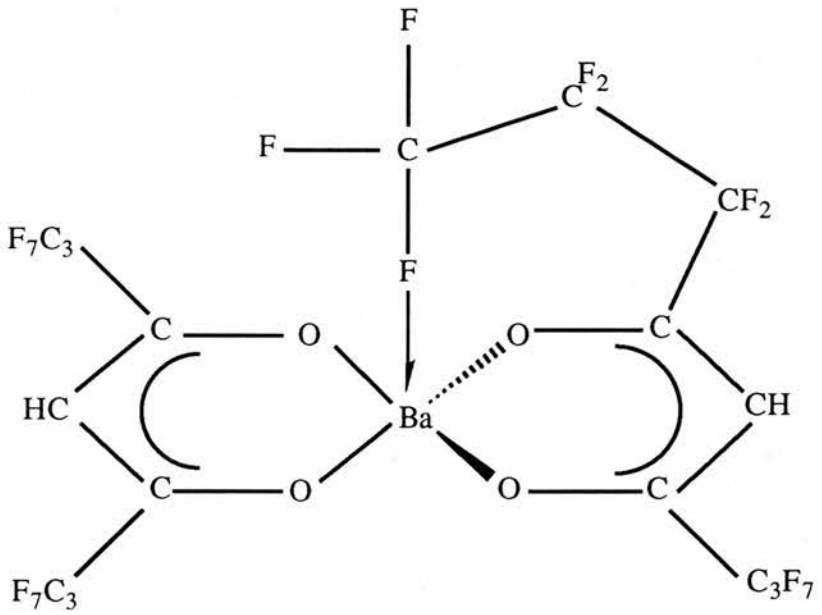

Figure 4.8; Proposed agostic interaction in [Ba(TDFND)$_2$].

The ^{19}F NMR studies of these complexes were limited to the TDFND complexes of barium, strontium and calcium and to [Ca(DFHD)$_2$]. At room temperature there were only three and four peaks for the TDFND and DFHD complexes respectively. To assess whether there were any agostic interactions these complexes were also tested down to 173 K. The series of spectra for all of these complexes are shown in Figures 4.9 to 4.12. The [Ba(TDFND)$_2$] was tested most extensively (at 293 K, 233 K, 203 K, 193K and 173K) whilst the other complexes were tested at 293 K and 193 K. If these interactions were taking place, there would be a substantial effect upon these spectra.

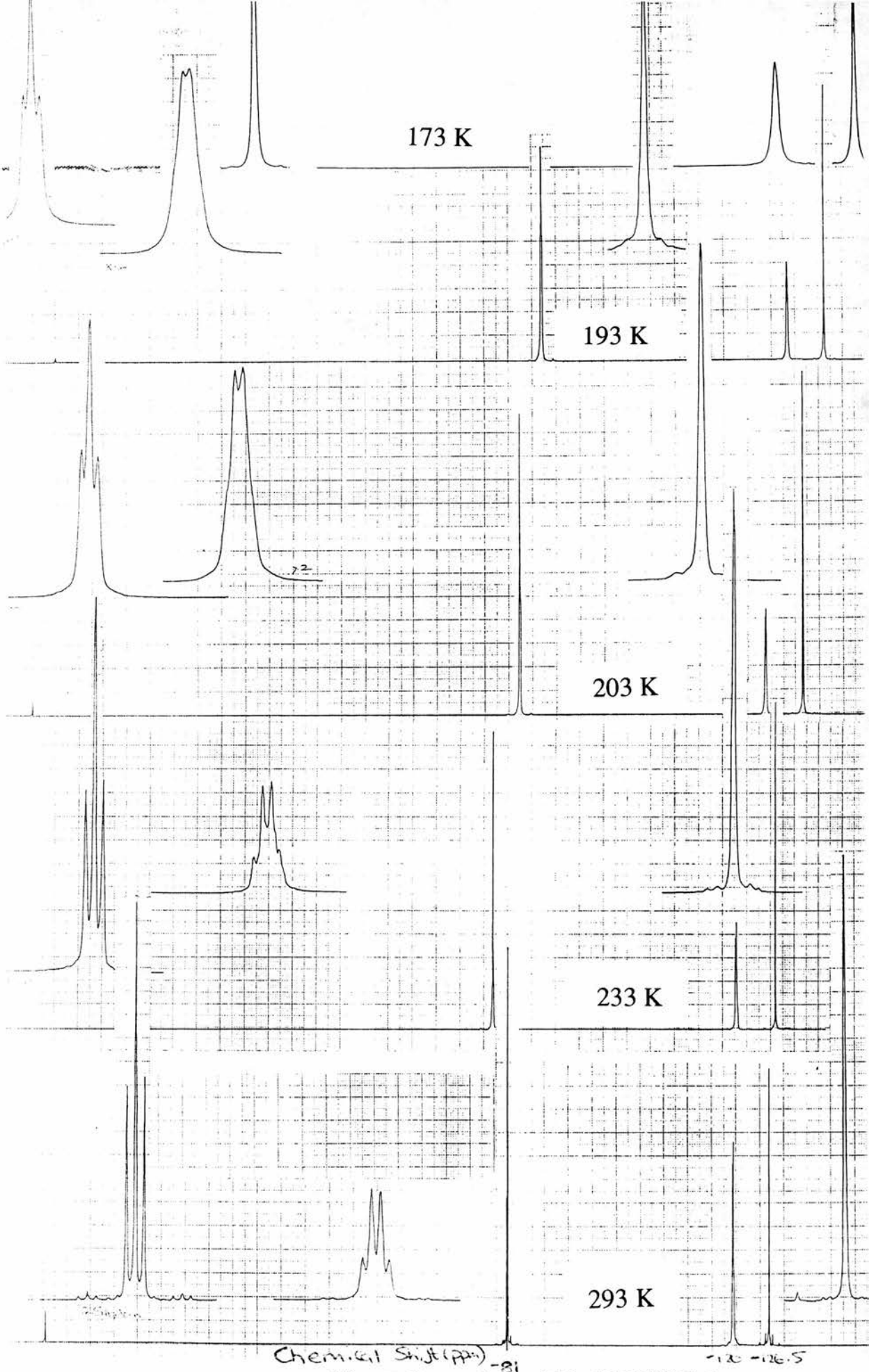

Figure 4.9; Low temperature ^{19}F NMR studies of [Ba(TDFND)$_2$]

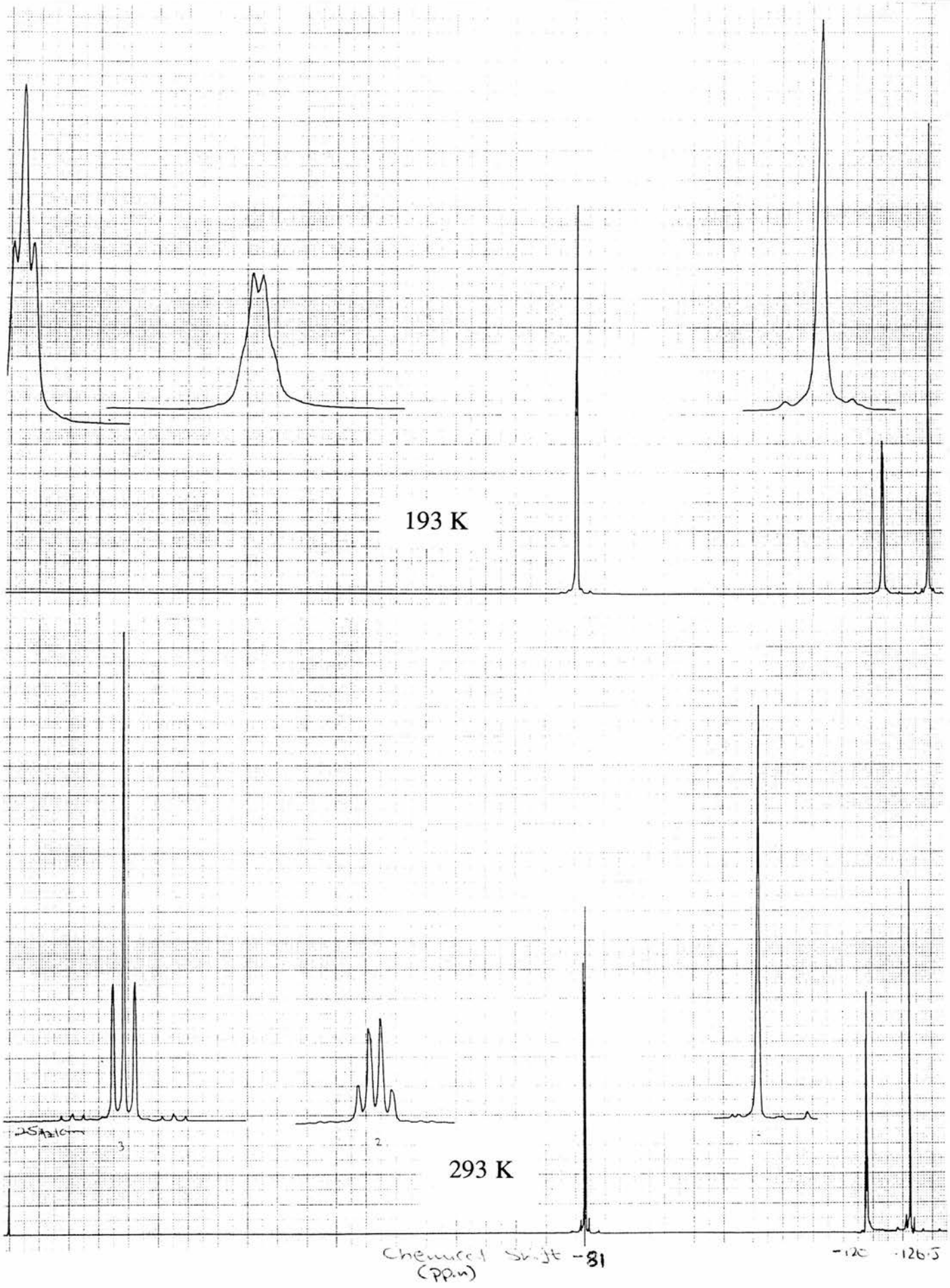

Figure 4.10; Low temperature ^{19}F NMR studies of [Ca(TDFND)$_2$]

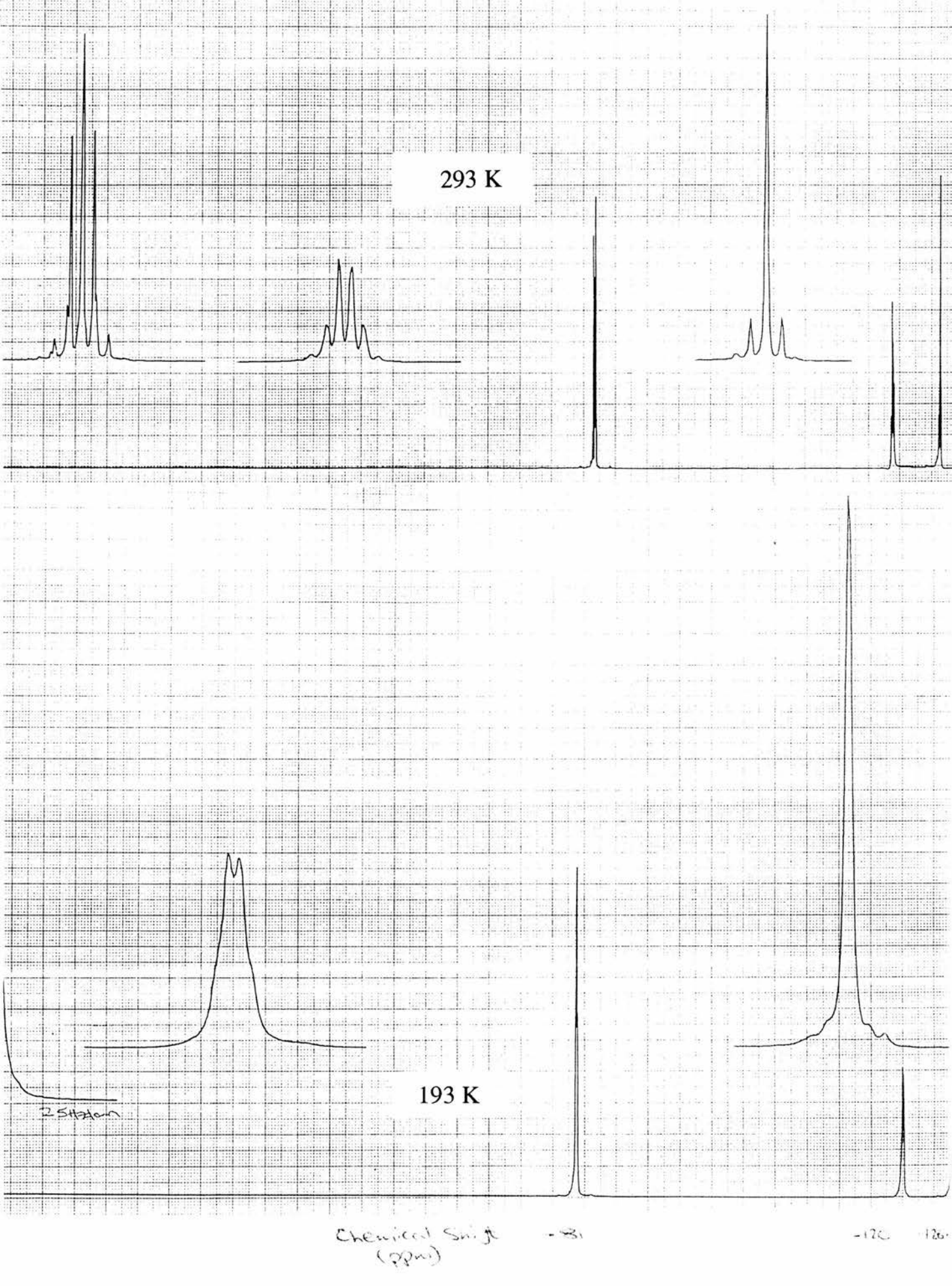

Figure 4.11; Low temperature ^{19}F NMR studies of [Sr(TDFND)$_2$]

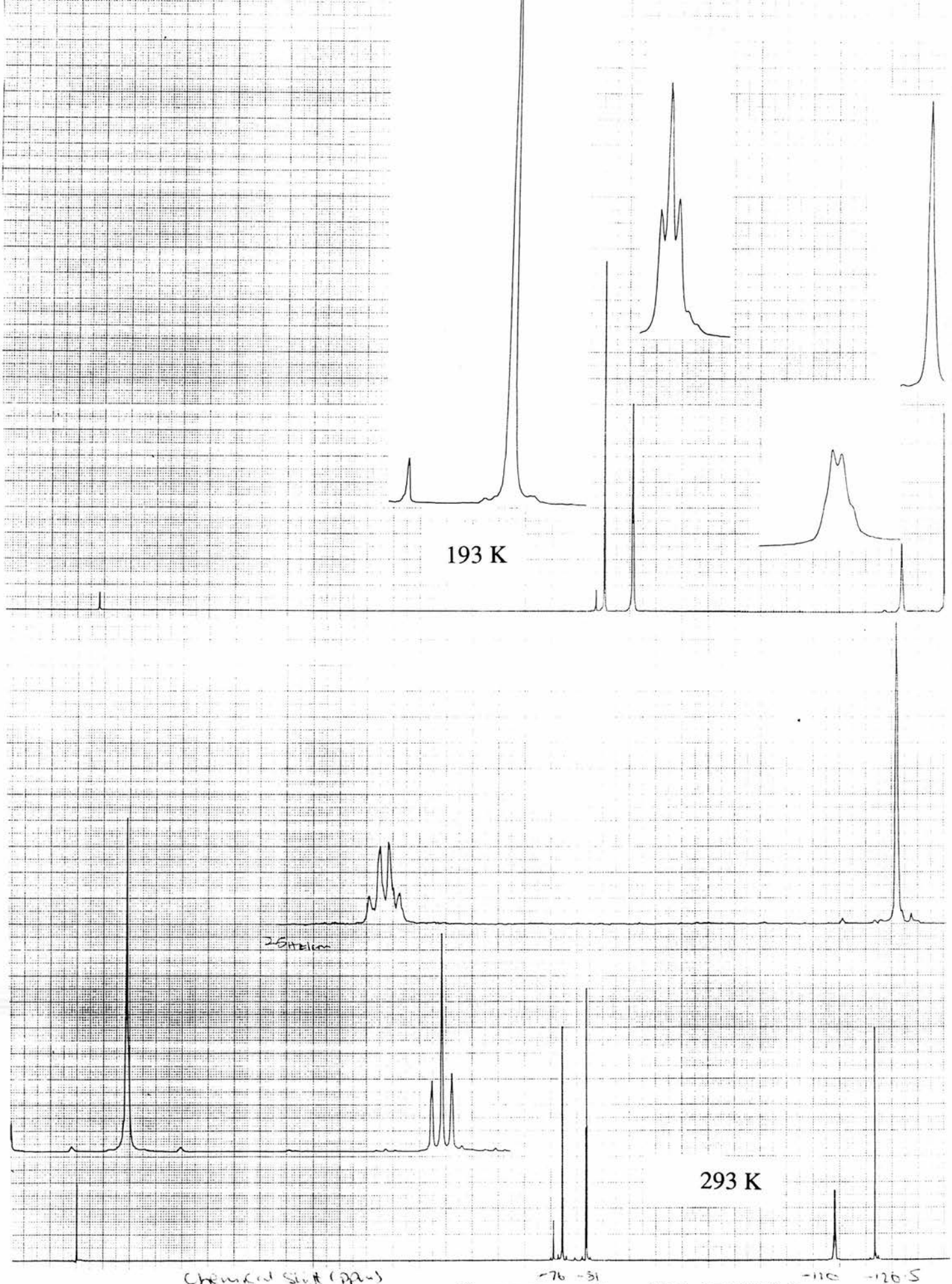

Figure 4.12; Low temperature ^{19}F NMR studies of $[Ca(DFHD)_2]$

Brookhart and Green[66] who first identified the phenomenon of agostic interactions involving hydrogen, stated that they lead to a substantial diminishing of J(^{13}C-H) when compared to non-bridged C-H groups and high field shifts in the ^{1}H and ^{13}C spectra. It is further stated that, whilst agostic interactions are fluxional at room temperature, they are static at reduced temperatures (typically 183 Kelvin). These facts show that the low temperature spectrum of [Ba(TDFND)$_2$] would be certain to show substantial shifts when compared to the room temperature spectrum of [Ba(TDFND)$_2$]. The ethanol adduct of the [Cu(TDFND)$_2$] complex has been shown to be free of agostic interactions (Section 4.2.4.3) and the absence of such shifts in the low temperature spectrum of [Ba(TDFND)$_2$] does, therefore, provide firm evidence of the absence of agostic interactions in this complex. Based upon this evidence it is our view that the volatility of these complexes can be put down purely to steric blocking of coordination sites on the metal reducing the availability of such sites for bridge bonding. Further comments on agostic interactions are provided in the crystal structure and IR sections of this chapter.

Table 4.4 lists the peaks and the assignments of the complexes which were subjected to ^{19}F NMR analysis. It is of interest to note that the chemical shifts of the C_3F_7 groups are identical for all of the complexes which closely matches the observation of the ^{1}H NMRs and indicates that there is a close relationship between the structures of the barium, strontium and calcium complexes. Figures 4.13 and 4.14 show the numbering of the carbon atoms in H(TDFND) and H(DFHD) respectively.

The identification of the two CF_2 groups was aided by reference to published work on the ^{19}F NMR spectra of C_3F_7 chains[67]. An example of this is the ^{19}F NMR spectra of 1-chloro-2-methoxy-

Table 4.4; ^{19}F NMR assignments;

β–DIKETONATE	CHEMICAL SHIFT (PPM)	MULTIPLICITY	ASSIGNMENT
	-81	t	$^{1}CF_3$
[Ba(TDFND)$_2$]	-120	q	$^{3}CF_2$
	-126.5	s	$^{2}CF_2$
	-81	t	$^{1}CF_3$
[Ca(TDFND)$_2$]	-120	q	$^{3}CF_2$
	-126.5	s	$^{2}CF_2$
	-81	t	$^{1}CF_3$
[Sr(TDFND)$_2$]	-120	q	$^{3}CF_2$
	-126.5	s	$^{2}CF_2$
	-76	s	$^{7}CF_3$
[Ca(DFHD)$_2$]	-81	t	$^{1}CF_3$
	-120	q	$^{3}CF_2$
	-126.5	s	$^{2}CF_2$

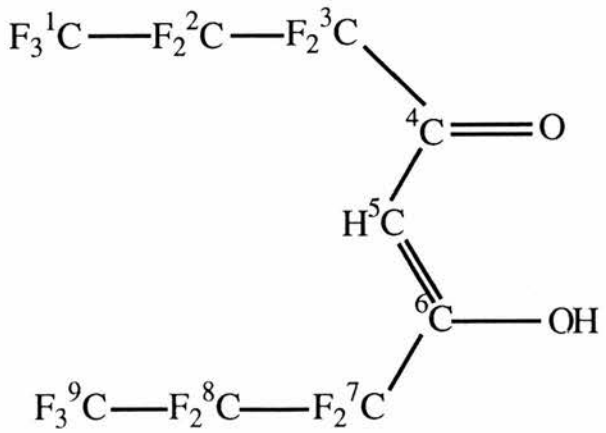

Figure 4.13; H(TDFND) showing numbered carbon atoms

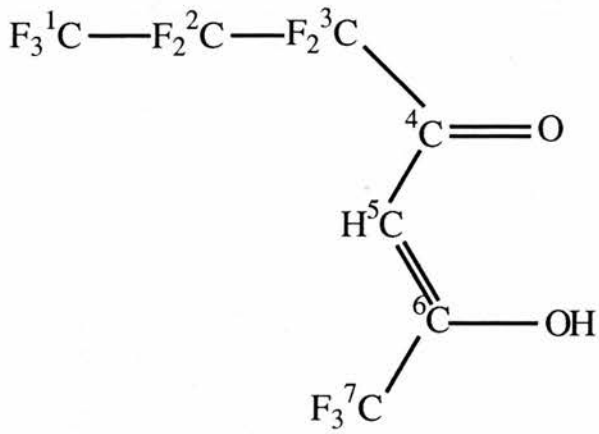

Figure 4.14; H(DFHD) showing numbered carbon atoms

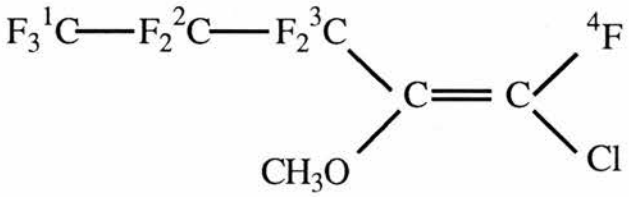

Figure 4.15; 1-chloro-2-methoxyfluoropent-1-ene

fluoropent-1-ene (Figure 4.15) the spectral assignment of which was carried out by Van Hamme and Burton[68]. The chemical shifts for fluorines on Carbons 1, 2 and 3 were -81.3 ppm, -120.0 ppm and -127.5 ppm respectively. There was a $J^4_{F\text{-}F}$ coupling between fluorines on C1 and C3 with a coupling constant of 7.4 Hz. The three bond $J^3_{F\text{-}F}$ couplings between fluorines on C1 and C2 and between those on C2 and C3 was essentially zero. The integrals have similar chemical shifts to those we found in the [Ba(TDFND)$_2$] side chain, although the position of C2 and C3 was reversed. The coupling constant between the fluorines of C1 and C3 was 8.5 Hertz.

4.2.4.3; THE CRYSTAL STRUCTURE OF [Cu(TDFND)$_2$(EtOH)];

The single crystal molecular structure of ethanolbis(1,1,1,2,2,3,3,7,7,8,8,9,9,9-tetradecafluorononanedione)-copper(II), employing a crystal obtained by the recrystallisation of [Cu(TDFND)$_2$] from aqueous ethanol, was determined using a data set produced on an Enraf-Nonius CAD 4 diffractometer by the SERC X-Ray crystallography service. The structural determination was undertaken at the University of Dundee under the direction of Dr John Barnes and John Paton and is descibed in Appendix 4.1.

Two projections of the structure (Figures 4.16 and 4.17) are provided. Figure 4.16 shows the fully labelled structure and clearly identifies the presence of a bound molecule of ethanol approximately perpendicular to the plane of the copper atom and β–diketone ligands. Figure 4.17 provides a good picture of the side chains and demonstrates that they take a staggered formation in order to minimise the fluorine-fluorine interactions. It is also clear from this figure that the side chains are well away from the copper atom thus providing further proof that agostic interactions are absent in this complex.

The presence of the ethanol in this complex is extremely unusual. We have not found any reference to other copper complexes with bound ethanol. It is particularly surprising that preferential binding over water has taken place, as one would have expected that the lesser size of the water molecule would have made its binding more sterically favourable.

Taking a more detailed look at this structure it is clear that the presence of the ethanol bound above the plane causes a distortion of the complex and forces the β–diketone rings below the plane to give

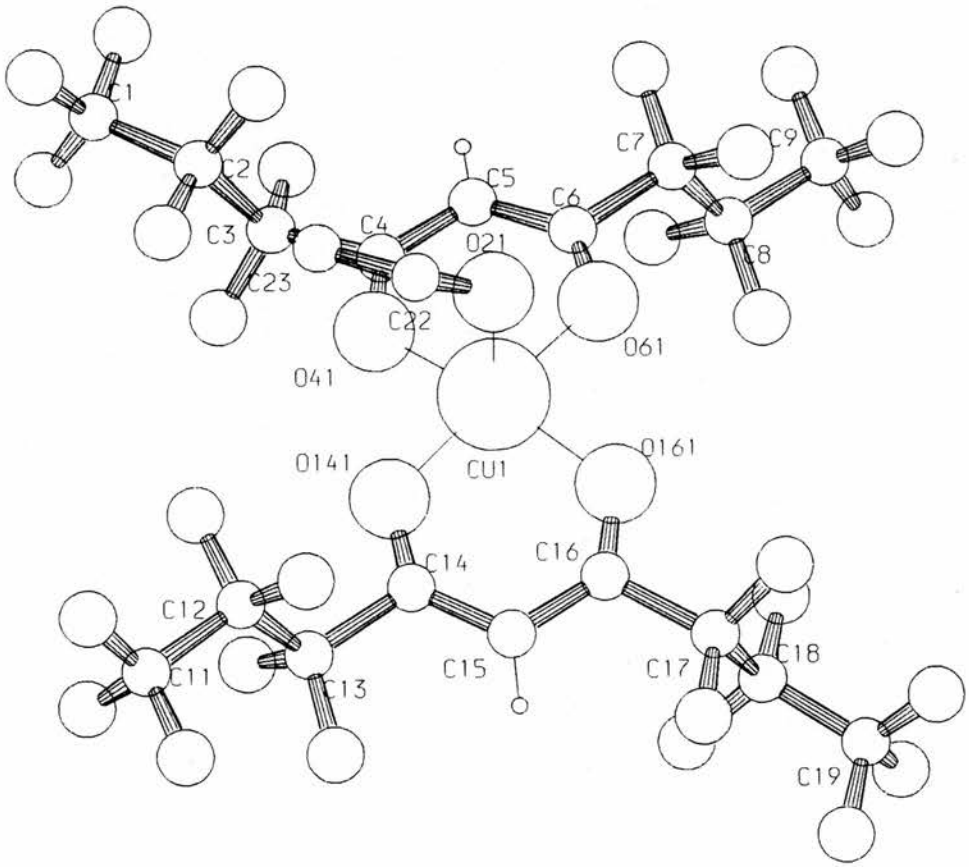

Figure 4.16; The crystal structure of [Cu(TDFND)$_2$(EtOH)] showing the bound ethanol molecule and including full atom labelling

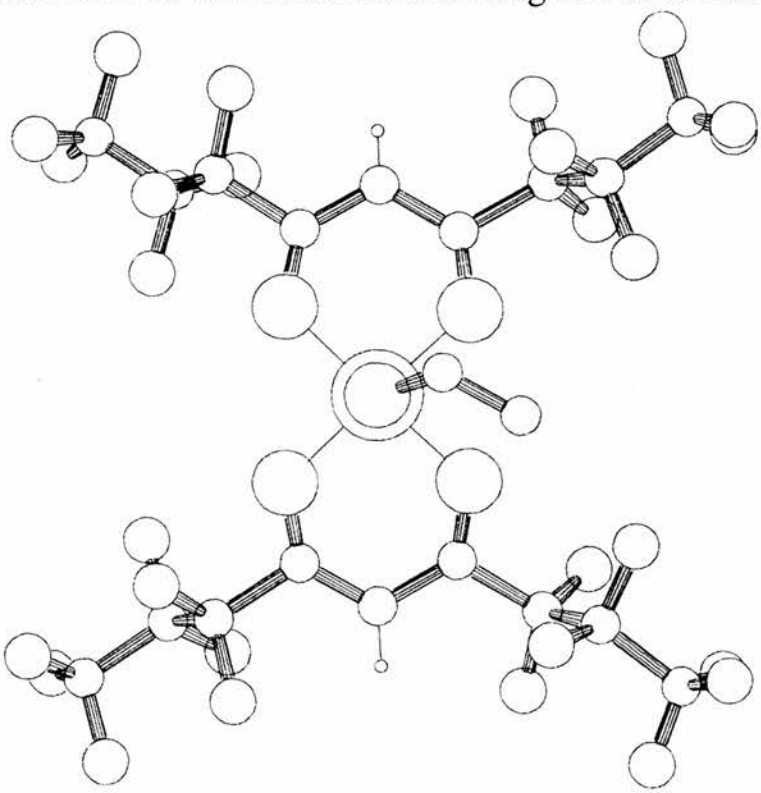

Figure 4.17; The crystal structure of [Cu(TDFND)$_2$(EtOH)] showing the structure of the fluoroalkyl chains

a classical square pyramidal structure. In this way the angle between the two ligands is reduced to below 180°C. This can be ascertained from an examination of the deviations from the plane of the four diketone oxygens. The O61-Cu-O141 and O41-Cu-O161 bond angles are 171.32° and 164.82° respectively. O21, the ethanol oxygen, has angles with the β-diketone oxygens in the range 91.87° to 100.09°. These angles confirm that the copper is above the plane of the β-diketone oxygens and show that there is a slight disortion in the square pyramidal structure. This is probably caused by the ethyl group of the ethanol which Figures 4.16 and 4.17 show to be bent over to one side (bond angles; Cu-O21-Cu22=132.02°, O21-C22-C23=114.55°)

Structures with a regular square-based pyramidal geometry with non-equivalent ligands are known, for example $[Cu(NH_3)_4(H_2O)](SO_4)$[69,70]. In this and related structures the four in-plane distances are of normal length (ca. 2.0 Å for O or N ligands) but the distance to the 5th ligand is 0.2-0.5 Å longer. The Cu(II) ion is also lifted out of the plane of the 4 in-plane ligand atoms by a distance ρ (ρ=0.1-0.5Å) with an inverse correlation to the 5th ligand distance. In $[Cu(NH_3)_4(H_2O)](SO_4)$, Figure 4.18[70], the copper atom is 0.194 Å above the plane and the oxygen is 2.34 Å above the plane whilst the Cu-N bond length is 2.03 Å.

Whilst we have a slightly different situation with the $[Cu(TDFND)_2(EtOH)]$ complex as there are two bidentate ligands, it is, nevertheless, clear that its structure is closely related to those of other copper square-based pyramidal complexes. The bond lengths between the copper atom and the β-diketone oxygens are in the range 1.930 to 1.950 Å whilst the bond length to the ethanol oxygen is increased to 2.212 Å. The copper atom is 0.20 Å above the plane of the four β-diketone oxygens.

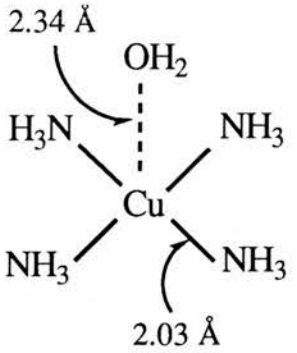

Figure 4.18; Square based pyramidal structure of $[Cu(NH_3)_4(H_2O)](SO_4)$ showing key bond lengths[70]

Another important fact about this structure is the absence of intermolecular interactions, there being no atom from an adjacent molecule within 4 Å of the copper atom. This is no great surprise as one would expect that the added shielding of the ethanol when combined with the steric bulk of the fluoroalkyl side chains would make adjacent molecules very distant. A comparison can be drawn here with $[Cu(ACAC)_2]$ and $[Cu(DPM)_2]$. In both of these cases there is no bound ethanol and the side groups have much less steric bulk, hence the intermolecular distances are much shorter. $[Cu(ACAC)_2]$ has relatively short intermolecular distances, the nearest atom from an adjacent molecule to copper being the methyne carbon at 3.01 Å. The closeness of the molecules to each other is undoubtedly the reason for the high sublimation temperature of this complex. In $[Cu(DPM)_2]$ the closest atom to the copper from an adjacent molecule is one of the tertiary butyl carbons at 3.78 Å whilst the closest ring atom is a carbon at 4.46 Å. Hence, we have progressively larger intermolecular distance as the steric bulk of the side chain is increased.

The structure of the side chains is of great interest as it enables us to obtain a better understanding of the structure of the TDFND complexes of other metals. There are two key features of these side chains which merit further discussion. Firstly, the chains take up a conformation so as to minimise the interaction between fluorines on adjacent carbon atoms. This is achieved by the chain having a staggered alignment and by the fluorines being located along opposite sides of the chain on adjacent carbons. This can clearly be observed in Figure 4.17. It is our belief that the optimum structure of these side chains, with the chains projecting sideways from the C-O bond explains the absence of agostic interactions in the barium complex. For an interaction to take place from carbon 3, the equivalent position of the intermolecular interaction in $[Ba(HFA)_2]$ described by Williams (Figure 2.12), the adjacent molecule would have to take up some of the room occupied by this side chain. It is our contention that alternative positions for this side chain are so sterically unfavourable, due to increased fluorine-fluorine interactions to preclude this possibility.

The second key feature of the side chains is that they are greatly distant from the central atom. In order for the chain to bend towards the central atom, all four fluorine atoms on carbons 2 and 3 would have to be on the same side of the chain. The steric unfavourability of this arrangement explains our observation that there are no intramolecular agostic interactions in $[Ba(TDFND)_2]$.

4.2.4.4; MICROANALYSIS;

The results of the microanalyses of each of the β-diketonates which we prepared are reported overleaf. These results are compared with the anhydrous and hydrated formulae of the β-diketonates as

appropriate.

$[Cu(TDFND)_2]$	Analysis	23.21% C, 0.18 % H
	$C_{18}H_2CuF_{28}O_4$ requires	24.61% C, 0.23 % H
	$C_{18}H_4CuF_{28}O_5$ requires	24.11% C, 0.44 % H
$[Ca(TDFND)_2]$	Analysis	24.37% C, 0.49% H
	$C_{18}H_2CaF_{28}O_4$ requires	25.23% C, 0.23% H
	$C_{18}H_4CaF_{28}O_5$ requires	24.71% C, 0.46% H
$[Sr(TDFND)_2]$	Analysis	22.81% C, 0.39% H
	$C_{18}H_2F_{28}O_4Sr$ requires	23.90% C, 0.22% H
	$C_{18}H_4F_{28}O_5Sr$ requires	23.44% C, 0.43% H
$[Ba(TDFND)_2]$	Analysis	22.17% C, 0.35% H
	$C_{18}H_2BaF_{28}O_4$ requires	22.71% C, 0.21% H
	$C_{18}H_4BaF_{28}O_5$ requires	22.23% C, 0.41% H
$[Y(TDFND)_3]$	Analysis	23.34% C, 0.44% H
	$C_{27}H_3F_{42}O_6Y$ requires	24.73% C, 0.23% H
	$C_{27}H_5F_{42}O_7Y$ requires	24.39% C, 0.37% H
$[Cu(DFHD)_2]$	Analysis	23.78% C, 0.27% H
	$C_{14}H_2CuF_{20}O_4$ requires	25.17% C, 0.30% H
	$C_{14}H_4CuF_{20}O_5$ requires	24.16% C, 0.58% H
$[Ca(DFHD)_2]$	Analysis	24.37% C, 0.28% H
	$C_{14}H_2CaF_{20}O_4$ requires	25.69% C, 0.31% H
	$C_{14}H_4CaF_{20}O_5$ requires	25.00% C, 0.60% H

$[Sr(DFHD)_2]$	Analysis	21.15% C, 0.47% H
	$C_{14}H_2F_{20}O_4Sr$ requires	23.93% C, 0.28% H
	$C_{14}H_4F_{20}O_5Sr$ requires	23.30% C, 0.56% H
$[Ba(DFHD)_2]$	Analysis	21.74% C, 0.47% H
	$C_{14}H_2BaF_{20}O_4$ requires	22.37% C, 0.27% H
	$C_{14}H_4BaF_{20}O_5$ requires	21.85% C, 0.52% H

$[Y(DFHD)_3]$	Analysis	22.78% C, 0.56% H
	$C_{21}H_3F_{30}O_4Y$ requires	25.02% C, 0.30% H
	$C_{21}H_5F_{30}O_5Y$ requires	24.58% C, 0.49% H

Three of the microanalysis results, those for $[Ba(TDFND)_2]$, $[Ca(TDFND)_2]$ and $[Ba(DFHD)_2]$, provide good matches for both carbon and hydrogen to the composition of the monohydrated complex. The microanalyses of $[Sr(TDFND)_2]$, $[Sr(TDFND)_2]$, $[Y(TDFND)_3]$ and $[Y(DFHD)_3]$ provide good matches to the hydrogen content which one would expect for a monohydrated species but the carbon contents are too low. These analyses are of themselves inconclusive and so a close examination of the results of other analytical techniques is required. The $[Cu(TDFND)_2]$, $[Cu(DFHD)_2]$ and $[Ca(DFHD)_2]$ microanalyses are contradictory as the carbon contents are closest to those of the monohydrate whilst the hydrogen contents are closest to those of the anhydrous species. Again it will be necessary to study the results of other analytical techniques before drawing definite conclusions about the hydration of these complexes.

4.2.4.5; MASS SPECTROMETRY;

In order that we might obtain some information on the degree of oligomerisation of these complexes, both in the vapour phase and in the solid state, we used a combination of Electron Impact Mass spectrometry and Fast Atom Bombardment Mass spectrometry. Our work was limited to the $[Cu(TDFND)_2]$, obtained from the β-diketonate preparation, and $[Ba(TDFND)_2]$ complexes since our main interest was in the barium complex. The copper complex was used for comparison as we assumed that, like other β-diketonate complexes of copper(II) including $[Cu(DPM)_2]$, this was a monomeric species (Section 2.3.1).

For the copper complex we undertook only electron impact mass spectrometry. The most important feature of this spectrum was the absence of peaks above the weight of the molecular ion (m/e=877). Other prominent representative peaks were observed at 708 (loss of C_3F_7) and 539 (loss of 2 x C_3F_7). No peaks were observed above m/e 877 hence, this species is probably monomeric in the gas phase.

Electron impact mass spectrometry of $[Ba(TDFND)_2]$ showed evidence of peaks above the molecular ion (951). However, these peaks (at 1284 and 1108) did not contain the barium isotope pattern and therefore do not seem to represent barium containing fragments. The other important peaks in this spectrum are those at 157, 333, 545 and 721 which represent $[BaF]^+$, $[Ba_2F_3]^+$, $[Ba(TDFND)]^+$ and $[Ba_2F_2(TDFND)]^+$ respectively. This leads us to conclude that it is unlikely that this species is monomeric in the gas phase, and to speculate that it is present as a dimer.

The FAB Mass spectrum (Figure 4.19) shows that the species is at least tetrameric in the solid state. This conclusion can be drawn from the peaks and assignments which are listed in Table 4.5. These

Figure 4.19; The FAB mass spectrum of [Ba(TDFND)$_2$]

show that some barium atoms in the solid are linked to at least three other bariums. Given that the crystals of the complex are long, fine needles, it is possible that the structure of this complex resembles that of $[Ba(HFA)_2]$ which was described in Section 2.3.3.1. However, the absence of agostic interactions and the increased volatility of this complex when compared to $[Ba(HFA)_2]$ indicate that there are likely to be fewer and weaker intermolecular interactions, as well as a lower coordination number, for the $[Ba(TDFND)_2]$ complex.

We are fortunate that there are 5 prominent isotopes of barium which give a characteristic pattern and ease the identification of barium containing fragments in the complex. The presence of these isotopes also enables us to identify the actual number of barium atoms in each fragment. It is possible to do this because the isotope pattern changes as the number of barium atoms changes. The reason for this change in the isotope pattern is explained most easily by studying the most dominent isotope, barium 138. The abundance of this isotope in barium is 71.66%. However the chance of having two atoms of this isotope in a Ba_2 fragment is only 71.66% of 71.66% ie. 51.35%. If we calculate the percentage possibilities of all of the isotopes for fragments containing Ba, Ba_2, Ba_3 and Ba_4 we obtain the patterns shown in Figure 4.20. The profile of these patterns can be observed in the FAB mass spectrum (Figure 4.19)

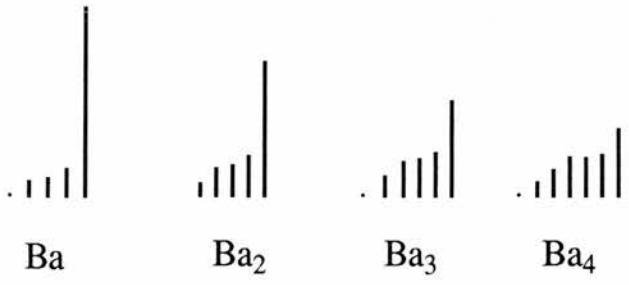

Figure 4.20; Isotope patterns for barium-containing fragments

A key feature of Table 4.5 is the number of complexes containing fluorine. Our co-workers have found in their CVD studies (Chapter 6) that TDFND complexes lay down fluoride films and the ease of formation of barium fluoride is confirmed by the presence of fluorine in these fragments and in certain of the fragments produced in the electron impact mass spectrum.

TABLE 4.5; $[Ba(TDFND)_2]$ FAB MASS SPECTROMETRY: PEAKS AND ASSIGNMENTS;

157 $[BaF]^+$	685 $[Ba_4F_7]^+$	1285 $[Ba_3F_3(TDFND)_2]^+$
333 $[Ba_2F_3]^+$	721 $[Ba_2F_2(TDFND)]^+$	1497 $[Ba_2(TDFND)_3]^+$
509 $[Ba_3F_5]^+$	1034 $[Ba_4F_4(TDFND)]^+$	1673 $[Ba_3F_2(TDFND)_3]^+$
545 $[Ba(TDFND)]^+$	1109 $[Ba_2F(TDFND)_2]^+$	2061 $[Ba_3F(TDFND)_4]^+$

4.2.4.6; DETERMINATION OF MOLECULAR WEIGHT IN SOLUTION;

In order to measure the molecular weight in solution we adopted a technique using a sealed system based upon the migration of solvent between two solutions until their molarity was equivalent. It is necessary to select a solvent with a low boiling point in order to speed the attainment of equilibrium. For this reason the solvent used for the copper complex was diethyl ether and that for the barium complex was methanol. As the molecular weight of the standard in one solution was known it was then possible to calculate the molecular weight of the test sample in the other solution. A full description of the experimental method and a diagram of the apparatus is provided in Section 4.3.1.3.

Using this technique we obtained a molecular weight for the $[Cu(TDFND)_2]$ of 979. When the experimental error is taken into account this is quite close to the expected value of 877 and certainly seems to indicate that the complex is monomeric in solution. This sample was, again, chosen as the control, because we were reasonably confident that it was a monomer.

Having gained this assurance about the reliability of our system, we then tested the barium complex. The molecular weight for this complex was 963.6 which is very close to the molecular weight of the anhydrous monomer, that being 951. We were able to conclude from this experiment that the complex is monomeric in solution in methanol.

The fact that this complex is monomeric in solution seems to contradict the evidence from the mass spectrometry studies. These had shown that the complex was oligomeric in the solid and probably dimeric in the vapour. However, the likely explanation of this fact is that the oligomeric structure is broken down in solution by the

coordination of the solvent (methanol) to the complex.

4.2.4.7; KEY IR BANDS OF THE β–DIKETONATE COMPLEXES;

A summary of the major IR bands for all of the DFHD and TDFND complexes is provided in Table 4.6. The main features in all cases are as follows. There is definite evidence of the products being fluorinated with the large bands in the range 1100-1300cm^{-1} in all cases. The C-O and C-C bands for each ligand are largely independent of the metal whilst there is the expected variation in the M-O bands. There is also a clear indication that all of these species are hydrated.

In order to further support our earlier comments on agostic interactions, it is important to examine the effect of such interactions on IR spectra. A detailed discussion of the effects of these interactions is provided by Brookhart and Green[66]. They explain that for hydrogen agostic interactions, ν(C-H) is found in the 2700-2350cm^{-1} region, which is lower than for normal C-H stretches. This is due to the longer than normal length of the agostic C-H bonds.

It is again beneficial to compare the [Cu(TDFND)$_2$] and the [Ba(TDFND)$_2$] complexes. As we are certain that there are no agostic interactions in the copper complex, if the ν(C-F) are in the same region of the spectrum and the peaks within this region are broadly similar we can conclude that such interactions are absent. Taking the relevant region for copper, the peaks are; 1115(s), 1140(s), 1170(s), 1220(s) and 1260(s) cm^{-1} and for barium; 1100(s), 1125(m), 1170(s), 1205(s), and 1280(m) cm^{-1}. Hence, the close relationship between these groups of peaks and the absence of a shift provide good confirmation of the absence of agostic interactions in the [Ba(TDFND)$_2$] complex.

Table 4.6; The assignments of the major IR bands of the TDFND and DFHD complexes;

COMPLEX	ν(M-O)	ν(C-F)	ν(C-C)	ν(C-O)	H_2O.
$[Ba(TDFND)_2(H_2O)]$	220-575	1100-1280	1515	1640	3250-3650
$[Ca(TDFND)_2(H_2O)]$	220-585	1115-1280	1510	1645	3250-3650
$[Sr(TDFND)_2(H_2O)]$	215-530	1115-1220	1510	1640	3250-3700
$[Cu(TDFND)_2(H_2O)]$*	215-540	1115-1260	1530	1635	3560, 3680
$[Y(TDFND)_3(H_2O)]$	285-585	1115-1200	1520	1635	3050-3550
$[Ba(DFHD)_2(H_2O)]$	290-570	1115-1270	1530-1555	1650	3200-3650
$[Ca(DFHD)_2(H_2O)]$	220-570	1120-1280	1520	1650	3250-3700
$[Sr(DFHD)_2(H_2O)]$	215-570	1115-1275	1520-1530	1655	3300-3700
$[Cu(DFHD)_2(H_2O)]$	200-590	1100-1300	1525-1540	1635	3140-3680
$[Y(DFHD)_3(H_2O)]$	215-570	1120-1270	1520	1640	3250-3750

* Complex prepared during the β-diketone preparation, not the ethanol-containing species.

4.2.4.8; SUBLIMATION TESTING;

All of the complexes were tested for their suitability as CVD precursors using the apparatus shown in Figure 4.21. This consists of an inlet tube, directed at the complex under test, through which flows dry nitrogen. The vessel containing the complex is heated using a Wood's metal bath , which can attain temperatures well in excess of oil baths. A

glass tube links this vessel with the collection vessel. This tube is heated, as required, with a paint-stripper to resublime any product which has deposited on the tube wall. The collection vessel is maintained at a low temperature by its immersion in liquid nitrogen. This vessel is attatched to an active vacuum system which maintains the pressure at, or below, 40 Torr to facilitate sublimation.

Table 4.7 lists the approximate sublimation temperatures for the β–diketonates. The expected order of increasing volatility is seen to hold true, ie. Cu>Y>Ca>Sr>Ba. A further discussion of the relative volatilities of the complexes is provided in Section 4.2.4.10.

Table 4.7; β-diketonate sublimation temperatures at 40 Torr;

β–diketonate	Sublimation Temperature*
$[Ca(TDFND)_2]$	160°C
$[Sr(TDFND)_2]$	165°C
$[Ba(TDFND)_2]$	195°C
$[Cu(TDFND)_2]$	100°C
$[Y(TDFND)_3]$	140°C
$[Ca(DFHD)_2]$	170°C
$[Sr(DFHD)_2]$	195°C
$[Ba(DFHD)_2]$	240°C
$[Cu(DFHD)_2]$	80°C
$[Y(DFHD)_2]$	165°C

* The temperatures given are those of the Wood's Metal bath, hence the actual sublimation temperatures are below these figures.

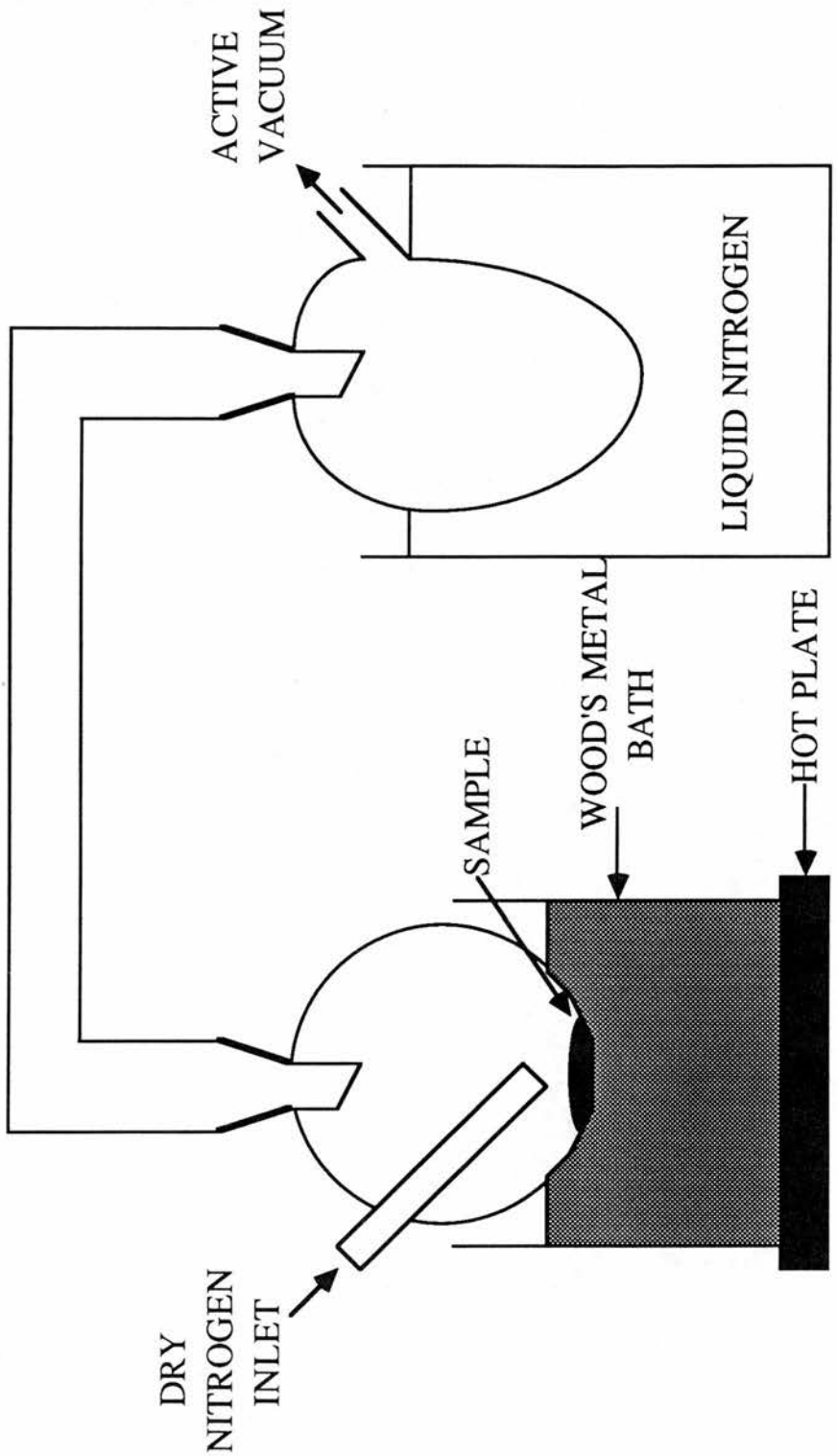

Figure 4.21; Apparatus used for sublimation testing

4.2.4.9; SIMULTANEOUS THERMAL ANALYSIS:

The STA traces for all of the complexes are provided in the appendix to this chapter. A discussion and assignment of the individual traces is now provided. It should be noted that the heating rate was usually 20 °C min^{-1}.

4.2.4.9.1; $[Ba(DPM)_2]$;

The STA of this complex is discussed in Section 3.3.2.4.

4..2.4.9.2; $[Ba(HFOD)_2]$;

This STA shows a considerable improvement when compared with that of $[Ba(DPM)_2]$. There is evidence of enhanced volatilisation, less decomposition and a far lower percentage of residue after analysis. However, it would appear that this precursor still has inadequacies not the least of these being the residue left after heating is complete.

The trough at 40°C is not accompanied by any weight loss. We would, therefore, conclude that this represents the melting points of an impurity in the product. The trough at 80°C coupled with a gradual, if small, loss of weight is likely to represent the loss of water. This water loss is much less than one mole, so the complex is likely still to be partially hydrated. A sharp peak at 180°C, without any weight loss, represents the sample melt. The onset of volatility is at 250°C and is indicated by a trough in the DTA and a 40% weight loss. A peak in the DTA and a sharp reduction in the rate of weight loss at 310°C seems to show that some decomposition is occuring. This is followed by a further rapid weight loss and a DTA trough at 330°C which may be further

volatilisation or a combination of volatilisation and decomposition. The residue is 10% which is much lower than the 21% and 24.1% residues which would result from total conversion to barium oxide and barium fluoride respectively. We are able to conclude that the minimum volatility probably exceeded 60% of the sample. Further thermal investigations of this complex are discussed in Chapter 6.

4.2.4.9.3; $[Ba(DFHD)_2]$;

The STA of $[Ba(DFHD)_2]$ shows a further improvement when compared to that of the $[Ba(HFOD)_2]$. There is a slight increase in the percentage volatilisation and an increase in the decomposition temperature.

The first trough in the DTA comes at 115°C and is accompanied by a weight loss of around 2% which is due to the loss of water. This represents the loss of slightly less than one water molecule for each barium centre. The next trough, at 205°C, has no loss of weight associated with it and is clearly the melting point of the complex. The trough at 295°C is accompanied by a near 90% weight loss and can be attributed to the volatilisation of the complex. The peak at 340°C is the onset of decomposition. This is followed by a long tail which shows steady decomposition of the residue. The two troughs at 830°C and 920°C are possibly due to residue melting points. The final residue, 8.48%, is less than that which we would expect for barium oxide, approximately 20.4%, or barium fluoride, 23.3%. As this is a highly fluorinated species, conversion to the fluoride is more likely. Hence, we are able to conclude that there has been a minimum of 65% volatilisation of the complex.

4.2.4.9.4; [$Ba(TDFND)_2$];

This analysis showed no decomposition at all and is clearly the most thermally stable barium β–diketonate so far prepared.

The initial trough in the DTA, at 80°C, marks the onset of a gradual weight loss of around 2% which is likely to represent the loss of water from the complex. The melt is at 187°C, a large trough being accompanied by a negligable weight loss. The final trough, at 295°C, represents sample volatilisation. There is no peak above this temperature and the weight loss at this point is almost 100%. With no apparent residue remaining we can conclude that total volatilisation has taken place.

In an attempt to obtain a better understanding of the effects of heating and subsequent water loss in the complex, a further sample was pre-heated at 180°C for an hour in the analyser. The STA of this sample was then taken. When compared with the sample which had not had this pre-heating, several changes were evident. The first of these was the absence of the 80°C trough and the accompanying weight loss. This provides confirmation that the sample has been dehydrated. The second difference is that the sublimation temperature is approximately 10% higher in the pre-heated sample. Finally, there has been an increase in the sample residue from 0 to 10%.

In order to confirm that [$Ba(TDFND)_2$] could be dehydrated successfully, we undertook a controlled dehydration by heating the complex at 100°C under active vacuum for 1 hour. This sample was then sublimed in the normal way and stored under dry nitrogen. The microanalysis (result of analysis shown overleaf) was then taken and found to be very close to the calculated stoichiometry for the anhydrous complex.

Found C 22.62%, H 0.13%

$C_{18}H_2BaF_{28}O_4$ requires C 22.71%, H 0.21%

Taking these factors together we have a clear indication that the sample dehydrates on heating to produce a species which is less volatile and less thermally stable than the hydrated sample. Further thermal investigations of this complex are discussed in Chapter 6.

4.2.4.9.5; $[Ca(DFHD)_2]$;

This complex was seen to volatilise at both a lower temperature and with less decomposition than the barium derivative. This can be attributed to the smaller size and lower atomic weight of calcium, reducing both the opportunities for oligomerisation and the energy required to volatilise the sample.

The change in slope of the DTA in the region 110-130°C is accompanied by an initial weight loss of 2-3%. It is possible that this represents the loss of water from the complex. There is no obvious melting of the sample, the next event being volatilisation at around 255°C. There is a small DTA trough at this temperature which coincides with a major increase in the rate of sublimation. The steep fall in weight loss just above this temperature and the associated DTA peak shows that decomposition is taking place. The sample residue is 3%. If the residue was entirely calcium oxide we would expect a residue of 8.6% whilst calcium fluoride would leave a 12% residue. As this is a highly fluorinated species, conversion to the fluoride is more likely. Hence, we have seen at least a 75% volatilisation of the sample.

4.2.4.9.6; [$Ca(TDFND)_2$];

The first DTA trough in this analysis is around 90°C and is likely to represent the sample melt. There is then a weight loss of approximately 1.5% close to 100°C which represents the loss of just less than one mole of water. The main weight loss is between 220 and 270°C and is accompanied by a trough in the DTA. This is clearly sample volatilisation. The residue is 0% so we can assume that total volatilisation with no decomposition has taken place.

4.2.4.9.7; [$Sr(DFHD)_2$];

This complex has, as would be expected, intermediate volatility between the calcium and barium complexes.

The large trough in the DTA with a minimum at 75°C and which extends to above 100°C and the corresponding weight loss of 5.2% is most likely to be the loss of solvent ethanol and of water from the complex. The small DTA trough at 160°C may be the melting point of the sample. Volatilisation is evident by the DTA trough at 264°C and the associated large weight loss. However, the rate of weight loss seems to vary markedly around this temperature, so it is possible that some decomposition is also taking place. Above 280°C the DTA peak is clearly indicative of decomposition. The sample residue of 3.9% is well below that expected for strontium oxide (14.8%) or strontium fluoride (17.9%). Again, the fluoride is the more likely deposition product so we are able to assume that at least 80% volatilisation has occurred.

4.2.4.9.8; [$Sr(TDFND)_2$];

The melt temperature of this sample is around 90°C and is quickly followed by the loss of water. The weight loss at this temperature is approximately 2% which corresponds to the loss of one mole of water. There is a further trough in the DTA which reaches a minimum at 230°C. This is accompanied by a near total weight loss to leave a residue of 2.5%. Due to the highly fluorinated nature of this complex we would expect this residue to be barium fluoride. As total conversion to barium fluoride would leave a residue of 13.9% we are able to conclude that the minimum volatilisation was 82%.

4.2.4.9.9; [$Cu(DFHD)_2$];

The trough in the DTA at around 60°C could represent the sample melt. There is a gradual decrease in weight from this temperature which could be attributed both to the onset of volatilisation and to the loss of water. Volatilisation is complete at 160°C to leave a sample residue of around 2%. Total conversion to copper oxide would leave a residue of 11.1% whilst copper fluoride would cause a 14.1% residue. The degree of volatilisation is therefore likely to be around 85%.

4.2.4.9.10; [$Cu(TDFND)_2$];

The STA of this complex shows that the copper derivative is by far the most volatile TDFND complex which we have investigated. The DTA trough at 65°C is the sample melt temperature. There is also a small weight loss at and below this temperature. This is most likely to

be a trace of petroleum residue which has been retained from the ligand preparation. There is no evidence of water loss in the analysis. The next trough, which has a minimum at 185°C is the sublimation temperature and the peak which follows at 190°C is the sample decomposition. The final residue is 2.2% which is well below that for total conversion to the fluoride (11.6%) or oxide (9.1%). If, as we expect, the fluoride is produced the minimum volatilisation will be 81%.

4.2.4.9.11; [$Y(DFHD)_3$];

The trough in the DTA at 70°C is likely to be the sample melt. There is a second trough with a minimum at 140°C which is accompanied by a gradual weight loss from the sample. This probably indicates the loss of water from the complex. The apparent peak at 170°C may just be a return to the baseline after the trough at 140°C and prior to the subsequent troughs. Above this temperature there are further dips in the DTA accompanied by a substantial loss in weight to leave a residue of 2.5%. Yttrium oxide would leave a residue of 22.4% whilst yttrium fluoride would leave a residue of 23.3%. Hence, there has been a sample volatilisation of around 90%.

4.2.4.9.12; [$Y(TDFND)_3$];

The STA of this complex shows that the complex sublimed in the range 170-230°C to leave essentially no residue . Other key features of the spectrum are the apparent absence of both a melting point, although the small trough at 70°C may be a melt, and of any exotherms below the sublimation temperature. The gradual reduction of the weight

loss curve commencing at 95°C may represent the loss of some water from the sample or the onset of volatilisation.

4.2.4.10; CONCLUSIONS FROM STA ANALYSIS;

If we consider first of all the volatility of these complexes, we can see that in certain cases the TDFND derivatives are by far the most volatile whilst in others the DFHD complex is at least as volatile as the TDFND. In order to explain this we must look at the individual elements and consider the relative importance of the various factors which influence volatility.

We have already reported that $[Cu(DPM)_2]$ and $[Cu(HFA)_2]$ have adequate volatility as CVD precursors. They are both monomeric species and, thus, increasing the steric crowding will not bring about a great improvement in the volatility of copper precursors. The reverse appears to be the case as $[Cu(TDFND)_2]$ is less volatile than both $[Cu(HFA)_2]$ and $[Cu(DFHD)_2]$. This is because the increase in molecular weight of the TDFND ligand is the dominant factor over reduced intermolecular interactions.

In the case of the yttrium complexes the metal is trivalent, so the presence of three ligands reduces the opportunities for intermolecular interactions. Furthermore, the increase in the molecular weight of the $[Y(TDFND)_3]$ complex relative to the $[Y(DFHD)_3]$ complex is much higher than in a divalent species, which reduces the volatility enhancement obtained from reduced intermolecular interactions. As a consequence the $[Y(TDFND)_3]$ complex is only slightly more volatile than the $[Y(DFHD)_3]$ complex.

For the strontium and calcium complexes something of a compromise situation exists. Both of these metals require an element of

steric crowding to prevent the formation of oligomeric complexes. As calcium is the smaller central atom, intermolecular interactions are less favoured than for strontium. Hence, there is less of an advantage in the calcium complex containing a bulky ligand and the result is that the volatilities of the DFHD and TDFND complexes are almost identical. For the strontium complex the steric bulk of TDFND does help complex volatility and results in incresed volatility relative to the DFHD complex.

Taking the case of the barium complexes, the extreme tendency to oligomerise means that the very large fluoroalkyl groups of TDFND are required. Hence, the increased molecular weight of the TDFND ligand relative to the DFHD ligand is more than compensated for by the reduced oligomerisation. This explains why the TDFND is the more volatile complex.

4.2.4.11; Probable molecular formulae of the DFHD and TDFND complexes;

4.2.4.11.1; $[Ba(TDFND)_2]$ and $[Ba(DFHD)_2]$;

We have clear evidence from STA, IR, micoanalysis and, for $[Ba(TDFND)_2]$, ^1H NMR that both of these complexes contain one molecule of bound water per barium centre. It is also certain that the $[Ba(TDFND)_2]$ complex dehydrates on heating to produce a less volatile, anhydrous species. We will discuss this dehydration further in Chapter 6 where the testing of $[Ba(TDFND)_2]$ on the CVD rig is described.

4.2.4.11.2; [Ca(TDFND)$_2$], [Ca(DFHD)$_2$], [Sr(TDFND)$_2$], [Sr(DFHD)$_2$], [Y(DFHD)$_3$] and [Y(TDFND)$_3$];

All the analyses which we undertook for [Ca(TDFND)$_2$] and indicate that there is one mole of bound water per calcium centre in the complex. However, [Ca(DFHD)$_2$], [Sr(TDFND)$_2$], [Sr(DFHD)$_2$] and [Y(DFHD)$_3$] have inconclusive microanalyses but both the STA and the IR in all of these cases point to the existence of a mole of bound water per metal centre. The IR for [Y(TDFND)$_3$] indicates that the complex is hydrated and the micro analysis has a high hydrogen content, probably confirming the presence of water in the complex. It is not possible to say with certainty whether the STA shows any water loss. On the basis of the IR and microanalysis we believe that [Y(TDFND)$_3$] contains one molecule of bound water per yttrium centre.

4.2.4.11.9; [Cu(DFHD)$_2$] and [Cu(TDFND)$_2$];

We have fully identified the crystal structure of this complex (Section 4.2.4.3) as being [Cu(TDFND)$_2$(EtOH)]. The crystal used was, however, obtained by the recrystallisation of the sample from aqueous ethanol. The samples of both [Cu(DFHD)$_2$] and [Cu(TDFND)$_2$] on which we did our analyses had not been so recrystallised and had not, therefore, been exposed to any ethanol. Hence, it is not possible in either case that bound ethanol is present, although it is possible that the complexes do contain bound water.

Both of these complexes show some evidence of water from their IR and STA analyses. Unfortunately, the microanalyses contradict this evidence and indicate that the complex is dehydrated. Whilst we are unable to draw definite conclusions about the state of hydration of these

complexes, the ability for $[Cu(TDFND)_2]$ to bind ethanol has been shown from the crystal structure and proves that neutral ligands can bind to this complex.

4.3; EXPERIMENTAL:

4.3.1; H(DFHD);

Sodium methoxide (7.8 g, 0.145 mol) was suspended in dry petroleum (boiling range 40-60°C). Ethylheptafluorobutyrate (32.3 g, 0.133 mol) was added over 30 minutes with vigorous stirring. After stirring for a further 30 minutes, trifluoroacetone (17.2g, 0.153 mol) was added over 1 hour. The resulting colourless solution was then stirred at room temperature for 24 hours. To this solution was added sulphuric acid ($50cm^3$, 6 mol dm^{-3}). The phases were separated and the aqueous layer extracted with petroleum (2 x 20 cm^3). The organic phases were combined and extracted with aqueous sodium ethanoate (60 cm^3, 260 gdm^{-3}) This aqueous phase was then added to an aqueous solution of $CuSO_4.5H_2O$ (12.6 g in 75 cm^3) and the resulting green precipitate was removed by filtration. This complex was washed twice with water (25 cm^3) to give bis(1,1,1,2,2,3,3,7,7,7-decafluoro-4,6-heptanedionato) copper(II).

The free ligand was obtained from the crude copper complex after washing with water and drying in vacuo. The solid was cooled in an ice bath and cold, concentrated sulphuric acid was added (3x 5 cm^3). The brown liquid was removed and distilled, the colourless product having a boiling range 100-104°C. Yield 12.3g, 29%.

4.3.2; H(TDFND);

The experimental technique, reagents and quantities were identical to those used for the H(DFHD) synthesis excepting that the ketone used in this case was heptafluoropropylmethylketone (32.4 g, 0.153 mol). The boiling range was 134-135°C and the yield (8.7 g, 31.8%).

4.3.3; [$Ba(DFHD)_2$];

A solution of H(DFHD) (3.08 g, 0.01 mol) in aqueous ethanol (30 cm^3, 1/1) was treated with NaOH (0.4 g, 0.01 mol) in aqueous ethanol (20 cm^3, 1/1). The resulting solution was added slowly to a stirred solution of barium (II) bromide dihydrate (1.67 g, 0.005 mol) in aqueous ethanol (50cm^3, 1/1). After stirring for one hour the ethanol was removed in vacuo. Water, (50 cm^3) was added and the solution evaporated in vacuo until a white precipitate formed. This was collected and dried in vacuo to give the product as a white powder.

IR; 290(w), 330(w), 355(w), 455(m), 525(m), 530(m), 570(s), 620(m), 665(m), 745(m), 775(m), 790(m), 900(m), 950(m), 1065(s), 1115(s), 1130(s), 1150(s), 1210(s, br), 1270(s), 1300(s), 1350(s), 1490(s), 1530(s), 1540(s), 1555(m), 1585(w), 1650(s), 3200-3650(m) cm^{-1}.

4.3.4; [$Ba(TDFND)_2$];

The same experimental method was used to prepare this complex from H(TDFND) (4.08 g, 0.01 mol).Yield 3.6 g, 75.7%.

On standing, the solution from the final filtration produced

colourless needles up to 2 cm in length, usually growing on the surface. These were identified as a further crop of the product by IR and ^1H NMR spectroscopy.

IR; 220(w), 240(w), 290(w), 330(w), 350(w), 370(w), 440(m), 510(m), 520(m), 575(w), 620(m), 660(w), 735(m), 740(m), 780(m), 860(m), 870(m), 910(m), 930(m), 950(m), 1045(w), 1065(w), 100(s), 1125(m), 1170(s), 1205(s), 1280(m), 1480(s), 1515(s), 1640(s), 3250-3650(w) cm^{-1}.

As we described earlier in this chapter we were able to calculate the amount of water in the complex by comparing the relative sizes of the δ3.3 and the δ4.8 peaks in the solvent spectrum and the product spectrum. For the solvent the ratio of the δ3.3 to the δ4.8 peak in the sample of D_4-methanol which we used was 1:2.56. By measuring the integrals for the barium complex and comparing them with those given for the solvent, we were able to conclude that approximately one mole of water was present. The data and calculations were as follows;

Integrals			Surplus of H in δ4.8 peak	water content
δ3.3	δ4.8	δ5.9		
10	46	19	20	1.05 moles

4.3.5; $[Sr(DFHD)_2]$;

This complex was similarly prepared from strontium (II) chloride dihydrate (1.33 g, 0.005 mol).

IR; 215(w), 295(w), 450(w), 525(w), 535(w), 570(m), 620(w), 670(w), 750(m), 780(w), 795(m), 900(m), 925(w), 955(m), 1085(m), 1115(s), 1145(s), 1205(s), 1225(s), 1275(m), 1305(s), 1350(m), 1490(s), 1520(s), 1530(s), 1655(s), 3300-3700(w) cm^{-1}.

4.3.6; $[Sr(TDFND)_2]$;

This complex was similarly prepared from strontium (II) chloride dihydrate (1.33 g, 0.005 mol).

IR; 215(w), 280(w), 290(w), 375(w), 455(m), 530(m), 630(m), 670(w), 745(m), 785(m), 850(w), 870(m), 920(m), 940(m), 960(m), 1060(m), 1115(s), 1140(s), 1175(s), 1220(s), 1350(s), 1510(s), 1640(s), 3250-3700(m) cm^{-1}.

4.3.7; $[Ca(DFHD)_2]$;

This complex was similarly prepared from calcium (II) chloride dihydrate (1.1 g, 0.005 mol).

IR; 220(w), 240(w), 295(w), 370(w), 390(w), 460(w), 530(m), 570(m), 630(w), 670(w), 745(m), 780(w), 800(w), 900(m), 930(w), 955(m), 1065(m), 1095(m), 1120(s), 1140(s), 1225(s), 1280(w), 1305(s), 1520(m), 1540(m), 1650(m), 3250-3700(w) cm^{-1}.

4.3.8; [$Ca(TDFND)_2$];

This complex was similarly prepared from calcium (II) chloride dihydrate (1.1 g, 0.005 mol).

IR; 220(w), 240(w), 260(w), 270(w), 290(w), 320(w), 330(w), 455(m), 530(m), 585(m), 625(m), 670(w), 740(m), 785(m), 875(m), 920(m), 945(m), 965(m), 1055(m), 1115(s), 1140(m), 1180(s), 1220(s), 1280(m), 1345(s), 1510(m), 1645(m), 3200-3650(w) cm^{-1}.

4.3.9; [$Cu(DFHD)_2$];

The sample was obtained during the purification of the H(DFHD). It was washed thoroughly with water then dried in vacuo prior to use.

IR; 200(m), 270(m), 290(w), 305(w), 325(w), 340(w), 405(w), 425(w), 495(w), 530(m), 545(m), 590(m), 630(m), 680(w), 745(m), 785(m), 805(m), 875(w), 905(s), 930(m), 960(s), 1040(m), 1070(s), 1100-1300(s), 1320(s), 1350(s), 1460(s), 1525(s), 1540(s), 1555(s), 1635(s), 3140(w), 3560(m), 3680(m) cm^{-1}.

4.3.10; [$Cu(TDFND)_2$];

The sample was obtained during the purification of the H(TDFND). It was washed thoroughly with water then dried in vacuo prior to use.

IR; 215(m), 240(w), 270(w), 290(m), 340(w), 430(w), 495(m), 525(m), 540(m), 640(m), 680(m), 745(m), 755(m), 770(w), 795(s), 870(m),

885(w), 925(s), 945(m), 960(m), 1070(m), 1115(s), 1140(s), 1170(s), 1220(s), 1260(s), 1340(s), 1510(m), 1530(s), 1535(s), 1595(m), 1610(m), 1635(s), 3560(m), 3680(m) cm^{-1}.

4.3.11; $[Y(DFHD)_3]$;

The same technique was used for this preparation excepting that 3:1 molar equivalents of β−diketone and base to metal salt were employed. The quantities used were; yttrium (III) nitrate pentahydrate (1.83 g, 0.005 mol), sodium hydroxide (0.60 g, 0.015 mol) and H(DFHD) (4.62 g, 0.015 mol).

IR; 215(m), 235(m), 255(w), 270(w), 295(w), 315(w), 340(w), 360(w), 390(w), 465(w), 525(m), 570(m), 620(w), 660(w), 740(m), 780(w), 795(m), 895(m), 925(w), 960(m), 1065(m), 1095(m), 1120(m), 1150(s), 1175(m), 1200(s), 1225(s), 1270(m), 1310(s), 1520(m), 1640(s), 3250-3750(w) cm^{-1}.

4.3.12; $[Y(TDFND)_3]$;

The same ratios of reagent were used as for the DFHD complex, but smaller quantities of reagents were used based upon yttrium (III) nitrate pentahydrate (1.22 g, 0.033 mol,).

IR; 285(m), 330(w),455(m), 535(s), 585(m), 625(m), 670(m), 745(s), 790(m), 875(m), 925(m), 945(m), 965(m), 1015(w), 1065(w), 1115(s), 1200(s, br), 1340(s), 1520(s), 1635(s), 3400(s, br), 3650(s) cm^{-1}.

4.3.13; Molecular weight determinations in solution;

In order to assess the molecular weight in solution we adopted a technique using the sealed system depicted in Figure 4.22. Two solutions containing a known weight of sample and standard respectively were placed in each of two bulbs and the solutions were left to equilibrate. We would expect to see a migration of the solvent from the weaker to the more concentrated solution until the solutions were of equal strength. It is necessary to measure the height of each column regularly in order to ascertain when the equilibrium state has been reached. By comparing the volumes after equilibration it would be possible to calculate the molecular weight of the complex under study.
The following equation is, therefore, representative;

$$g_1 / M_1L_1 = g_2 / M_2L_2$$

g_1 = mass of sample
g_2 = mass of standard
M = molecular weight
L = final column length

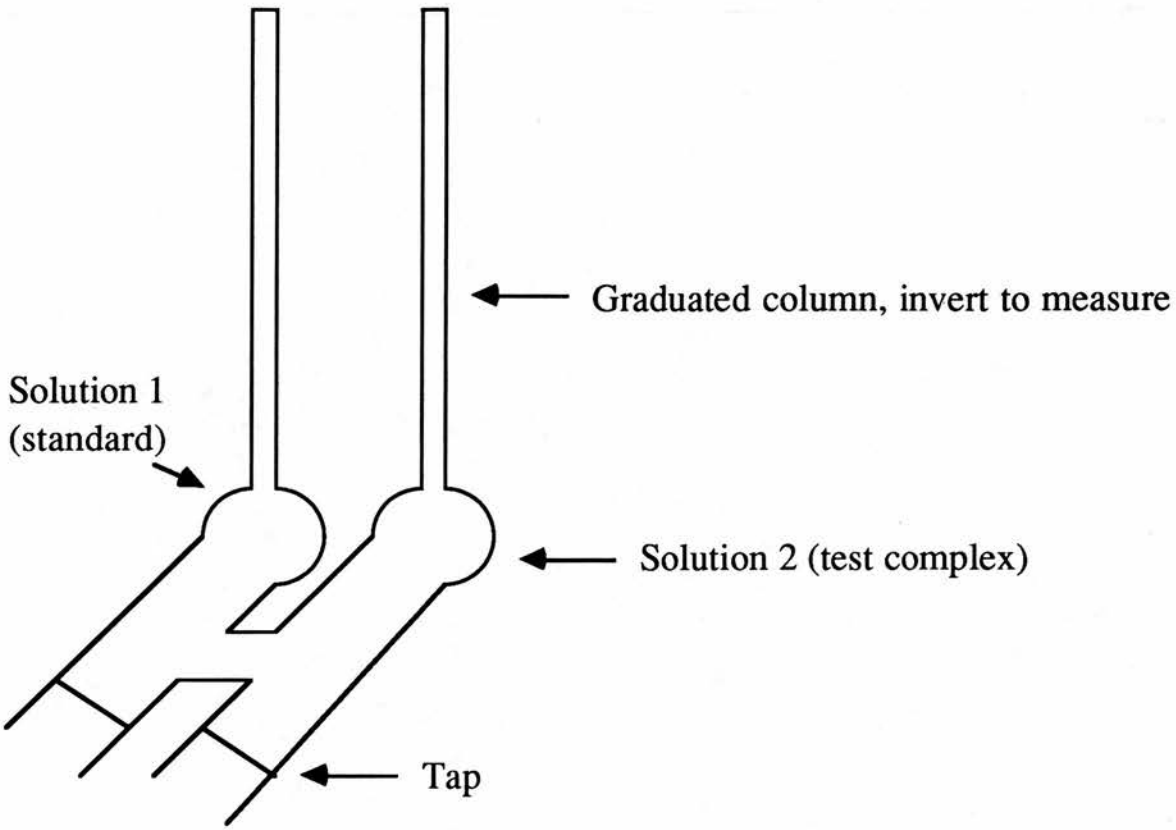

Figure 4.22; Apparatus used to determine the solution phase molecular weight of selected β–diketonates;

APPENDIX 4.1;

THE DETERMINATION OF THE CRYSTAL STRUCTURE OF bis(1,1,1,2,2,3,3,7,7,8,8,9,9,9-tetradecafluorononane-4-6-dione) ethanol copper (II)

Experimental;

Turquoise, plate-like crystals were obtained by recrystallising bis(1,1,1,2,2,3,3,7,7,8,8,9,9,9-tetradecafluorononanedione) copper (II) from aqueous ethanol (1:1) at 278 K. These crystals were stable indefinitely at this temperature in the mother liquor under air.

A crystal 0.42 x 0.36 x 0.08 mm was sealed in a Lindemann glass capillary. Cell dimensions were refined from 25 carefully centred reflections ($8°\leq\theta\leq13°$) using an Enraf-Nonius CAD4 diffractometer (SERC service at QMW, London). 5902 measured reflections yielded 5422 unique data (R_{int} = 0.0108) of which 3117 with $F\geq3\sigma(F)$ were used in the refinement.

Data were collected for the range $1.5°\leq\theta\leq25°$ for index limits $-12\leq h\leq11$, $-14\leq k\leq14$, $0\leq l\leq15$ and corrected for absorption by a ψ scan technique on the diffractometer.

Crystallographic Data;

Formula $C_{20}H_8F_{28}O_5Cu$ M_r=923.813, triclinic, $P\bar{1}$, a=11.269(4) Å, b = 12.331 (2) Å, c = 12.890 (2) Å, α = 96.89 (2) °, β = 108.93 (3) °, γ=109.63(3)°, V=1541.54 $Å^3$, Z=2, D_x=1.989 Mgm^{-3}, λ ($M_oK\alpha$)= 0.71069 Å, μ=8.37 cm^{-1}, F(000)=897.95, T=293 K.

The use of direct methods calculations, employing the SHELXS86[71] program, in Space group $P\bar{1}$ did not give a satisfactory solution. The best E-MAP showed overlapping fragments of the molecule and gave poor figures of merit. The symmetry was then

lowered to P_1 and further E-MAPS were calculated. The best map showed large parts of two molecules which were obviously connected by a centre of symmetry. After one set of least squares refinements a new electron density map was calculated and the position of the centre of inversion was located as accurately as possible. The symmetry was then raised to $\bar{P}_1$ and the coordinates of one of the molecules was adjusted to move the centre of symmetry to the origin . The analysis was then completed in $\bar{P}_1$. All other non - hydrogen atoms were found during conventional extension and refinement using least squares and difference Fourier map techniques and employing the SHELX76[72] program system. At a late stage in the refinement it became clear that an ethanol molecule was coordinated at right angles to the main coordination plane. Atomic geometry calculations used XANADU[73] and drawings were prepared with PLUTO[74].

Final Refinement;

(Minimising $\Sigma\omega|F_o-|F_c||^2$) 495 refined parameters. R=0.0649, ωR=0.0677, $\omega=2.16051/(\sigma^2(F) + 0.000628\ F^2)$, mean shift / e.s.d. =0.0006, max. shift / e.s.d.= +0.091, max. peaks on final difference map= 0.499, -0.407 e $Å^{-3}$.

Table 1. Bis(tetradecafluorononanedione) copper(II)

Coordinates X 10^4 for non hydrogen atoms
with e.s.d's in parentheses. Ueq X 10^3.

$$U_{eq} = (1/3)\Sigma_i\Sigma_j U_{ij} a_i^* a_j^* \mathbf{a}_i . \mathbf{a}_j$$

	x/a	y/b	z/c	Ueq
CU1	-2262(1)	652(1)	633(1)	49(1)
C1	2285(15)	5441(10)	4359(12)	133(5)
F11	2094(9)	5596(7)	5280(7)	215(4)
F12	2277(8)	6394(6)	4015(8)	234(4)
F13	3345(6)	5304(6)	4513(7)	175(3)
C2	990(10)	4361(7)	3494(8)	92(3)
F21	-135(6)	4455(4)	3437(7)	163(3)
F22	1068(7)	4406(5)	2480(5)	169(3)
C3	906(8)	3124(7)	3637(6)	75(2)
F31	1887(4)	2924(4)	3406(4)	107(1)
F32	1135(5)	3172(5)	4720(3)	133(2)
C4	-517(6)	2148(5)	2855(5)	51(2)
O41	-672(4)	1892(3)	1849(3)	59(1)
C5	-1435(7)	1632(6)	3328(5)	60(2)
C6	-2662(6)	705(5)	2700(5)	52(2)
O61	-3159(4)	190(3)	1658(3)	54(1)
C7	-3604(7)	167(5)	3321(5)	54(2)
F71	-3329(4)	992(3)	4247(3)	84(1)
F72	-4915(4)	-162(4)	2641(3)	73(1)
C8	-3427(7)	-907(6)	3707(6)	63(2)
F81	-3715(5)	-1746(4)	2801(4)	99(2)
F82	-2076(4)	-568(4)	4376(4)	103(2)
C9	-4278(11)	-1468(8)	4366(8)	91(3)
F91	-5525(6)	-1752(6)	3825(6)	160(3)
F92	-4027(6)	-2395(5)	4625(5)	128(2)
F93	-3866(7)	-710(6)	5354(5)	150(3)
C11	532(10)	2441(8)	-2730(8)	89(3)
F111	1749(6)	2502(6)	-2218(6)	139(3)
F112	559(6)	3444(5)	-2889(6)	145(3)
F113	41(8)	1675(7)	-3720(5)	175(3)
C12	-355(7)	1962(6)	-2058(6)	67(2)
F121	121(6)	2832(4)	-1124(5)	128(2)
F122	-1619(5)	1763(5)	-2689(5)	136(2)
C13	-344(6)	833(5)	-1698(5)	54(2)
F131	-544(4)	38(3)	-2604(3)	85(1)
F132	898(4)	1068(4)	-925(3)	87(1)
C14	-1432(6)	328(5)	-1197(5)	47(2)
O141	-1196(4)	992(3)	-285(3)	58(1)
C15	-2481(6)	-768(5)	-1768(5)	49(2)
C16	-3462(6)	-1268(5)	-1341(5)	48(2)
O161	-3584(4)	-848(3)	-471(3)	51(1)
C17	-4576(7)	-2534(5)	-2006(5)	57(2)
F171	-4671(4)	-2789(3)	-3081(3)	88(1)
F172	-5789(4)	-2567(3)	-2057(3)	83(1)
C18	-4269(10)	-3488(6)	-1453(7)	87(3)
F181	-2993(6)	-3366(5)	-1336(6)	137(2)
F182	-4269(7)	-3280(4)	-417(4)	142(2)
C19	-5234(18)	-4756(10)	-2052(13)	142(7)
F191	-4905(9)	-5472(5)	-1461(7)	199(4)
F192	-6441(9)	-4924(6)	-2300(10)	228(5)
F193	-5077(11)	-5063(6)	-3008(8)	217(5)
O21	-3486(5)	1691(4)	17(4)	84(2)
C22	-3239(11)	2660(9)	-472(10)	137(5)
C23	-2048(13)	3592(10)	138(12)	163(6)

Supplementary Table.

Bis(tetradecafluorononanedione) copper(II)
Anisotropic temperature factors X 10^3
with e.s.d's in parentheses

	U11	U22	U33	U23	U13	U12
CU1	53(1)	46(1)	41(1)	8(1)	22(1)	10(1)
C1	135(11)	79(7)	150(11)	-5(7)	73(10)	-6(8)
F11	193(8)	154(7)	190(7)	-70(6)	70(7)	-14(5)
F12	163(7)	78(4)	327(12)	41(6)	6(7)	-20(4)
F13	75(4)	130(5)	240(8)	-28(5)	41(5)	-7(4)
C2	84(7)	67(5)	103(7)	6(5)	42(5)	3(5)
F21	73(4)	68(3)	310(9)	8(4)	53(5)	19(3)
F22	201(7)	117(4)	102(4)	44(4)	25(4)	-12(4)
C3	76(6)	72(5)	57(4)	5(4)	29(4)	6(4)
F31	59(3)	105(4)	125(4)	-16(3)	21(3)	25(3)
F32	108(4)	149(4)	49(2)	19(3)	5(2)	-30(3)
C4	52(4)	50(4)	45(4)	7(3)	18(3)	16(3)
O41	63(3)	54(2)	50(2)	7(2)	28(2)	7(2)
C5	67(5)	59(4)	37(3)	3(3)	21(3)	9(4)
C6	58(4)	61(4)	49(4)	21(3)	28(3)	28(4)
O61	55(3)	56(2)	39(2)	9(2)	20(2)	8(2)
C7	59(5)	57(4)	48(4)	12(3)	26(3)	20(3)
F71	113(3)	73(2)	81(3)	11(2)	67(3)	30(2)
F72	52(3)	99(3)	80(3)	40(2)	33(2)	32(2)
C8	54(5)	73(5)	63(4)	30(4)	27(4)	19(4)
F81	152(4)	72(3)	102(3)	27(3)	78(3)	53(3)
F82	62(3)	123(4)	131(4)	68(3)	32(3)	37(3)
C9	104(8)	92(6)	84(6)	51(5)	44(6)	31(6)
F91	69(4)	231(7)	204(6)	152(6)	67(4)	41(4)
F92	150(5)	126(4)	166(5)	102(4)	95(4)	69(4)
F93	206(7)	157(5)	116(4)	62(4)	109(5)	56(5)
C11	86(7)	97(7)	107(7)	61(6)	50(6)	37(6)
F111	94(4)	178(6)	190(6)	103(5)	90(4)	54(4)
F112	176(6)	122(4)	229(7)	123(5)	142(5)	81(4)
F113	212(7)	189(6)	95(4)	43(4)	93(5)	12(6)
C12	59(5)	62(5)	90(5)	30(4)	41(4)	22(4)
F121	207(6)	64(3)	155(5)	29(3)	128(5)	45(3)
F122	66(3)	176(5)	217(6)	149(5)	65(4)	65(3)
C13	49(4)	62(4)	48(4)	17(3)	19(3)	19(3)
F131	104(3)	68(2)	96(3)	14(2)	69(3)	24(2)
F132	56(3)	127(4)	92(3)	62(3)	30(2)	41(3)
C14	52(4)	51(4)	42(3)	19(3)	21(3)	20(3)
O141	62(3)	53(2)	47(2)	5(2)	28(2)	5(2)
C15	57(4)	45(3)	41(3)	9(3)	20(3)	15(3)
C16	44(4)	46(3)	46(4)	11(3)	11(3)	15(3)
O161	51(3)	49(2)	43(2)	5(2)	19(2)	11(2)
C17	52(4)	48(4)	58(4)	4(3)	18(3)	13(3)
F171	97(3)	72(3)	49(2)	-8(2)	22(2)	-4(2)
F172	51(3)	74(3)	94(3)	1(2)	17(2)	6(2)
C18	106(7)	48(4)	101(6)	22(4)	42(6)	21(5)
F181	108(4)	97(4)	214(6)	57(4)	50(4)	57(4)
F182	245(7)	91(3)	87(3)	49(3)	65(4)	56(4)
C19	205(15)	69(8)	179(13)	42(8)	101(12)	58(10)
F191	266(9)	70(4)	215(7)	54(4)	49(7)	51(5)
F192	120(6)	91(5)	410(15)	53(6)	78(8)	-5(5)
F193	322(13)	85(4)	198(7)	-13(5)	95(8)	51(6)
O21	89(4)	73(3)	107(4)	41(3)	44(3)	41(3)
C22	105(8)	94(7)	184(11)	43(8)	31(8)	29(7)
C23	128(11)	107(9)	211(13)	25(9)	42(10)	24(8)

Supplementary Table

Bis(tetradecafluorononanedione) copper(II)
Coordinates x 10^4 for hydrogen atoms

	x/a	y/b	z/c
H51	-1246	1912	3999
H151	-2585	-1207	-2403

Table 2.Bis(tetradecafluorononanedione) copper(II)

Interatomic distances (A) and angles(°)

O41 ---CU1	1.939(3)	O61 ---CU1	1.937(5)
O141---CU1	1.930(5)	O161---CU1	1.950(3)
O21 ---CU1	2.212(6)	F11 ---C1	1.278(20)
F12 ---C1	1.306(16)	F13 ---C1	1.218(19)
C2 ---C1	1.557(12)	F21 ---C2	1.290(14)
F22 ---C2	1.345(13)	C3 ---C2	1.533(13)
F31 ---C3	1.323(12)	F32 ---C3	1.325(9)
C4 ---C3	1.548(8)	O41 ---C4	1.237(8)
C5 ---C4	1.382(11)	C6 ---C5	1.365(7)
O61 ---C6	1.260(7)	C7 ---C6	1.554(11)
F71 ---C7	1.346(8)	F72 ---C7	1.336(7)
C8 ---C7	1.521(11)	F81 ---C8	1.333(9)
F82 ---C8	1.367(8)	C9 ---C8	1.532(14)
F91 ---C9	1.247(12)	F92 ---C9	1.322(13)
F93 ---C9	1.322(11)	F111---C11	1.286(13)
F112---C11	1.270(13)	F113---C11	1.314(11)
C12 ---C11	1.545(15)	F121---C12	1.331(9)
F122---C12	1.310(9)	C13 ---C12	1.521(11)
F131---C13	1.335(8)	F132---C13	1.336(7)
C14 ---C13	1.552(10)	O141---C14	1.241(7)
C15 ---C14	1.374(7)	C16 ---C15	1.387(10)
O161---C16	1.246(8)	C17 ---C16	1.552(7)
F171---C17	1.344(8)	F172---C17	1.333(9)
C18 ---C17	1.526(12)	F181---C18	1.349(14)
F182---C18	1.329(12)	C19 ---C18	1.498(12)
F191---C19	1.302(17)	F192---C19	1.227(22)
F193---C19	1.330(22)	C22 ---O21	1.405(14)
C23 ---C22	1.342(13)		

O61	-CU1	-O41	92.1(2)	O141	-CU1 -O41	85.6(2)
O141	-CU1	-O61	171.3(2)	O161	-CU1 -O41	164.8(2)
O161	-CU1	-O61	88.0(2)	O161	-CU1 -O141	92.0(2)
O21	-CU1	-O41	100.1(2)	O21	-CU1 -O61	91.9(2)
O21	-CU1	-O141	96.8(2)	O21	-CU1 -O161	95.1(2)
F12	-C1	-F11	103.7(13)	F13	-C1 -F11	111.5(12)
F13	-C1	-F12	113.5(13)	C2	-C1 -F11	106.5(11)
C2	-C1	-F12	107.5(10)	C2	-C1 -F13	113.4(11)
F21	-C2	-C1	112.8(10)	F22	-C2 -C1	104.7(9)
F22	-C2	-F21	107.0(8)	C3	-C2 -C1	116.1(9)
C3	-C2	-F21	109.5(8)	C3	-C2 -F22	106.1(8)
F31	-C3	-C2	108.7(7)	F32	-C3 -C2	106.0(7)
F32	-C3	-F31	109.3(7)	C4	-C3 -C2	110.9(7)
C4	-C3	-F31	110.8(6)	C4	-C3 -F32	111.0(6)
O41	-C4	-C3	113.7(6)	C5	-C4 -C3	119.1(6)
C5	-C4	-O41	127.2(5)	C4	-O41 -CU1	125.9(4)
C6	-C5	-C4	121.9(6)	O61	-C6 -C5	128.9(7)
C7	-C6	-C5	117.7(6)	C7	-C6 -O61	113.3(4)
C6	-O61	-CU1	123.9(4)	F71	-C7 -C6	110.0(5)
F72	-C7	-C6	110.1(5)	F72	-C7 -F71	107.6(7)
C8	-C7	-C6	113.0(7)	C8	-C7 -F71	107.6(5)
C8	-C7	-F72	108.4(5)	F81	-C8 -C7	108.9(6)
F82	-C8	-C7	107.9(5)	F82	-C8 -F81	106.7(7)
C9	-C8	-C7	116.6(8)	C9	-C8 -F81	108.2(6)
C9	-C8	-F82	108.1(6)	F91	-C9 -C8	111.6(8)
F92	-C9	-C8	109.3(10)	F92	-C9 -F91	111.4(8)
F93	-C9	-C8	109.5(7)	F93	-C9 -F91	109.6(11)
F93	-C9	-F92	105.1(8)	F112	-C11 -F111	110.9(7)
F113	-C11	-F111	105.4(10)	F113	-C11 -F112	108.9(9)
C12	-C11	-F111	110.0(9)	C12	-C11 -F112	112.0(10)

C12	-C11	-F113	109.4(7)	F121	-C12 -C11	105.6(6)
F122	-C12	-C11	107.3(7)	F122	-C12 -F121	110.4(8)
C13	-C12	-C11	117.1(8)	C13	-C12 -F121	108.1(6)
C13	-C12	-F122	108.2(6)	F131	-C13 -C12	107.7(6)
F132	-C13	-C12	109.1(5)	F132	-C13 -F131	106.9(6)
C14	-C13	-C12	112.5(7)	C14	-C13 -F131	111.2(5)
C14	-C13	-F132	109.3(5)	O141	-C14 -C13	113.0(4)
C15	-C14	-C13	118.5(6)	C15	-C14 -O141	128.5(7)
C14	-O141	-CU1	125.6(4)	C16	-C15 -C14	120.6(6)
O161	-C16	-C15	129.1(5)	C17	-C16 -C15	117.5(6)
C17	-C16	-O161	113.4(6)	C16	-O161 -CU1	124.0(4)
F171	-C17	-C16	110.7(6)	F172	-C17 -C16	109.1(6)
F172	-C17	-F171	107.0(5)	C18	-C17 -C16	111.7(5)
C18	-C17	-F171	108.4(7)	C18	-C17 -F172	109.8(7)
F181	-C18	-C17	108.0(7)	F182	-C18 -C17	108.2(8)
F182	-C18	-F181	107.5(7)	C19	-C18 -C17	116.7(8)
C19	-C18	-F181	108.7(11)	C19	-C18 -F182	107.3(10)
F191	-C19	-C18	110.6(10)	F192	-C19 -C18	113.3(14)
F192	-C19	-F191	111.4(14)	F193	-C19 -C18	109.0(13)
F193	-C19	-F191	104.3(14)	F193	-C19 -F192	107.8(13)
C22	-O21	-CU1	132.0(7)	C23	-C22 -O21	114.5(10)

APPENDIX 4.2;

STA ANALYSES

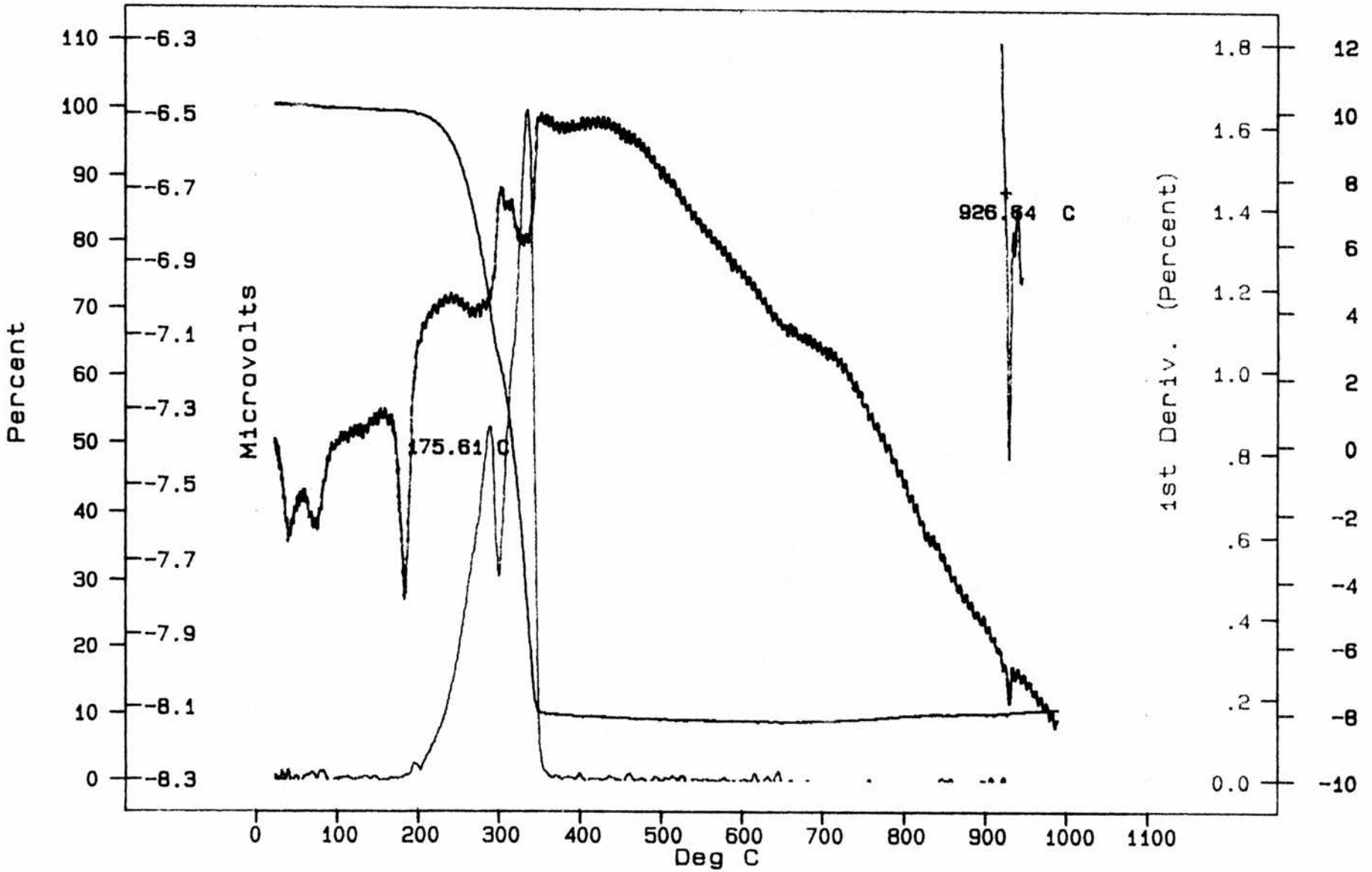

VERSION: C4.20

Figure A.4.2.1; [Ba(HFOD)$_2$]

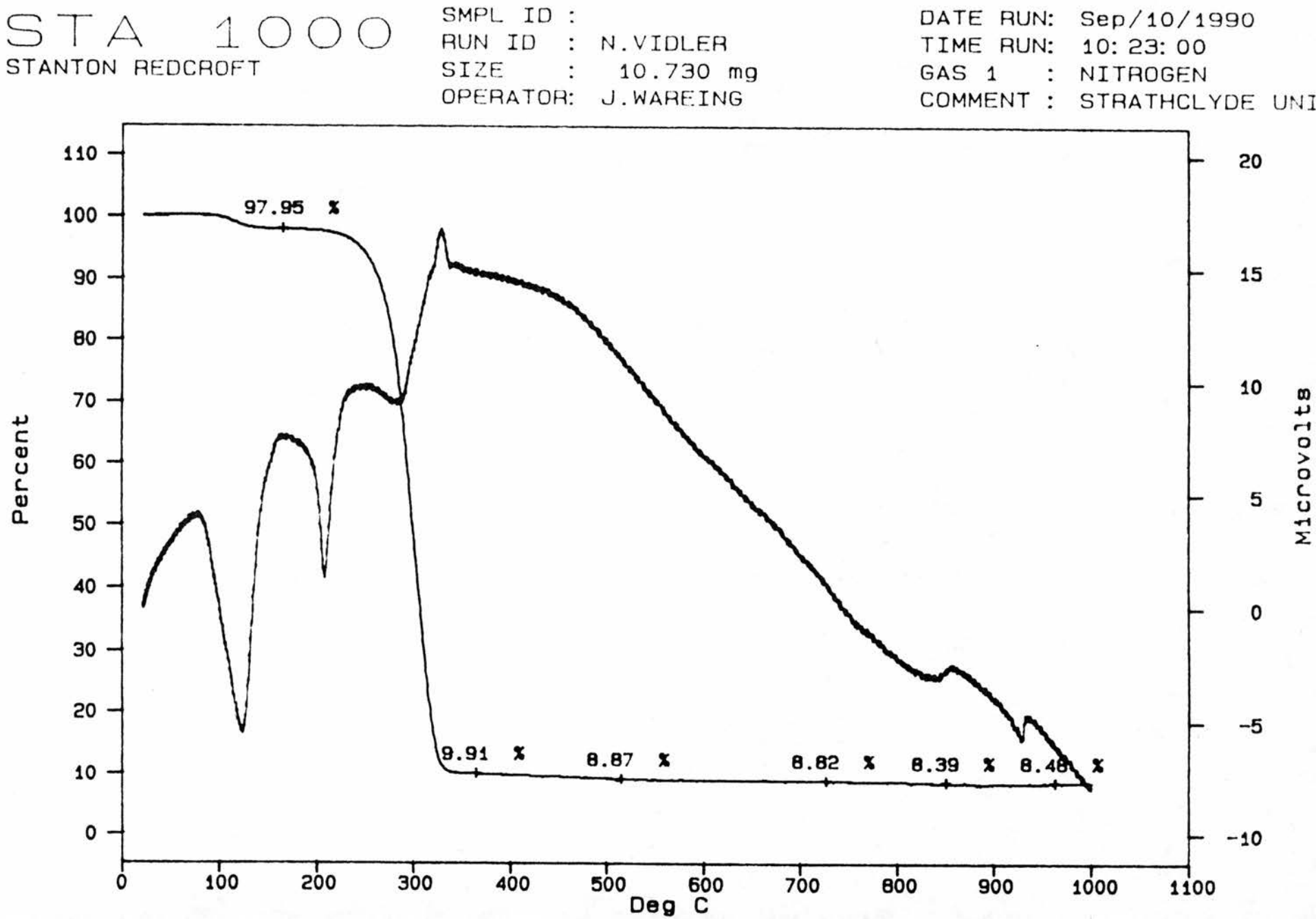

Figure A.4.2.2; [Ba(DFHD)$_2$]

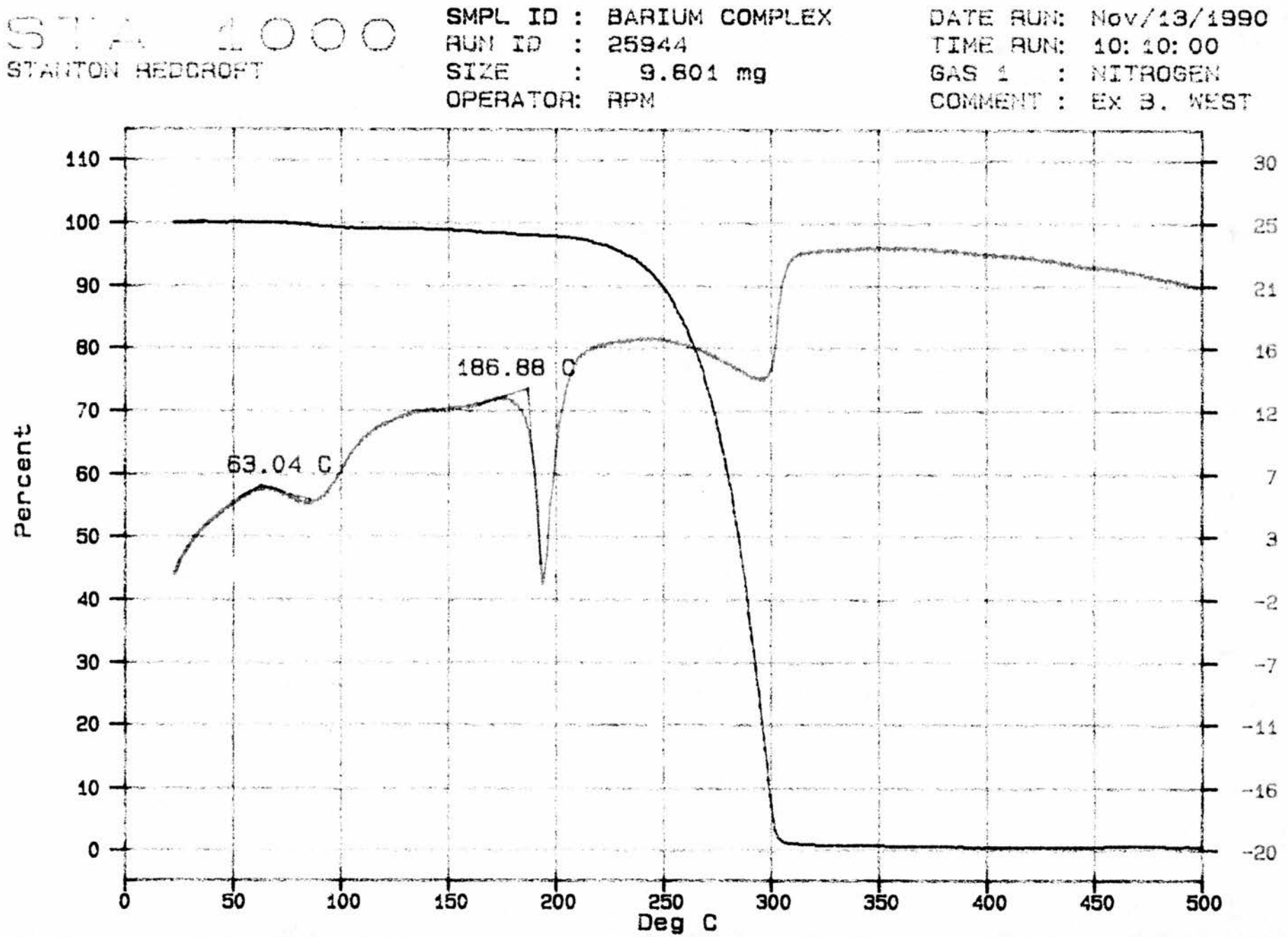

Figure A.4.2.3; [Ba(TDFND)$_2$]

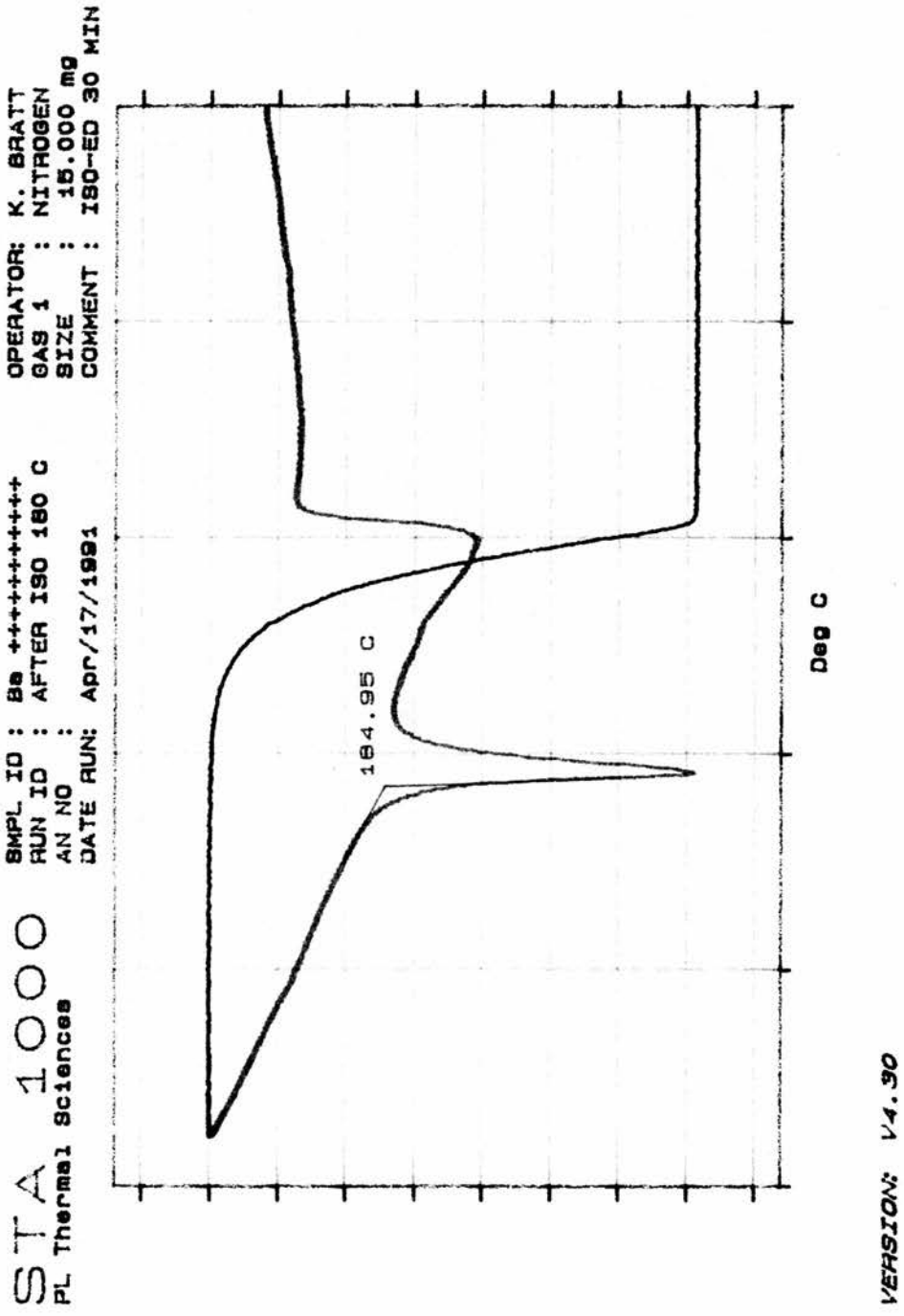

Figure A.4.2.4; [Ba(TDFND)$_2$] after pre-heating to 180°C for 1 Hour

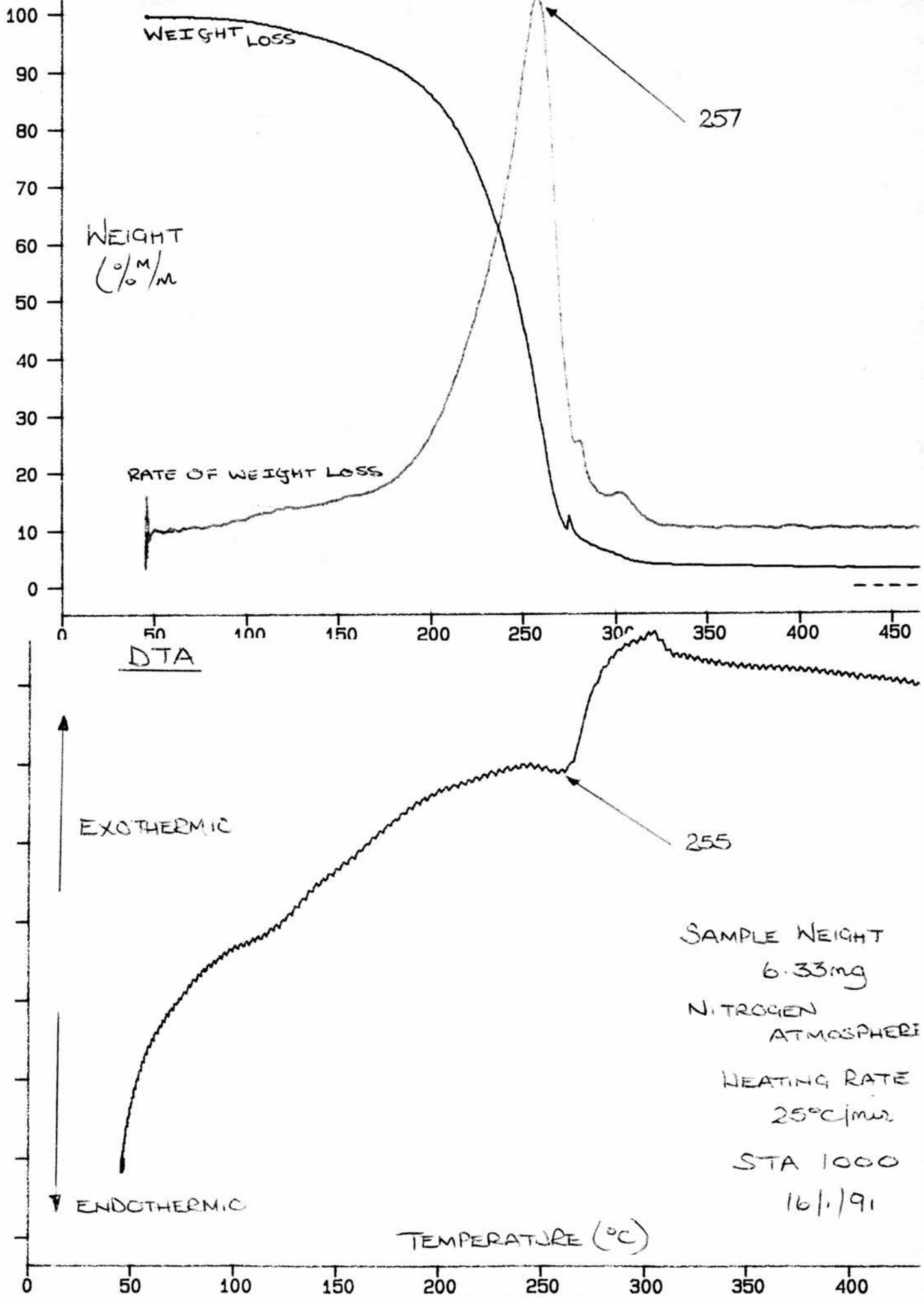

Figure A.4.2.5; [$Ca(DFHD)_2$]

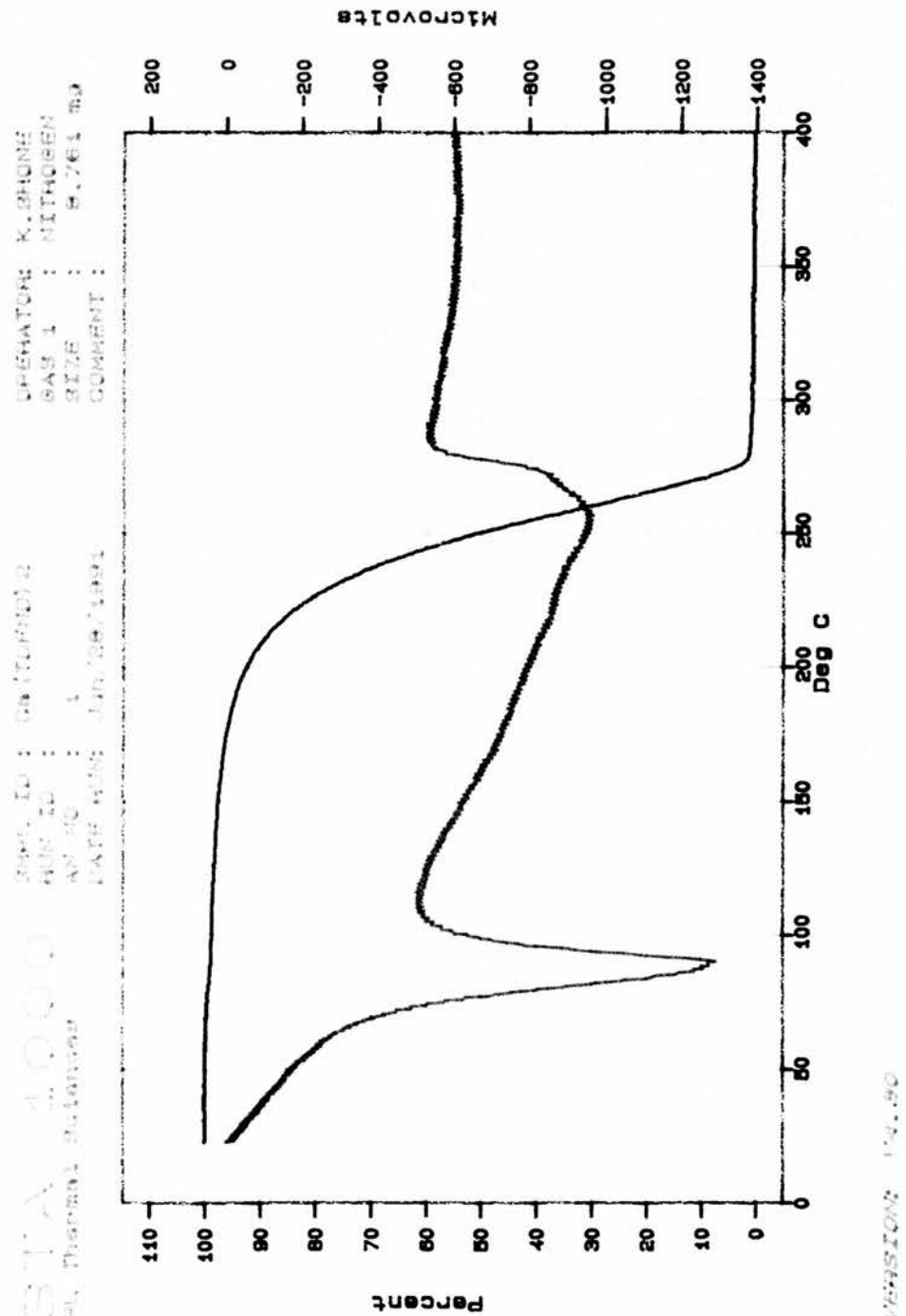

Figure A.4.2.6; [Ca(TDFND)$_2$]

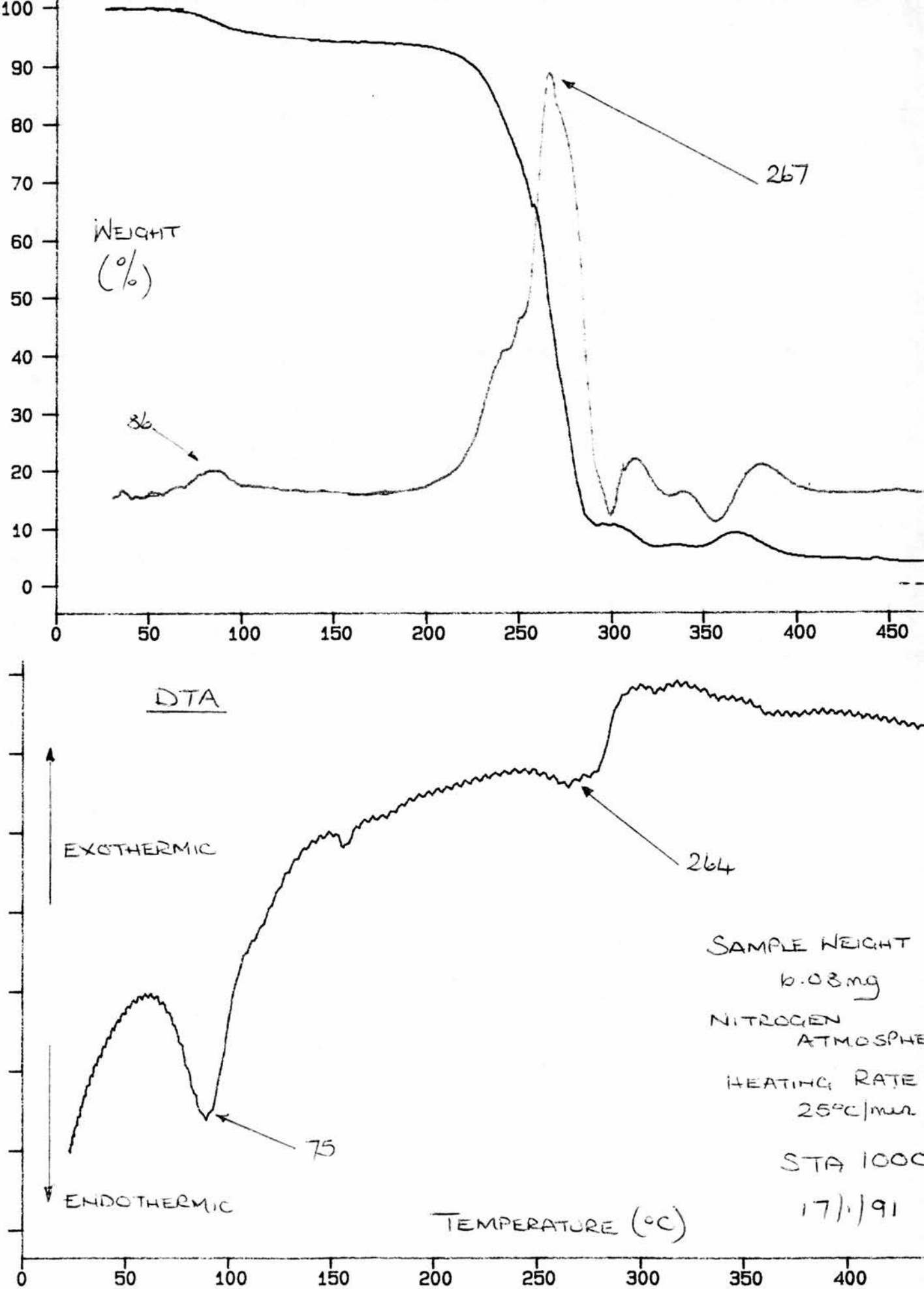

Figure A.4.2.7; [$Sr(DFHD)_2$]

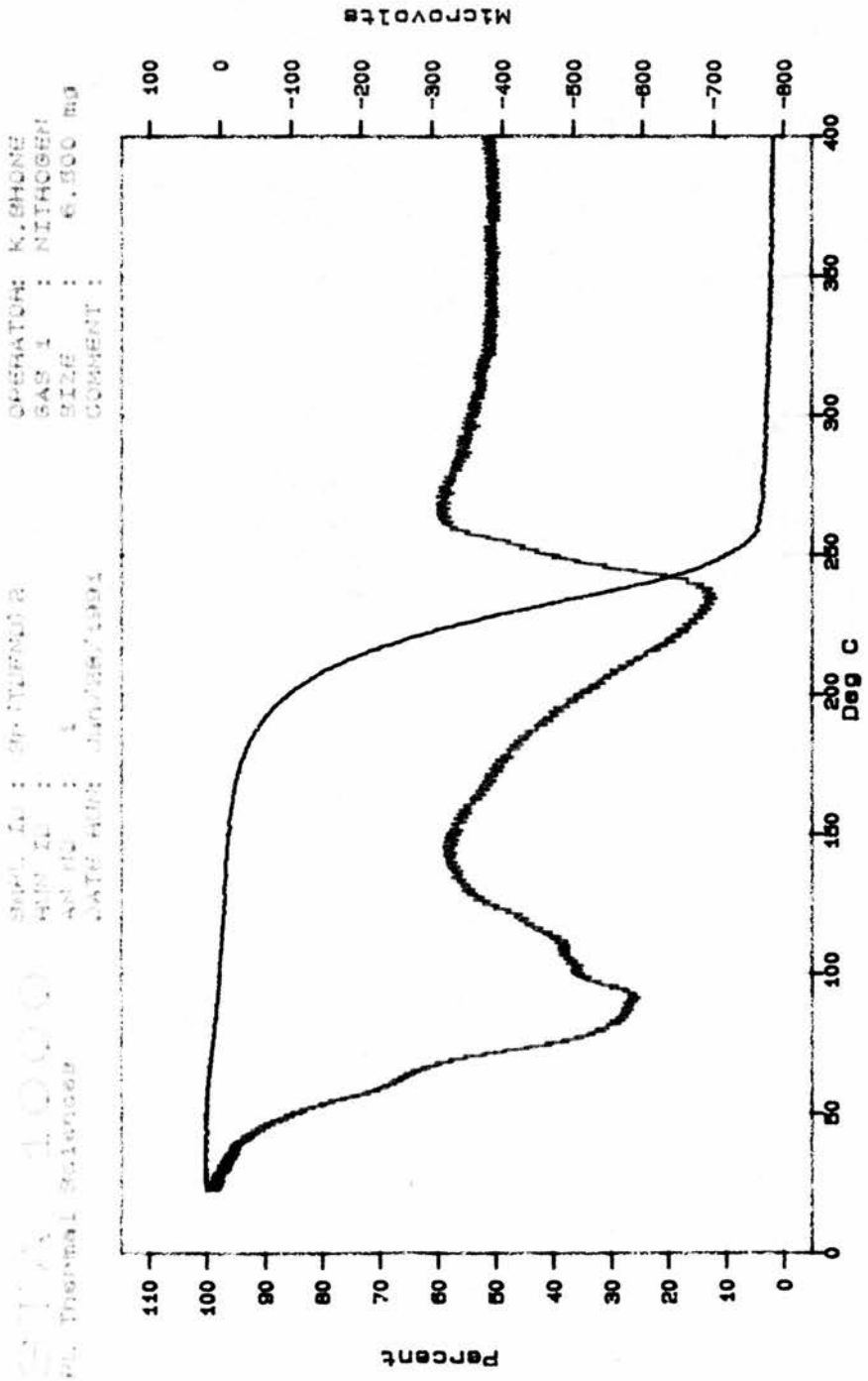

Figure A.4.2.8; [Sr(TDFND)$_2$]

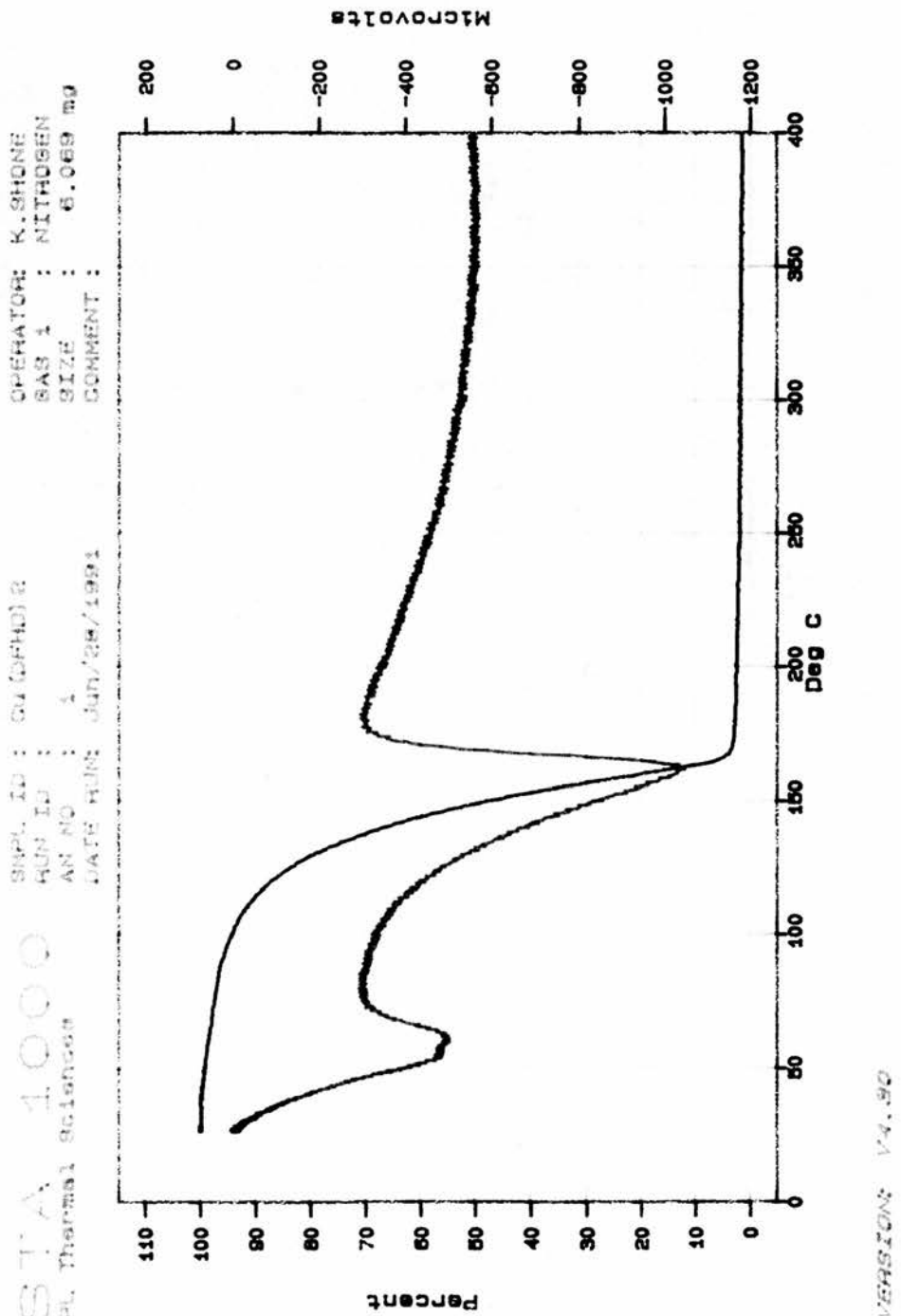

Figure A.4.2.9; $[Cu(DFHD)_2]$

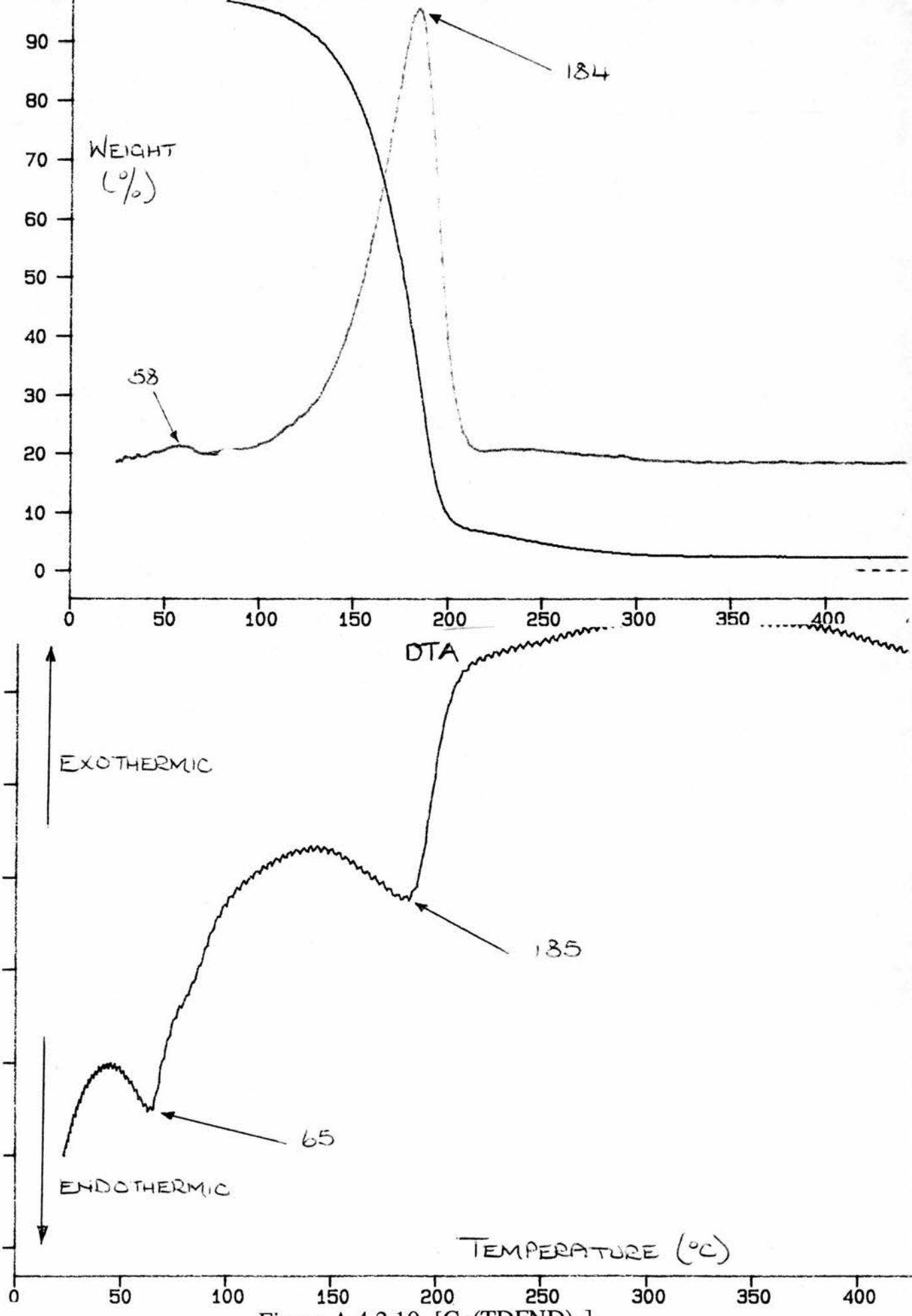

Figure A.4.2.10; [Cu(TDFND)$_2$]

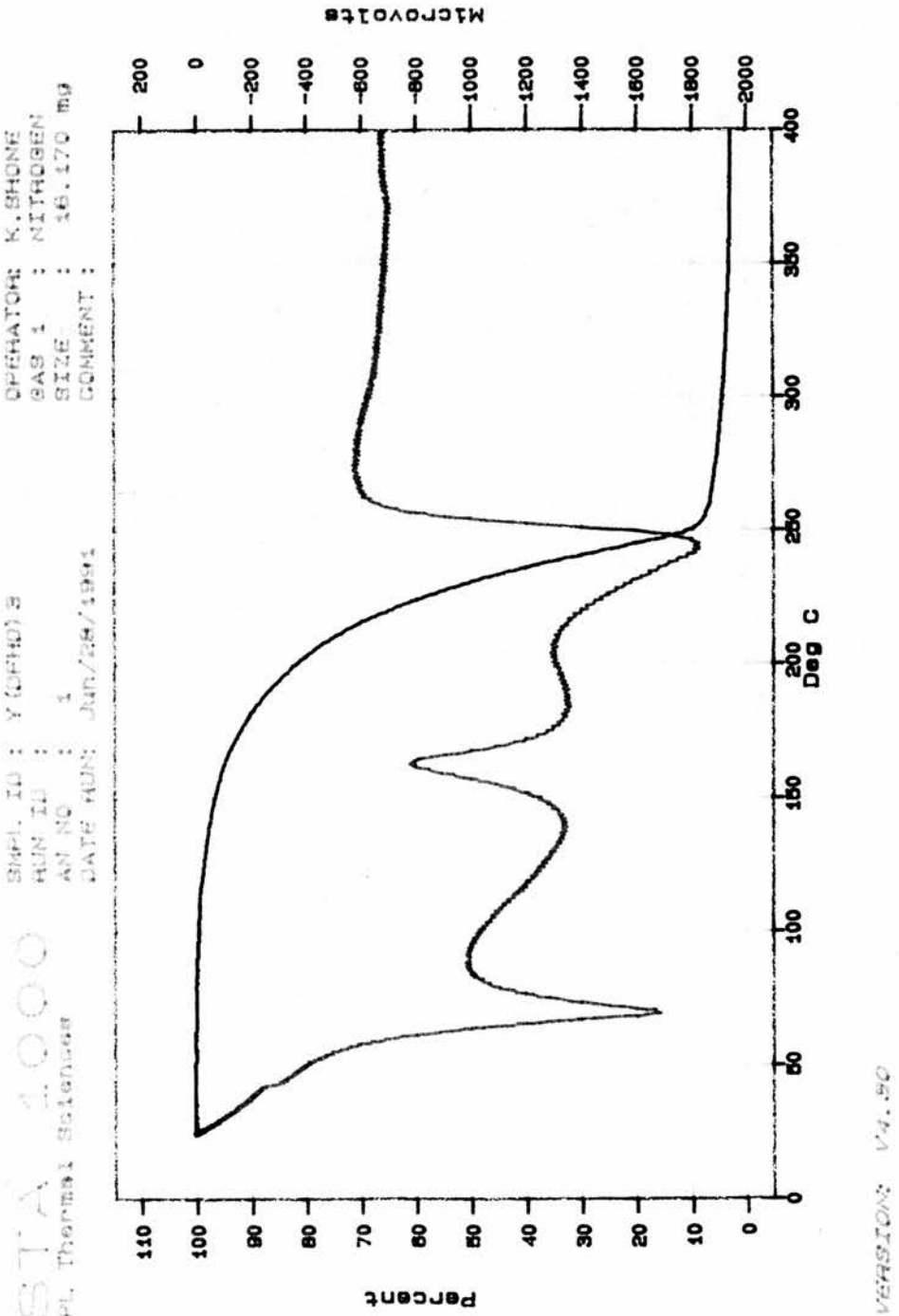

Figure A.4.2.11; [$Y(DFHD)_3$]

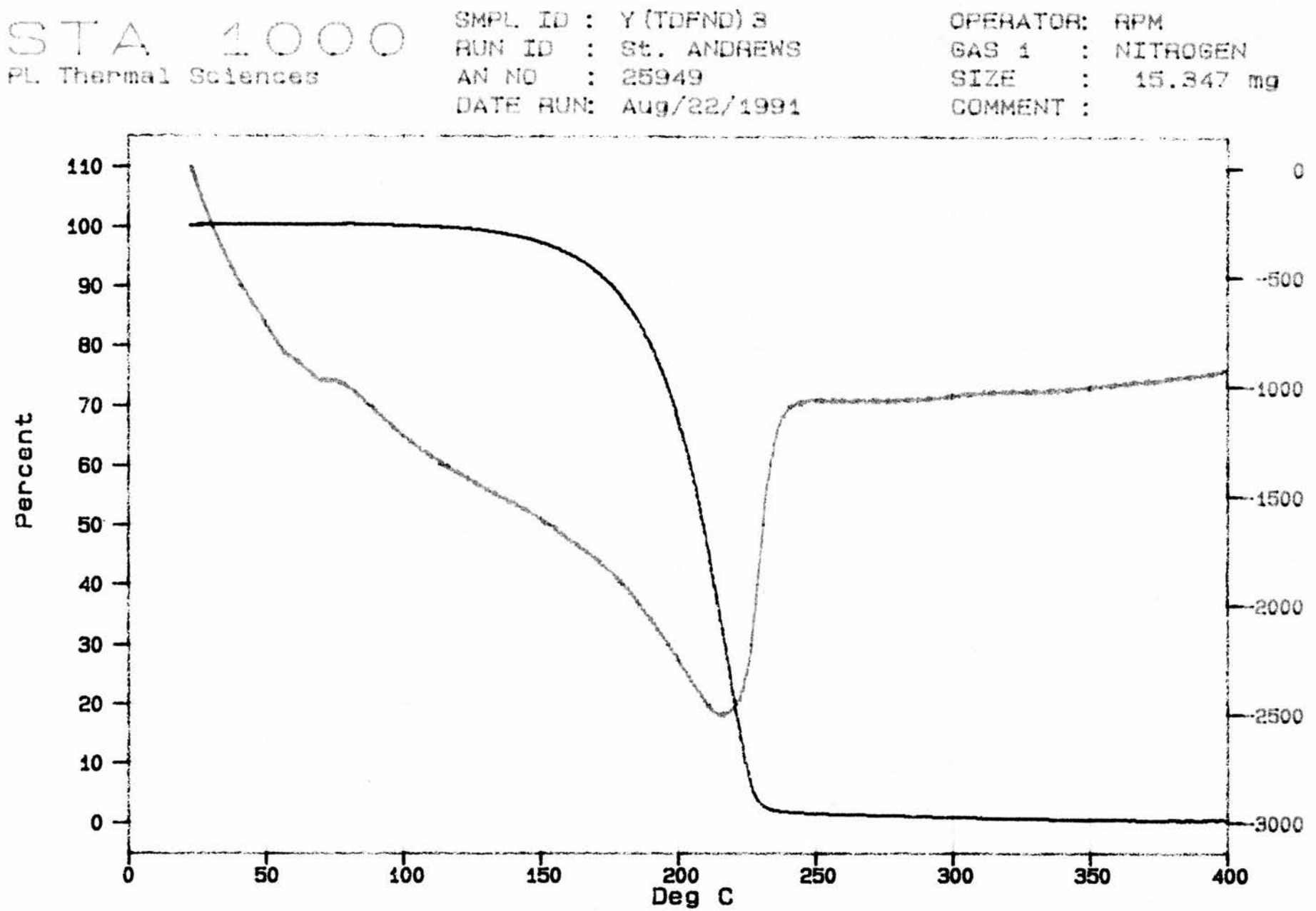

Figure A.4.2.12; [Y(TDFND)$_3$]

CHAPTER 5

THE PREPARATION AND ANALYSIS OF ALKOXIDES AND FLUOROALKOXIDES

5.1; INTRODUCTION;

In Chapter 2 the principal advantage of using alkoxide precursors was discussed. This is their capability of breaking down at the substrate surface to deposit a metal oxide film. It is important for film quality to maximise the oxygen content at this stage, thus reducing the need for either the later inclusion of oxygen or the addition of oxygen to the carrier gas stream.

In the same chapter there was a description of the main problems with alkoxides, these being involatility, decomposition and air sensitivity. Despite such problems much work has been done on barium alkoxides, principally by Caulton[75,76], Hubert-Pfalzgraf[77] and ourselves[78], in an effort to overcome these difficulties and reap the benefits of an oxide film. Four principal types of alkoxide have been developed for this purpose, namely alkoxides with bulky alkyl or phenyl groups, siloxides, bidentate alkoxyalkoxides and fluoroalkoxides. We will first review the work of Caulton on sterically hindered alkoxides and siloxides prior to a discussion of our own investigations.

5.1.1; The Preparation and crystal structure of two sterically hindered alkoxides[75];

The two sterically hindered alkoxides of barium which Caulton prepared and identified were the tertiary butoxide (t-BuO) and the Phenoxide (OPh).

These were prepared by direct reaction of the alcohol with the metal in THF. For the phenol the reaction was complete at room temperature after 50 minutes, whilst it was necessary to reflux the t-butanol at 70°C for 60 minutes. Crystallisation was undertaken from

toluene layered pentane at -20°C. The melting point for the phenoxide was 226-228°C and for the t-butoxide >340°C.

The melting points reported for these complexes, particularly that for the tertiary butoxide, would lead one to conclude that they are likely to be unsuitable for CVD use. Indeed, the description of the tertiary butoxide melting point as >340°C indicates to us that Caulton failed to melt this complex intact (our work with other ligands has shown that barium alkoxides and β–diketonates decompose around or below 250°C). These initial thoughts are reinforced when an examination is made of the structure of these complexes. The phenoxide has a molecular formula of $[HBa_5(O)(OPh)_9(THF)_8]$, Figure 5.1, whereas the molecular formula of the tertiary butoxide is $[H_3Ba_6(O)(t\text{-}BuO)_{11}(OCEt_2CH_2O)(THF)_3]$, Figure 5.2. The crystal structures of both complexes contain a square-based pyramidal core, $Ba_5(\mu_5\text{-}O)$, supported by μ_2 and μ_3 phenoxide or butoxide ligands.

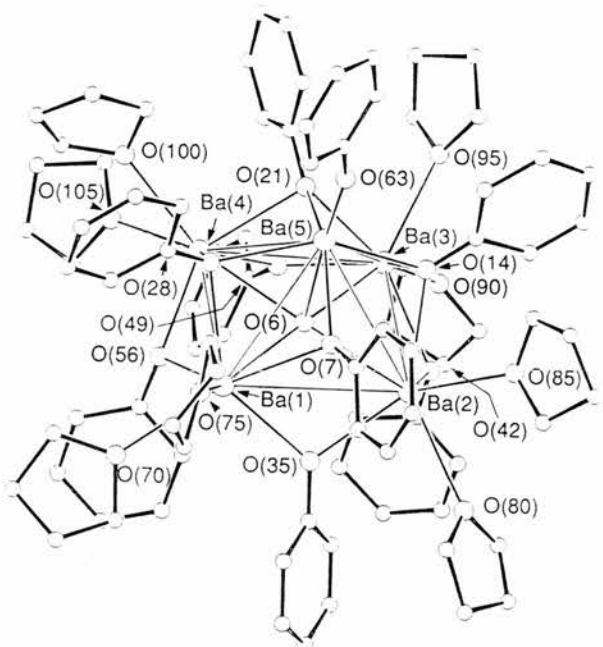

Figure 5.1; The crystal structure of $[HBa_5(O)(OPh)_9(THF)_8]$[75]

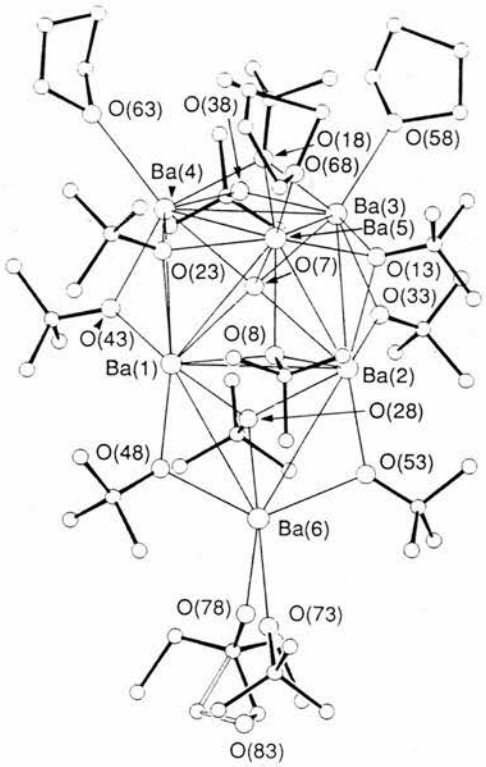

Figure 5.2;
The crystal structure of $[H_3Ba_6(O)(t\text{-}BuO)_{11}(OCEt_2CH_2O)(THF)_3]$[75]

5.1.2; The preparation and crystal structure of $[Ba_3(OSiPh_3)_6(THF)].0.5\ THF$[79];

Caulton found that it was not possible to react triphenylsilanol with barium granules even in the presence of a catalyst. However, it was found that if gaseous ammonia was bubbled through a solution of

triphenyl silanol in THF, ready reaction with barium granules would occur. Although Caulton was unable to identify the reaction mechanism with certainty, it was clear that the ammonia was acting as a catalyst.

Figure 5.3 shows the crystal structure of the complex which contains a core of three barium atoms forming a triangle. The relatively low molecular weight of this cluster would lead one to speculate that the complex might be more volatile than the alkoxide complexes which have already been described. This is indeed the case as Caulton reports that the species can be sublimed between 200 and 220°C under a pressure of 10^{-2} Torr. As no information is supplied on product decomposition at this temperature, it is not possible to speculate whether this complex is suitable for CVD applications.

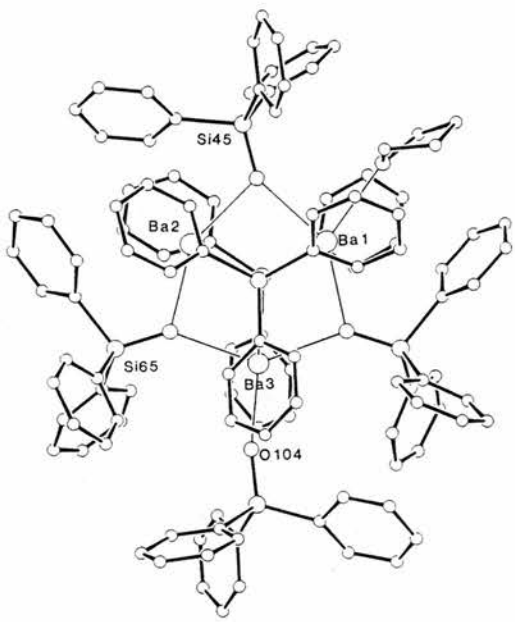

Figure 5.3; The crystal structure of $[Ba_3(OSiPh_3)_6(THF)].0.5\ THF$[79];

5.2; THE PREPARATION OF ALKOXIDES CONTAINING BULKY ALKYL OR PHENYL GROUPS;

In our early attempts to overcome the problems of involatility of alkoxides, we tried to introduce bulky groups into the alkoxides. This was the same method as that pursued by Caulton[75], although our investigations preceded their publications. We hoped that bridging bonds, as described in Chapter 2, would be prevented from forming by the steric crowding caused by the use of these bulky groups.

At the time when we commenced this work, in the summer of 1988, the best barium precursor reported for CVD use was $[Ba(DPM)_2]$. Given this fact, it was decided to attempt to form branched alkoxides with similar side groups to the $[Ba(DPM)_2]$ complex. Tertiary butanol, $(CH_3)_3COH$, the exact equivalent of H(DPM), was not chosen as it is a solid at room temperature and, therefore, not easy to handle. Instead we selected the tertiary amyl alcohol, $(CH_3)_2(C_2H_5)COH$. We found that this alkoxide was easy to prepare by direct reaction of the alcohol with the metal and that reaction was complete after 2-3 hours of reflux in the absence of a catalyst.

5.2.1; The preparation and analysis of barium tertiary amyl alkoxide;

The pre-dried and distilled alcohol was refluxed with barium granules under an atmosphere of dry nitrogen for three hours, after which time the reaction was complete. The slightly opaque solution was filtered hot and the alcohol was then removed in vacuo to leave the alkoxide as a solid residue.The spectra of the alcohol and of the alkoxide are shown in Figures 5.4 and 5.5 respectively, whilst an assignment of the peaks in the alkoxide spectrum is provided in Table 5.1.

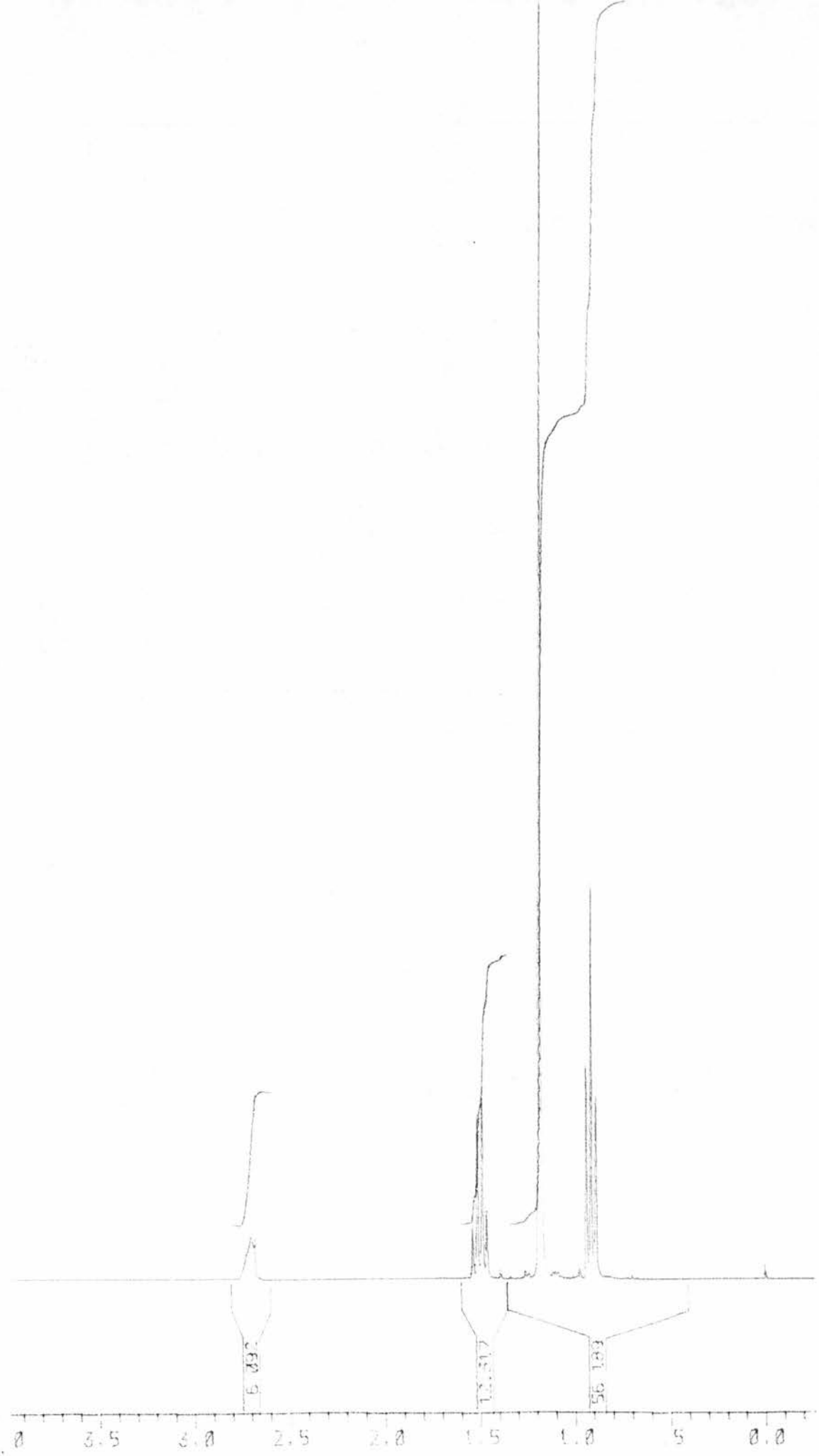

Figure 5.4; ^{1}H NMR of tertiary amyl alcohol

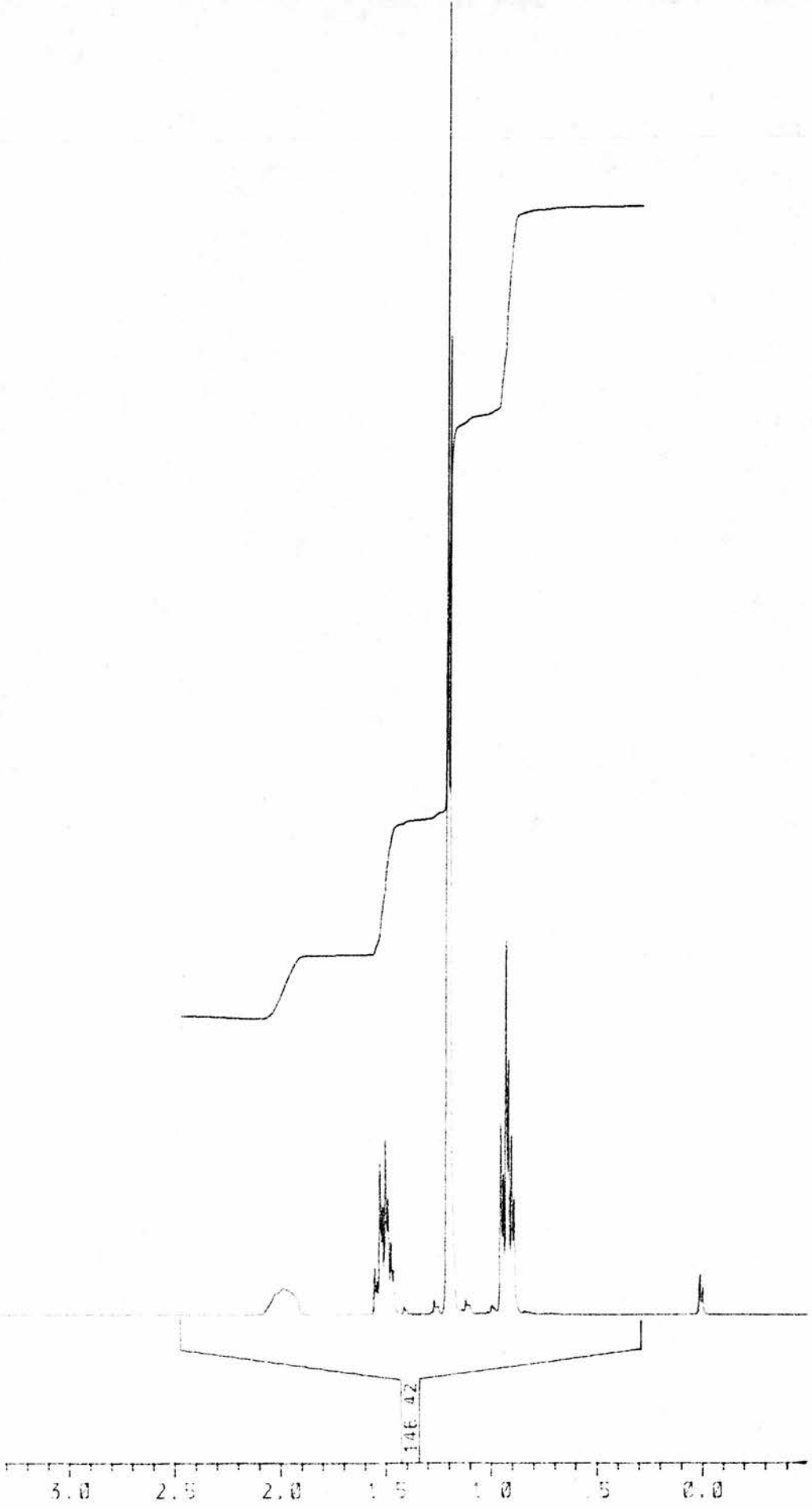

Figure 5.5; ^{1}H NMR of barium tertiary amyl alkoxide

Analysis was undertaken using IR, ^1H NMR and Microanalysis techniques. For the ^1H NMR it was necessary to assess the solubility in various solvents. The alcohols were unsuitable as exchange with the product might occur and the alkoxide was insoluble in both DMSO and THF. It was, however, slightly soluble in methylene chloride so this was chosen as the solvent.;

Table 5.1; Peaks and assignments for the ^1H NMR of barium t-amyl alkoxide;

Chemical shift (δ)	Integral	Assignment
0.95(triplet of triplets)	33	$^4CH_3$
1.20(triplet)	65	$^1CH_3$
1.55(quartet of doublets)	22	$^3CH_2$
2.00(broad singlet)	11	H_2O

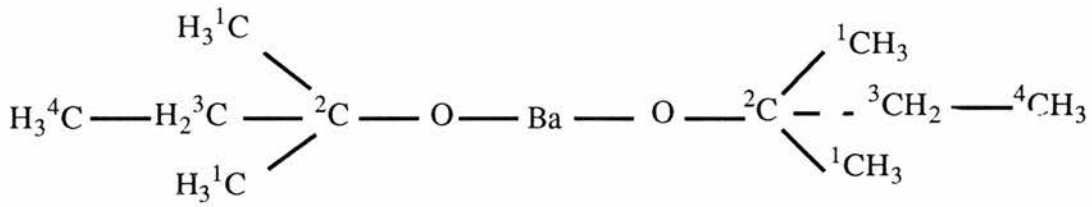

Figure 5.6; Barium tertiary amyl alkoxide, simple structure omitting additional barium-oxygen bonding and bound water.

The only peak in the ^1H NMR which causes problems with its assignment is that at δ2.00. The two possibilities for this peak are water and the presence of bound alcohol in the complex. The more likely assignment is water as the integral fits the presence of one mole of

water almost exactly. However, it was necessary to assess further analytical techniques to come to a definite conclusion.

This can best be achieved by considering the microanalysis of the complex. If we examine the result of the analysis and compare it with the simple alkoxide, the hydrated alkoxide and the alkoxide with two moles of bound alcohol respectively the result is quite conclusive;

$C_{10}H_{22}BaO_2$ requires C 38.53%, H 7.11%
$C_{10}H_{24}BaO_3$ requires C 36.47%, H 7.29%
$C_{20}H_{46}BaO_4$ requires C 49.28%, H 9.44%
found C 36.24%, H 7.24%

It can be seen from this analysis that the species most closely matching the experimental value is that containing a mole of water.

The IR spectrum is able to offer some confirmation of this finding and contains other peaks which indicate that the alkoxide has been prepared successfully. There is a large band in the 3100-3600 cm^{-1} region which is less intense than that found in the IR of the alcohol and could indicate that water is present in the complex. The expected group of peaks between 270 and 530 cm^{-1} are Ba-O stretching bands. Additionally, we would expect a large C-O stretching peak in the 1000 cm^{-1} region and there are peaks close to 1000 cm^{-1} in the alkoxide.

The clear problem with this assignment is the origin of the water in the complex (the reaction was carried out in a dry nitrogen atmosphere using pre-dried reagents). The most likely explanation is that the complex is ultra-sensitive to water and that contamination from the atmosphere occurred either during sample transference or reflux.

In order to test the suitability of the complex for CVD use we

attempted to sublime the complex. This was carried out by placing a sample of the solid in a flask fitted with a vacuum connection and a cold finger. The flask was put under active vacuum and then slowly heated to 200°C. Once this temperature was reached the sample was seen to be decrepitating and, as a result, a large quantity adhered to the cold finger. Whilst it was difficult to examine the sample closely during this process due to the highly mobile powder, it did not appear that this process was accompanied by sublimation. On continued heating the remaining sample on the base of the flask decomposed to a brown solid.

5.2.2; The preparation of other sterically hindered alkoxides of barium;

Three other barium alkoxides which we investigated were the derivatives of 2-butanol, 2,6-ditertiarybutyl phenol and 3-methyl-3-pentanol. The preparation of all of these alkoxides was undertaken using the same method as for the tertiary amyl alkoxide. We were only able to prepare the 2-butoxide effectively. The ditertiarybutylphenol derivative was seen to be unstable, with the solution changing from clear to orange during the reaction, whilst 3-methyl-3-pentanol reacted only slowly and failed to react adequately even under reflux conditions. All of the reactions were carried out under a dry nitrogen atmosphere and all products were seen to decompose badly on heating in vacuo. There was no evidence of any sublimation.

The 2-butanol reacted fully after 3 hours of reflux to produce a pale yellow solution. The alcohol was removed under vacuum, leaving an off-white solid residue. This solid was found to be involatile, but was clearly highly soluble in its own alcohol. However, other alcohols could not be used as solvents because of the risk of alcohol exchange and solubility in other solvents was inadequate. We were, therefore, unable

to produce a satisfactory ^1H NMR spectrum.

The microanalysis of the complex does not point conclusively to any obvious composition for the complex. The result of the analysis and the possible formulae for the unsubstituted alkoxide, the hydrate and the dialcohol species are as follows;

Found C 29.23%, H 6.25%
$C_8H_{18}BaO_2$ requires C 33.92%, H 6.36%
$C_8H_{20}BaO_3$ requires C 31.89%, H 6.64%
$C_{16}H_{38}BaO_4$ requires C 44.34%, H 8.81%

It can be seen from this analysis that the only possibilities are the hydrated alkoxide and the unsubstituted alkoxide. If the IR analysis is examined the hydrated species can be discounted due to the absence of any peaks between 3000 and 3600 cm^{-1}. However, the group of peaks between 275 and 595 cm^{-1} provide clear evidence of metal-oxygen bonds.

Taking into account the IR evidence, the product discolouration, the inaccuracy of the microanlysis and the product involatility it is anticipated that the alkoxide has a complicated, oligomeric structure. It is also possible that the product is an oxo species, which, as was described earlier, is known for some other barium alkoxides. If this were the case the discrepancy in the microanalysis would be greatly reduced.

5.2.3; Conclusion;

When both our own research and that of Caulton was taken into consideration we concluded that it was most unlikely to be possible to

prepare an alkoxide based upon branched or bulky alkyl chains. An alternative strategy was, therefore, required.

It was stated in Chapter 2 that the β–diketonates owed their volatility to the fact that four rather than two oxygens are able to bind to each barium. If it were possible to mimic this structure then this might prove to be a fruitful method of preparing a volatile alkoxide.

5.3; THE PREPARATION AND ANALYSIS OF ALKOXY ALCOHOLS;

Probably the best method of mimicing the β–diketonates is to use an alcohol of the alkoxy ethanol type ($CH_2(OH)CH_2OR$). For a volatile product to be prepared it is necessary for the metal to react with the hydroxy groups of the alcohol to remove a proton then for the alkyl chain to bend around the metal and form a bond through a lone pair on the oxygen atom (Figure 5.7a). A problem with these compounds is the possibility of the lone pair on the alkoxy oxygen being donated to an adjacent barium centre (Figure 5.7b).

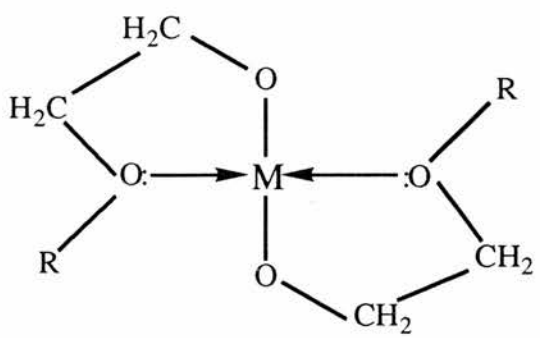

Figure 5.7a; Intramolecular bonding in a 2-alkoxy ethoxide complex

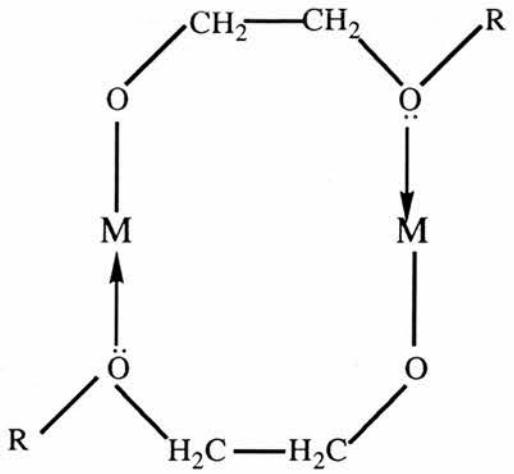

Figure 5.7b; Intermolecular bonding in a 2-alkoxy ethoxide complex

We chose to investigate the simplest of these compounds, using 2-methoxyethanol ($CH_3OCH_2CH_2OH$) as our alcohol. The use of 2-methoxy ethanol had previously been reported by Hubert-Pfalzgraf[77] who employed it to prepare an yttrium alkoxide. The structure of this yttrium complex was found to be decameric as a crown.

5.3.1; The preparation and analysis of barium 2-methoxyethoxide;

We prepared the alkoxide by direct reaction of the dry alcohol with barium metal in a dry nitrogen atmosphere. A rapid, exothermic reaction ensued, with all of the barium being consumed after 3 minutes.

It was not possible to recrystallise the product from diethyl ether. Sublimation testing produced only slight evidence of volatility and the product decomposed to a black powder on prolonged heating. We concluded that it was unsuitable for use as a CVD precursor.

Further analysis was not undertaken as, after our initial research, Caulton published a paper describing the preparation and structural determination of this complex. An overview of his work with

this ligand is now provided.

5.3.2; The preparation and structural identification of barium 2-methoxyethoxide[76];

Some time after concluding our unpublished research with this alcohol Caulton[76] prepared the barium alkoxide using different conditions from those which we had employed. The complex so prepared was reported as being volatile and could be sublimed at 160°C under a pressure of 10^{-1} Torr. However, the sublimate was obtained in a low yield of 30%. As we indicated in Chapter 2, it is necessary both to maintain a steady vapour pressure and to be able to re-use the precursor. This is most unlikely to be possible with such a low yield of sublimate, so our earlier view that this is not a suitable precursor for CVD is confirmed by this work.

Whereas we prepared the barium 2-methoxy ethoxide from barium granules and neat alcohol, Caulton undertook the reaction in toluene. As would be expected from our results, a rapid, exothermic reaction took place. Recrystallisation was undertaken from toluene / pentane.

In contrast to the reported structures of the phenoxide and t-butoxide, which had square pyramidal $Ba_5(\mu_5\text{-}O)$ units, this structure incorporates a fully encapsulated oxoligand (Figure 5.8). Each barium is coordinated to 8 oxygen atoms in this structure. The ligand is bound in three ways; through the terminal oxygen only, through both oxygens to one barium or through both oxygens to two adjacent barium centres to form a bridge. The molecular formula is $[H_4Ba_6(\mu_6\text{-}O)(OCH_2CH_2OCH_3)_{14}]$.

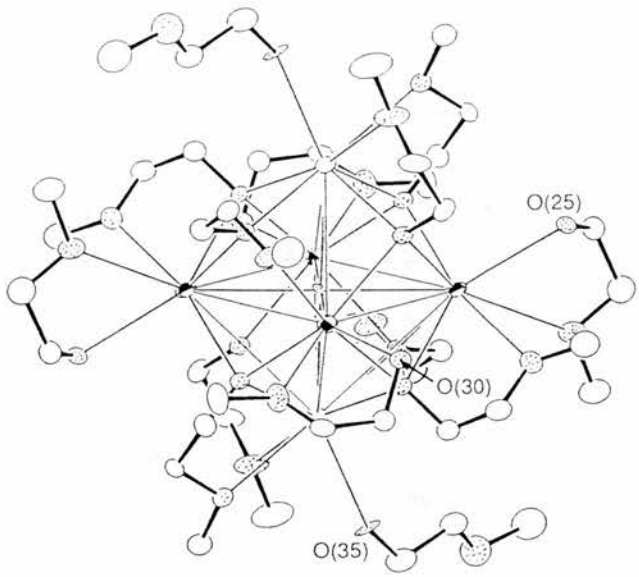

Figure 5.8; The crystal structure of
$[H_4Ba_6(\mu_6\text{-}O)(OCH_2CH_2OCH_3)_{14}]$[76]

Although this complex is unsuitable for CVD use it is certainly the most volatile barium alkoxide so far prepared. There may be future potential in this type of ligand, particularly if the methyl group is replaced by fluoroalkyl groups.

5.4; THE PREPARATION AND ANALYSIS OF BARIUM 1,1,1-TRIFLUOROETHOXIDE;

As we were unable to prepare a precursor of adequate volatility using bulky alkyl groups or bidentate alkoxides, we decided to investigate a new class of barium alkoxides. At this time it had been reported[18] that $[Ba(HFOD)_2]$ was both more volatile and more thermally stable than the DPM complex. We decided to apply the use of

fluorinated alkyl chains to alkoxides and, therefore, considered the preparation of barium fluoroalkoxides. We limited our investigations to the commercially available fluorinated derivative of ethanol in the belief that its highly fluorinated, compact nature would maximise the shielding around the barium centre.

5.4.1; The preparation of barium 1,1,1-trifluoroethoxide;

All of the operations were carried out under a dry nitrogen atmosphere using standard Schlenk techniques. 1,1,1-trifluoroethanol was dried and distilled prior to use. The ethoxide was prepared by direct reaction of the metal with the alcohol. The highly exothermic reaction was complete after 20 minutes. Recrystallisation was attempted at -20°C from diethyl ether. The crystals thus produced, like those of $[Ba(TDFND)_2]$, were unable to stand solvent removal and were converted to a dry powder under vacuum conditions.

5.4.2; The analysis of barium 1,1,1-trifluoroethoxide;

The ^1H NMR spectrum of barium trifluoroethoxide (Figure 5.9) was taken using deuterated methylene chloride as the solvent. A comparison is provided between the ^1H NMR of the alkoxide and the parent alcohol in Figure 5.10. Deuterated methylene chloride was used as the solvent in each case. The peaks and assignments were as shown in Table 5.3;

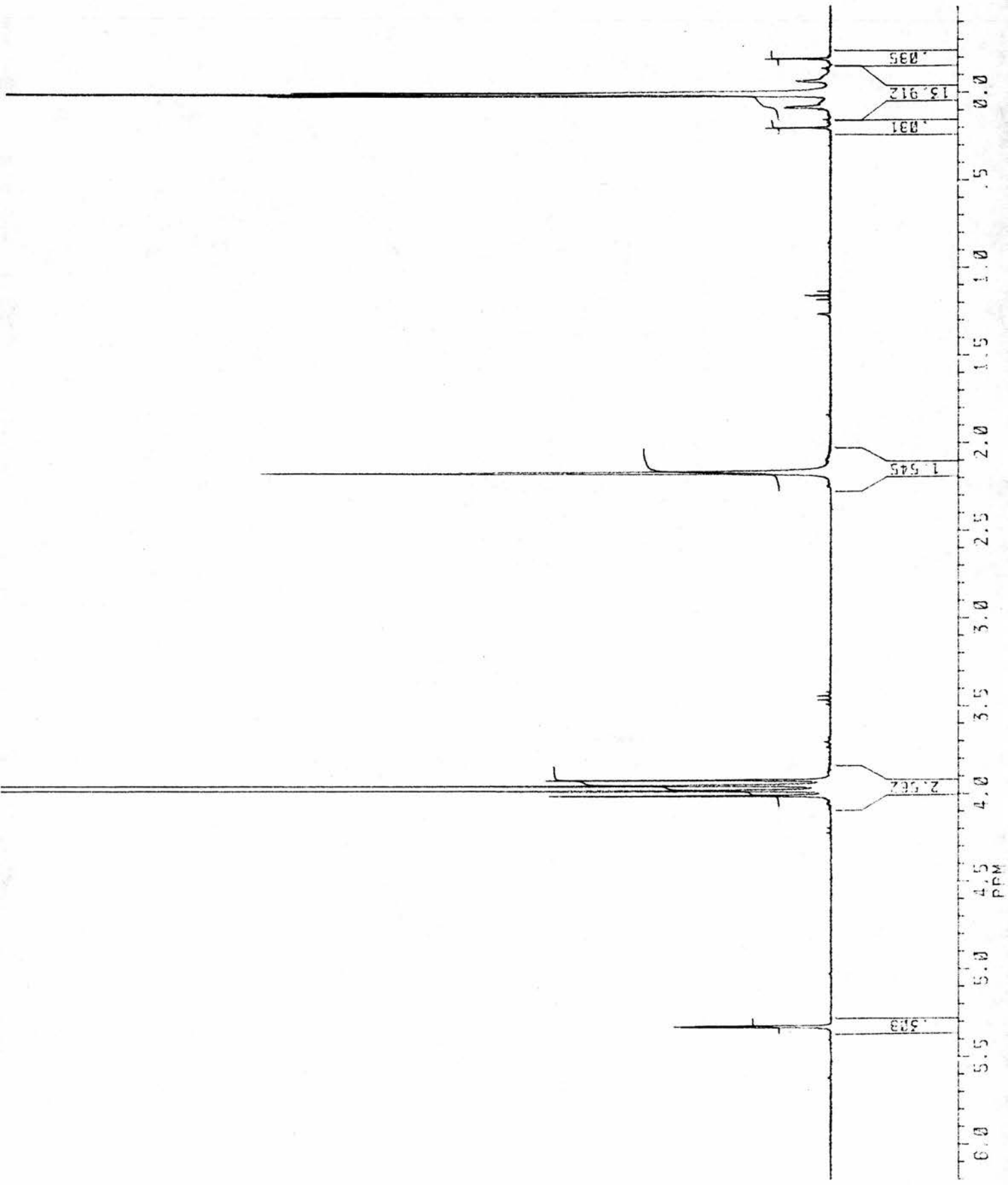

Figure 5.9; The ^{1}H NMR of barium trifluoroethoxide

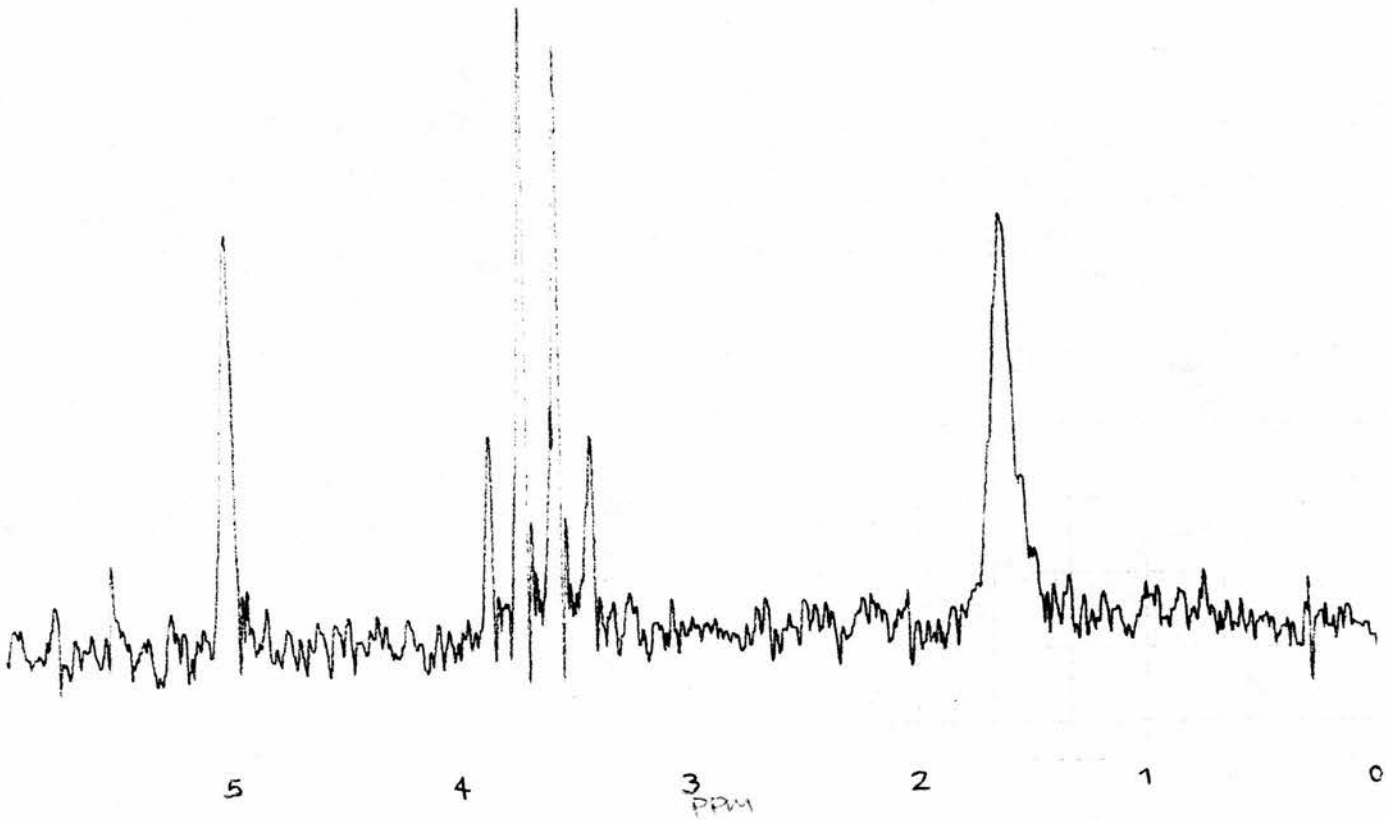

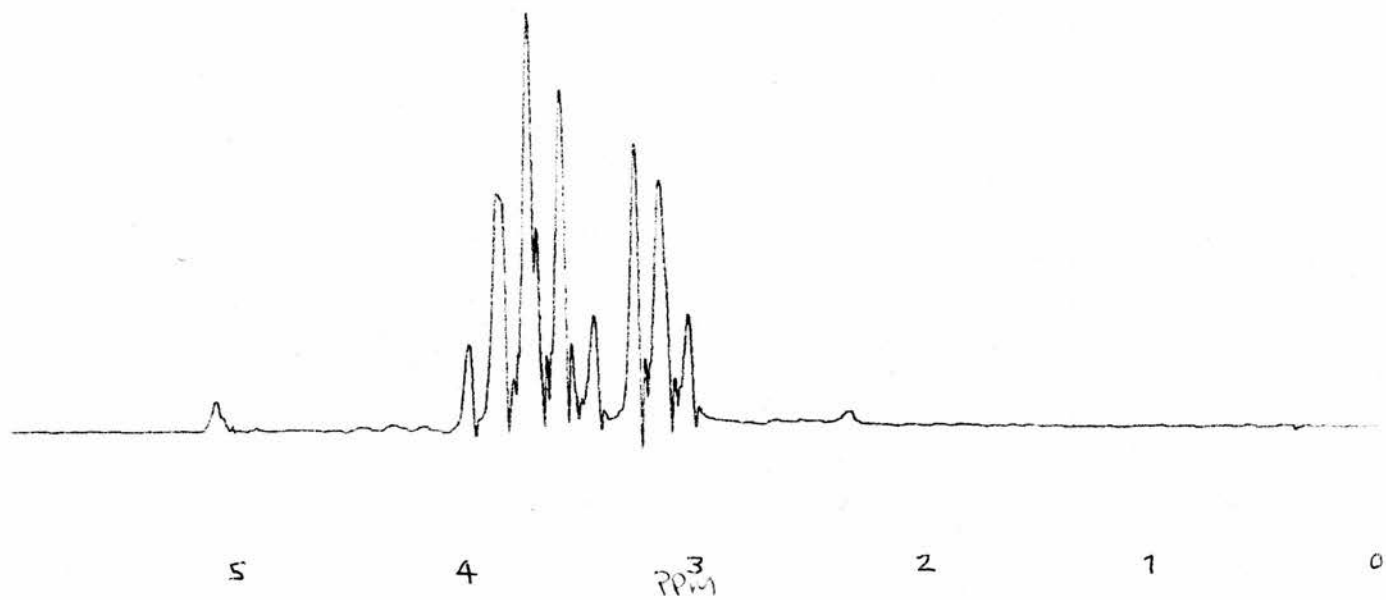

5.10; A comparison between the ^{1}H NMR of trifluoroethanol and that of barium trifluoroethoxide

Table 5.3; Peaks and assignments for the ^{1}H NMR spectra of trifluoroethanol and barium trifluoroethoxide

Sample	δ	Integral	Assignment
Trifluroethanol	3.15 (t)		OH
	3.8 (quintet)		CH_2
Barium trifluoroethoxide	2.1(s)	12.8	OH
	4.0 (quartet)	26.0	CH_2

The ^{19}F NMR spectrum was taken and showed only one peak, a triplet, at -77.1 ppm. The ^{13}C NMR has two peaks, a quartet at 124.9 ppm (coupling constant 271 Hz) and a quartet at 62 ppm (coupling constant 32 Hz).

It is clear from the ^{1}H NMR spectrum that there is still some alcohol in the product but we believe it is likely that it is bound to the metal. This is indicated by the shift in the OH proton and by the change from quintet and triplet to quartet and singlet of the two peaks. The apparently simple nature of both this spectrum and of the ^{19}F and ^{13}C NMR spectra can be explained by a proton exchange going on between the alkoxide and the alcohol in the solution phase.

In an attempt to freeze out this phenomenon, the low temperature ^{1}H NMR of the complex was taken. This was done at 223 K and was identical to that at room temperature, so we were able to conclude that the hydrogens were identical even at this low temperature.

The main peaks of the IR spectrum form a good fit with what we would have anticipated. The band at 1010 cm^{-1} is likely to be the result of C-O stretching[61], whilst the bands between 520 and 215 cm^{-1} are indicative of metal-oxygen bonds. There are no peaks in the region

3000-3600 cm^{-1} so we may conclude that there is no residue of alcohol present. However, there is a broad peak around 2600 cm^{-1} which, according to Williams and Fleming[80] is the expected location for a bound alcohol molecule. If this is a correct assignment it fits in well with our other spectral evidence for this complex. Finally, the bands between 1080 and 1300 cm^{-1} are attributable to carbon-fluorine bonding.

Further confirmation of the presence of bound alcohol comes from the microanalysis of the complex;

Found	C 17.8%, H 1.84%
$C_4H_6BaF_6O_2$	requires C 14.0%, H 1.2%
$C_8H_{10}BaF_{12}O_4$	requires C 17.9%, H 1.86%

The second formula is seen to fit the microanalytical data almost exactly and represents a complex of formula $[Ba(OR)_2(ROH)_2]_n$. We propose that the hydrogen is effectively shared between two alkoxides bound to the metal (Figure 5.11)

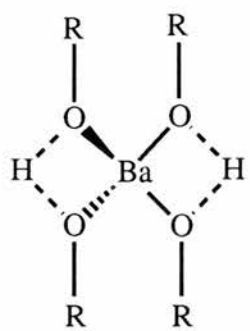

Figure 5.11; Proposed structure of barium trifluoroethoxide

5.4.3; Sublimation testing of barium 1,1,1-trifluoroethoxide;

We attempted the sublimation of this alkoxide using the same apparatus as had been used for the β–diketonates, that is with the system under active vacuum with a dry nitrogen stream passing over the complex under study (Section 4.2.4.8). There was no marked evidence of sublimation, even with the heater bath at 250°C, and decomposition set in at 180°C. It was our belief that the heating of the sample to this temperature had driven off the bound alcohol which we had previously identified.

In an effort to prevent the alcohol being driven off, we introduced a bubbler containing dry trifluoroethanol into the nitrogen stream. This stabilised the alkoxide at higher temperatures and increased the onset of decomposition to 240°C. There was, however, still no evidence of sublimation despite the heater bath temperature being raised to 270°C on this occasion.

As we described in chapter 2, the introduction of an amine base into the carrier gas had been reported by Barron[48] to increase greatly the volatility of certain diketonates. Hence, we applied this to the trifluoroethoxide and passed the nitrogen through triethylamine prior to entry into the heated flask. Again the complex decomposed with no evidence of sublimation, at a slightly enhanced temperature of around 200°C.

5.5; EXPERIMENTAL DETAILS:

5.5.1; Barium tertiary amyl alkoxide;

Because tertiary amyl alcohol does not react with magnesium, it was dried using barium granules. The alcohol was added to barium granules (ca. 5g) in the presence of an iodine catalyst. This was refluxed for 3 hours under a nitrogen atmosphere, after which time all of the barium had been consumed, and then distilled.

To the dry alcohol (400 cm^3) was added barium granules (7.5 g, 0.057 mol). The reagents were again refluxed for 3 hours after which time all of the metal had been consumed. The solution was then filtered hot in order to prevent product precipitation and the unreacted alcohol was removed in vacuo. The product was a slightly off-white solid.

IR; 270(m), 355(m), 380(m), 435(m), 475(s), 500(m), 530(m), 875(s), 955(s), 985(m), 1010(w), 1040(M), 1160(s), 1210(m), 1280(w), 1350(m), 3100-3600(w) cm^{-1}.

5.5.2; Barium-2-butoxide;

The alcohol was pre-dried over molecular sieves. It was then dried further by reaction of 100 cm^3 of the alcohol with 5 g of barium. The alcohol was then purified further by distillation.

Barium (2.5 g, 0.018 mol) was refluxed for two hours with the alcohol (50 cm^3). After this time all of the metal had been consumed. The yellowish solution was filtered hot and a yellow-white solid was obtained after the alcohol had been removed under vacuum.

IR; 275(s), 390(m), 415(s), 450(s), 475(m), 510(s), 595(w), 765(m), 775(m), 810(m), 900(s), 950(s), 980(s), 1025(s), 1125(s), 1255(m) cm^{-1}.

5.5.3; Barium 2-methoxy ethoxide;

Barium granules (5.0 g, 0.036 mol) were added to the dry alcohol (50 cm^3) contained in a three necked flask fitted with a double surface condenser. A vigorous reaction ensued involving the rapid evolution of hydrogen and total consumption of the barium metal after 3 minutes. The solution was, again, filtered hot and the solvent was removed in vacuo.

IR; 280(s), 380(s), 430(w), 470(m), 540(s), 715(w), 820(s), 885(s), 945(s), 1000(s), 1050-1130(s), 1185(s), 1230(s), 1270(s), 1315(m), 1580(w), 1895(w), 1950(w), 1990(w), 2075(w) cm^{-1}.

5.5.4; Barium 1,1,1-trifluoroethoxide;

1,1,1-trifluoroethanol was pre-dried with $CuSO_4$ / $NaHCO_3$ (the latter to remove traces of acid) and distilled prior to use.

To barium granules (5.05g, 0.037 mol) was added dry 1,1,1-trifluroethanol (80 cm^3) contained in a three necked flask fitted with a double surface condenser. Evolution of gas commenced immediately on the addition of the alcohol. After 20 minutes the reactants had warmed to the alcohol's boiling point and reaction was complete. On cooling for 30 minutes the product crystallised out to form a solid mass in the flask. Diethyl ether (100 cm^3) was then added to dissolve the solid prior to filtration. The filtered solution was then

placed in the freezer at -20°C for recrystallisation.

IR; 215(w), 235(w), 255(w), 270(w), 280(w), 290(w), 315(w), 340(w), 385(m), 520(w), 660(m), 795(s), 840(s), 965(s), 1010(s), 1080(s), 1150(s), 1250(s), 1300(s), 2650(m,br) cm^{-1}.

CHAPTER 6

A SUMMARY OF CVD WORK CARRIED OUT AT THE UNIVERSITY OF STRATHCLYDE USING BOTH NEW AND ESTABLISHED PRECURSORS

6.1: INTRODUCTION:

The majority of the work described in this chapter was carried out by Douglas Gilliland at the University of Strathclyde under the supervision of Professor Michael Hitchman. However, the analysis of used samples removed from the CVD apparatus and the associated assessment of the level of decomposition was undertaken by ourselves.

This chapter is, of necessity, a summary of the most important investigations carried out at Strathclyde, which are ongoing. A more detailed and finalised report of this work must await the publication of Douglas Gilliland's thesis.

6.2: THE CVD SYSTEM:

A description of the basic structure of a CVD apparatus was provided in Chapter 1. The apparatus which was used by our co-workers was manufactured specifically for superconductor CVD by Archer Technicoat. It consists of four ovens for precursor pots, linked to the reactor by heated lines. These are maintained at a minimum of 10-15°C above the sublimation temperature of the precursors to prevent deposition in the lines. The reactor itself is warm-walled with the temperature being held at 200-250°C, depending upon the precursor used (Most precursors required a temperature of around 200°C whilst [$Ba(DPM)_2$] needed an increased temperature of 250°C because of its higher volatilisation temperature). This heating was necessary to prevent the deposition of precursors on the reactor walls. The reactor contains a heater platform capable of a maximum temperature of 950°C.

In all cases the pressure used in the system was 10 Torr and the substrate temperature was usually 730°C although in certain cases a

slightly lower temperature was used. The carrier gas was Air Products 5.0 Grade Argon (99.999% purity) delivered at a flow rate of 200 standard cubic centimetres per minute (sccm).

During the deposition of YBCO, the oxygen was introduced to the system via line four. As the complexes are co-deposited, the oxygen and all three of the precursor vapours first meet, and are mixed, immediately before they enter the reactor. In this way it has proved possible to co-deposit oxide films. Despite this action, however, some complexes still deposit fluoride films.

6.3: SAMPLE PREPARATION:

In order to assist reproducibility, all precursors were pelleted using a standard technique (Fgure 6.1). 0.75g of the sample was placed in a metal container to which was applied a pressure of 3000 Kg. The sample was, thus, compacted to a depth of 2-3 mm.

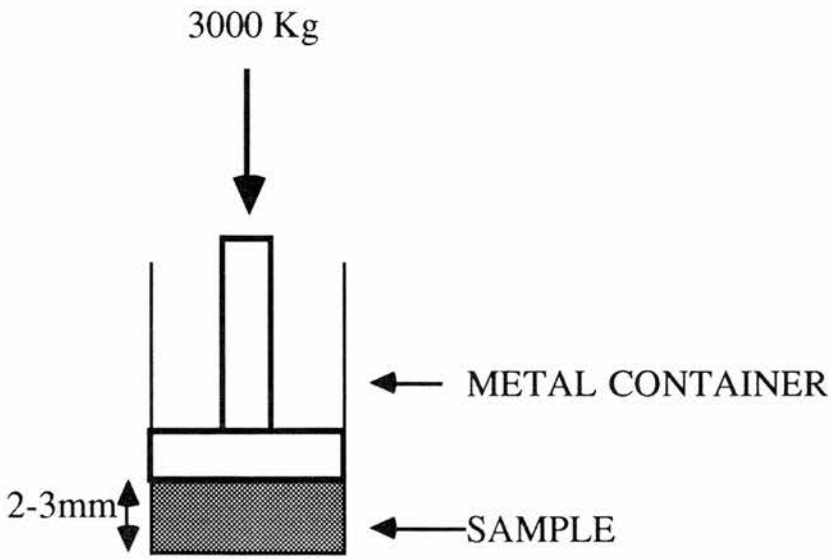

Figure 6.1; Preparation of a pelleted sample

6.4: PRECURSOR PERFORMANCE:

In order to obtain YBCO films reproducibly using the pelleted materials it is important that the precursors satisfy two conditions. Firstly, the precursor must be volatile below its decomposition temperature and, secondly, it must be stable at this temperature for an exposure time of 6-8 hours.

All of the precursors which have so far been evaluated for CVD use have been discussed in earlier chapters. An assessment of the performance of, and the film quality produced from, precursors of copper, yttrium, barium, calcium and strontium which have been used up to the present time is now given.

6.4.1; Copper;

The two precursors which were used for the CVD of this metal were $[Cu(ACAC)_2]$ and $[Cu(DPM)_2]$. The $[Cu(ACAC)_2]$ was found to be sublimable at 150°C. After 3-4 hours of heating some slight decomposition had occurred, making this a less than ideal preccursor. X-Ray Diffraction (XRD) results indicate that the deposited film is either copper metal, copper (I) oxide (Cu_2O) or copper (II) oxide (CuO) depending upon the conditions used. For example, low temperature deposition in the absence of oxygen will lay down copper metal whilst using the same temperature with oxygen will produce a Cu_2O film.

The $[Cu(DPM)_2]$ was tested in order to see whether this brought about any improvement in thermal stability and a lowering of deposition temperature. This proved to be the case. $[Cu(DPM)_2]$ was deposited in the range 110-140°C and had not suffered any

decomposition after repeated use. It was also found that this complex was able to maintain a stable vapour pressure throughout more than ten deposition runs.

This precursor has been used to produce successfully a film containing copper, yttrium and barium which was found to be semiconducting. The other precursors used in this case were $[Y(DPM)_3]$ and $[Ba(HFOD)_2]$. Work to assess the chemical composition of films containing copper only, prepared using $[Cu(DPM)_2]$, are ongoing.

6.4.2; Yttrium;

$[Y(DPM)_3]$ was found to be an ideal precursor as it satisfied the major criteria of a low volatilisation temperature and good thermal stability. The temperature used for the volatilisation of the complex was varied in the range 110-140°C. There was no apparent decomposition of the sample, even after repeated use. As with $[Cu(DPM)_2]$ it was possible to maintain a steady vapour pressure of this complex throughout deposition runs. Figure 6.2 shows clearly that the complex is capable of producing consistent film thicknesses over a series of runs using the same deposition conditions.

An XRD examination of the deposited film showed that yttrium (III) oxide (Y_2O_3) had been deposited. The films were of good quality and there were some indications of textured growth.

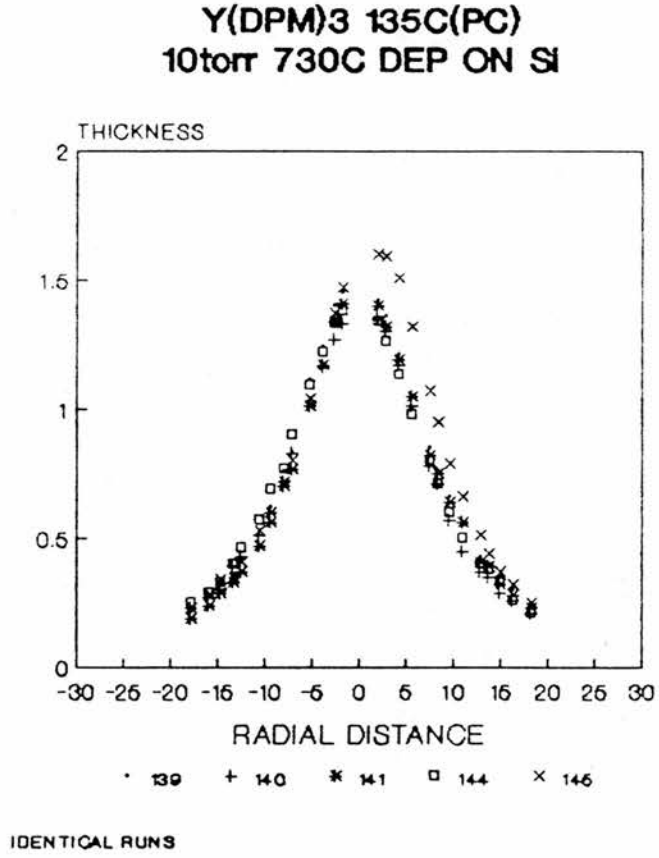

Figure 6.2; Film thicknesses from a series of five deposition runs using identical conditions

6.4.3; Barium;

6.4.3.1; [$Ba(DPM)_2$];

Whilst initial work with this complex showed that it was of low volatility and thermal stability, more recent research has produced some good quality films. It has been possible to obtain a film composition with a Y:Ba:Cu ratio close to 1:2:3 using [$Cu(DPM)_2$], [$Y(DPM)_3$] and [$Ba(DPM)_2$]. The temperatures inside the precursor pots were 107°C, 115°C and 241°C respectively. However there was still a rapid drop in the [$Ba(DPM)_2$] vapour pressure after 30 minutes at this temperature,

thus hindering the reusability of this sample.

6.4.3.2; [$Ba(HFOD)_2$];

[$Ba(HFOD)_2$] was transported in the temperature range 180-190°C. It was found that this complex was capable of producing a remarkably consistent deposition profile. Table 6.1 demonstrates the consistency attained using this complex. The tests outlined in this table were run over a three day period and involved a total run time of 28 hours.

This reproducibility can, in part, be explained by an analysis of the residue after its use in the CVD apparatus. The examination of the used complex was undertaken using three techniques, namely ^1H NMR, IR and STA, in order to achieve a valid comparison with the complex prior to the CVD runs.

It should first be stated that the used complex differs in appearance from the pure white unused sample as it has a light brown colouration. The used complex dissolves to a large extent in methanol to give a brown solution, although a brown residue does remain. The ^1H NMR spectrum of the filtered sample was taken in deuterated methanol for this reason. The peaks, integrals and assignments for this spectrum are described in Table 6.2.

Table 6.1; [$Ba(HFOD)_2$] deposition trial;

RUN	GROWTH RATE(μm/hour)	TOTAL HEATING TIME
1	0.57	
2	0.57	
3	0.56	11 HOURS
	END OF DAY 1	
4	0.47	
5	0.48	
6	0.47	
7	0.41	19 HOURS
	END OF DAY 2	
8	0.78	
9	0.75	
10	0.69	
11	0.58	28 HOURS

The following conditions applied to this trial:

Source temperature=180°C*

Temperature inside the precursor pot 167°C*

System pressure=10 Torr

Deposition temperature=700°C

Precursor weight=0.75 g

Warm-up time=1 hour

* 180°C was the temperature of the heater box surrounding the steel precursor container. The thermocouple inside the pot touching the chemicals showed a lower value of 167°C. Both temperatures are provided as the use of the thermocouple is a recent addition intended to provide a better idea of the thermal properties of the complex.

Table 6.2; ^1H NMR Spectral details and assignments for the $[Ba(HFOD)_2]$ CVD residue.

CHEMICAL SHIFT (δ)	INTEGRAL	ASSIGNMENT
0.95 (s)	16	impurity
1.10 (s)	92	CH_3
1.20 (s)	13	impurity
2.625 (broad)	15	water
5.80 (s)	9	C-H
6.70 (s)	1	impurity
7.35 (s)	5	solvent

The comparable spectral details for the unused sample are provided in Chapter 7. In this case there were only three peaks, these representing the tertiary butyl groups, water and the methyne proton.

Although the discovery of the nature of the impurities in the used complex might increase our understanding of the decomposition process,we were more concerned with the size of the impurity integrals relative to those of the $[Ba(HFOD)_2]$. It is clear from this comparison that the vast majority of the $[Ba(HFOD)_2]$ sample has not decomposed, although it should be added that a further 10% of the sample was insoluble in the NMR solvent. The continued presence of water in the complex was also a vital observation. Further comment of the relevance of this will be made shortly.

The STA comparison of the used and unused samples is shown in Figure 6.3. It can be seen that there are notable differences between the two complexes. The used complex clearly contains far less water

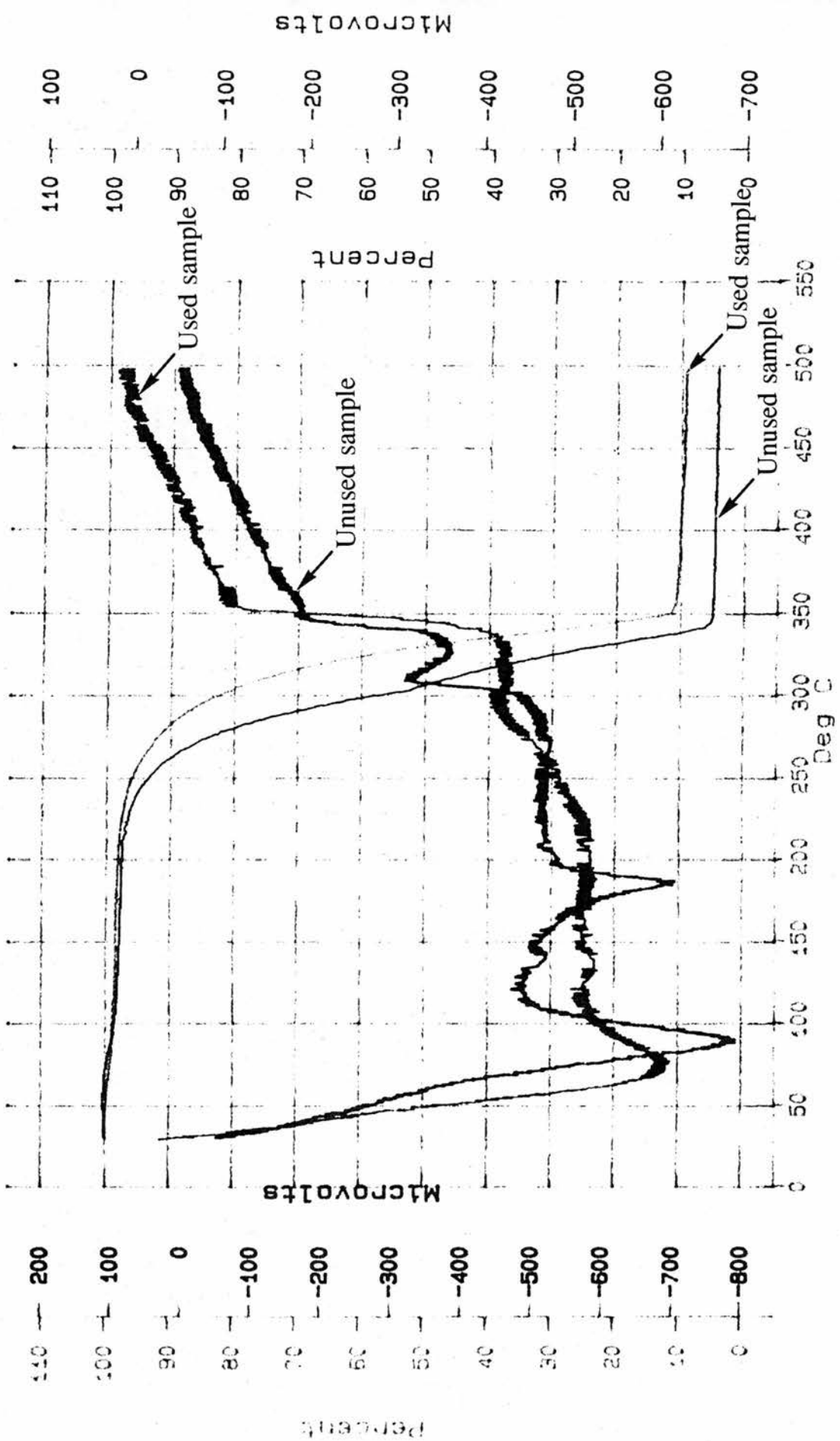

Figure 6.3; A comparison of the STA analyses of used and unused $[Ba(HFOD)_2]$

than the unused complex and does not have the melting point at 185°C. Furthermore, it has a far larger exotherm after sublimation and a residue around twice the size of that in the unused complex. The likely explanation for this is that a structural rearrangement occurs to produce a second structure which is almost as volatile as that found in the unused sample. This leads to a different STA profile but allows for continued volatility of the complex.

The IR peaks were as follows; 215(w), 240(w), 290(w), 335(w), 370(w), 450(w), 470(m), 530(m), 565(w), 580(w), 620(w), 685(m), 735(m), 750(m), 790(m), 825(m), 900(m), 930(m), 955(m), 1010(m), 1055(m), 1110(s), 1150(s), 1220(s), 1270(s), 1340(s), 1505(s), 1635(s), 3250-3550(w) cm^{-1}.

The IR analysis confirms the observations which were made in the ^1H NMR analysis. A comparison of the peaks from the used sample with those obtained for the un-used sample (provided in Chapter 7) shows that the two samples are extremely similar. The conclusion from this particular analysis would be that the sample is mainly intact but has undergone limited decomposition.

The aspect of the IR spectrum which is of most interest is the presence of a small water peak which shows that the sample has not completely dehydrated. In fact the amount of retained water, as observed in the ^1H NMR, is surprisingly high. This may be due, in part, to the exposure of the sample to the air during and after the removal from the CVD rig, allowing the sample to partially rehydrate.

However, we believe that some bound water was retained after the CVD runs and that the presence of this water in the new structure was the key to the retention of volatility. The retention of at least some

of this water is clearly continuing to prevent oligomerisation and, thus, enables reproducible deposition rates to be maintained throughout a series of CVD runs.

It appears that there is something of a contradiction between the result of CVD testing and the STA of $[Ba(HFOD)_2]$. According to the STA the complex decomposes close to its sublimation temperature but this does not happen in the CVD rig. It must be remembered that the heating conditions were greatly different in the two cases. In this STA the temperature is increased steadily at a rate of 20°C per minute, so the product is not held at its sublimation temperature. Furthermore, the analysis is carried out at atmospheric pressure and will involve higher temperatures as a result. In CVD, however, the product is held at the sublimation temperature (which is relatively low as the pressure is only 10 Torr) and it may be that the fact that this temperature is not exceeded is greatly responsible for the lack of decomposition.

The as-deposited films for barium deposition only were found, by XRD, to be barium (II) fluoride (BaF_2). The optimum conditions for the deposition of a mixed oxide layer involved the heating of the barium precursor to 185°C. When used with $[Cu(ACAC)_2]$ and $[Y(DPM)_3]$ which were heated to 150°C and 140°C respectively the resultant film had the following composition; $YBa_{1.3}Cu_{2.2}$.

6.4.3.3; $[Ba(DFHD)_2]$;

$[Ba(DFHD)_2]$ was transported in the slightly higher temperature range of 200-210°C under a pressure of 10 Torr. There was some visible decomposition at vapourisation temperatures above 205°C after 90-120 minutes of heating.

A comparison can be made with the $[Ba(HFOD)_2]$ for the

preparation of a mixed oxide film using comparable conditions to those described above. In this case it was necessary to vapourise the precursor at 210°C and this produced a film composition of $YBa_{1.6}Cu_4$. Whilst this is a marginally better composition than for the $[Ba(HFOD)_2]$, the associated decomposition has prevented the attainment of the same reproducibility.

6.4.3.4; $[Ba(TDFND)_2]$;

$[Ba(TDFND)_2]$ was transported in a similar temperature range to $[Ba(HFOD)_2]$, but was found to deposit at a far greater rate. The problem with this ligand, however is that the rate of deposition falls as runs are repeated. The largest fall is seen after the first run, which we believe may be caused by the sample being dehydrated. The removal of water produces vacant sites in the complex which might result in sample oligomerisation and is likely to render the anhydrous sample less volatile than the hydrated sample.

However, the situation is somewhat paradoxical. As we have already described, the $[Ba(HFOD)_2]$ complex appears to have decomposed to some extent during the deposition process. Despite this it appears to continue to produce films at a reasonably constant rate. $[Ba(TDFND)_2]$, on the other hand, does not appear to have undergone the same degree of decomposition yet its volatility decreases rapidly as the series of runs progresses. Figure 6.4 clearly shows this phenomemon.

If we now examine the DTA of both the used and the un-used complexes (Figure 6.5) we can see that there is no great change between the two. Taking first of all the DTA of the un-used sample, which we

examined in detail in Chapter 4, the most important feature for our purposes is the relatively steep drop from 140 to 170°C. We have already atrributed this to the loss of bound water from the complex. This feature is absent from both of the analyses of used samples and may be because the sample is wholly dehydrated after the CVD runs.

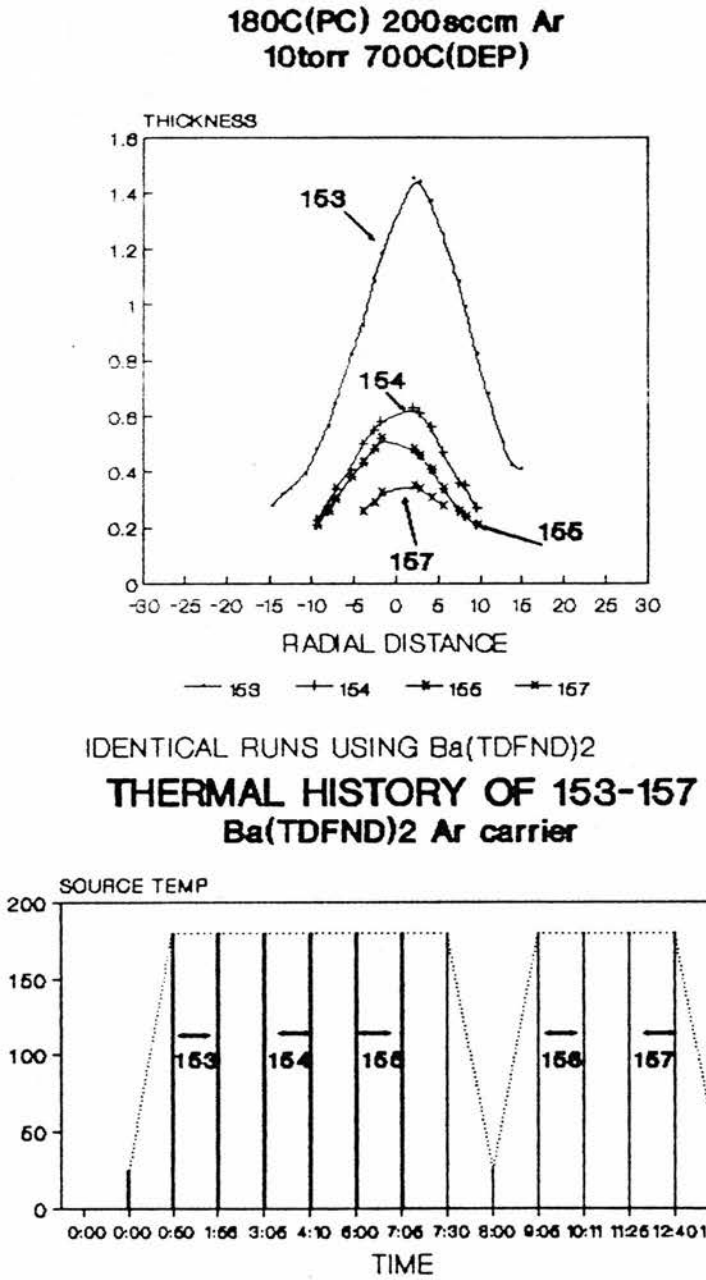

Figure 6.4; The film thicknesses produced from a series of four deposition runs using [$Ba(TDFND)_2$]

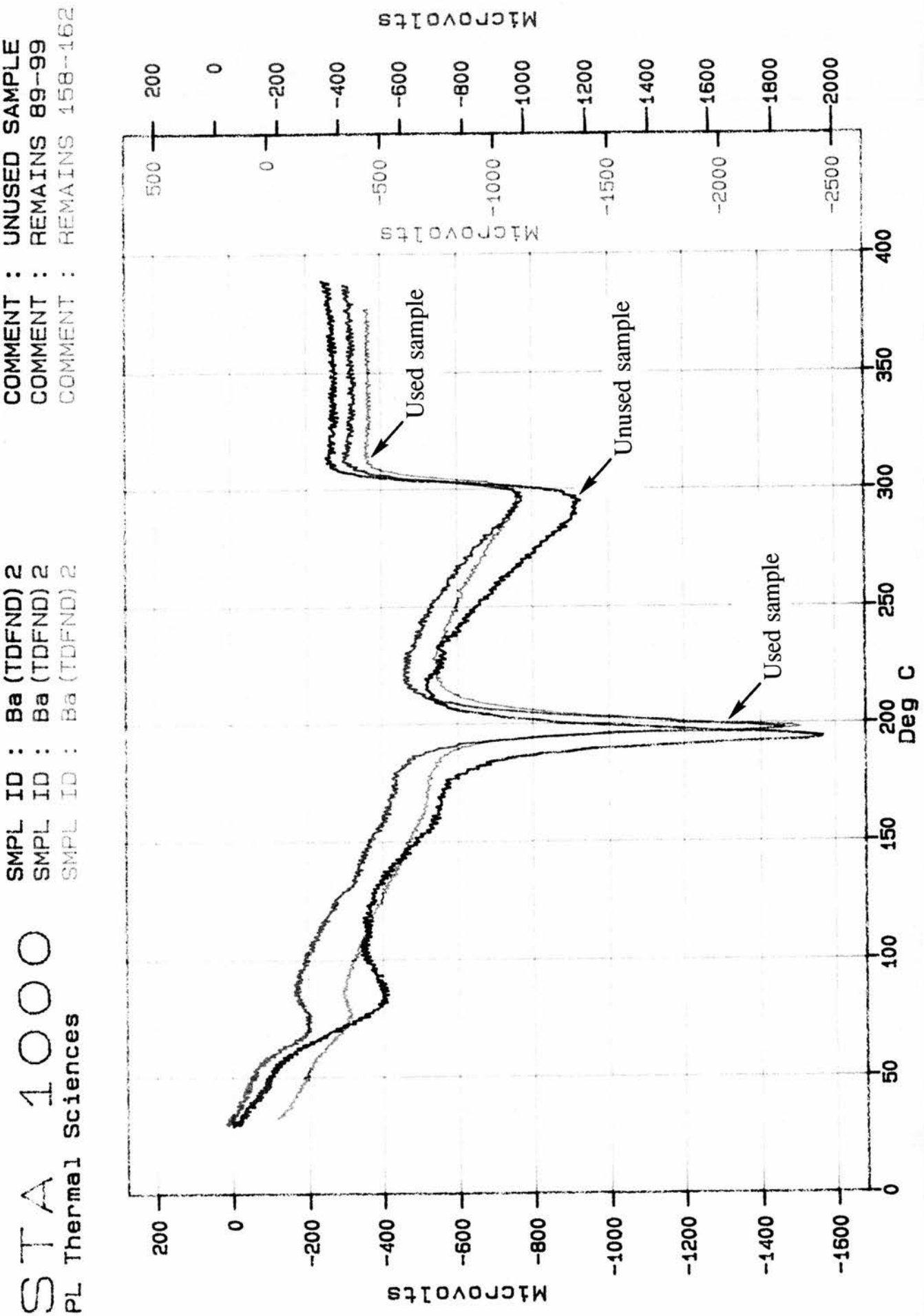

Figure 6.5; DTA comparison of used and un-used [$Ba(TDFND)_2$]

This ties in well with our finding described in Chapter 4 that it is possible to dehydrate this complex by maintaining a temperature of 100°C for 1 hour under vacuum conditions. The other notable feature of the DTA is that the used samples sublime at a temperature around 10°C higher than that required to sublime the un-used sample. A dehydration of this sample leading to increased intermolecular interactions is a possible explanation for this phenomenon.

A comparison of the three weight loss curves (Figure 6.6) shows them to be almost identical and indicates that volatilisation is almost total in all cases as the residue is always essentially zero.

It has been intimated that the [$Ba(TDFND)_2$] has not decomposed to any great extent. The STA shows that the volatility of the complex is maintained and that there is only a very small residue remaining after the completion of the analysis. An examination of the IR and ^1H NMR of the used sample will confirm the level of decomposition of the complex and whether dehydration has taken place.

The ^1H NMR of the complex was taken in D_4-methanol and was found to dissolve totally in this solvent, leaving no residue, to produce a light brown solution. The fact that the sample was entirely soluble enables a good comparison between the amount of decomposed product and of intact complex in the residue to be made using this technique. The spectrum of this sample was seen to be identical to that of the unused complex, except for the greatly reduced size of the OH peak. This can be attributed to the loss of water from the sample during the heating process.

In a further effort to examine the extent of decomposition the ^{19}F NMR of the sample was taken. We were particularly interested to see whether any barium fluoride had been produced during the heating process. Again the peaks in the spectrum of the used sample at -81, -120

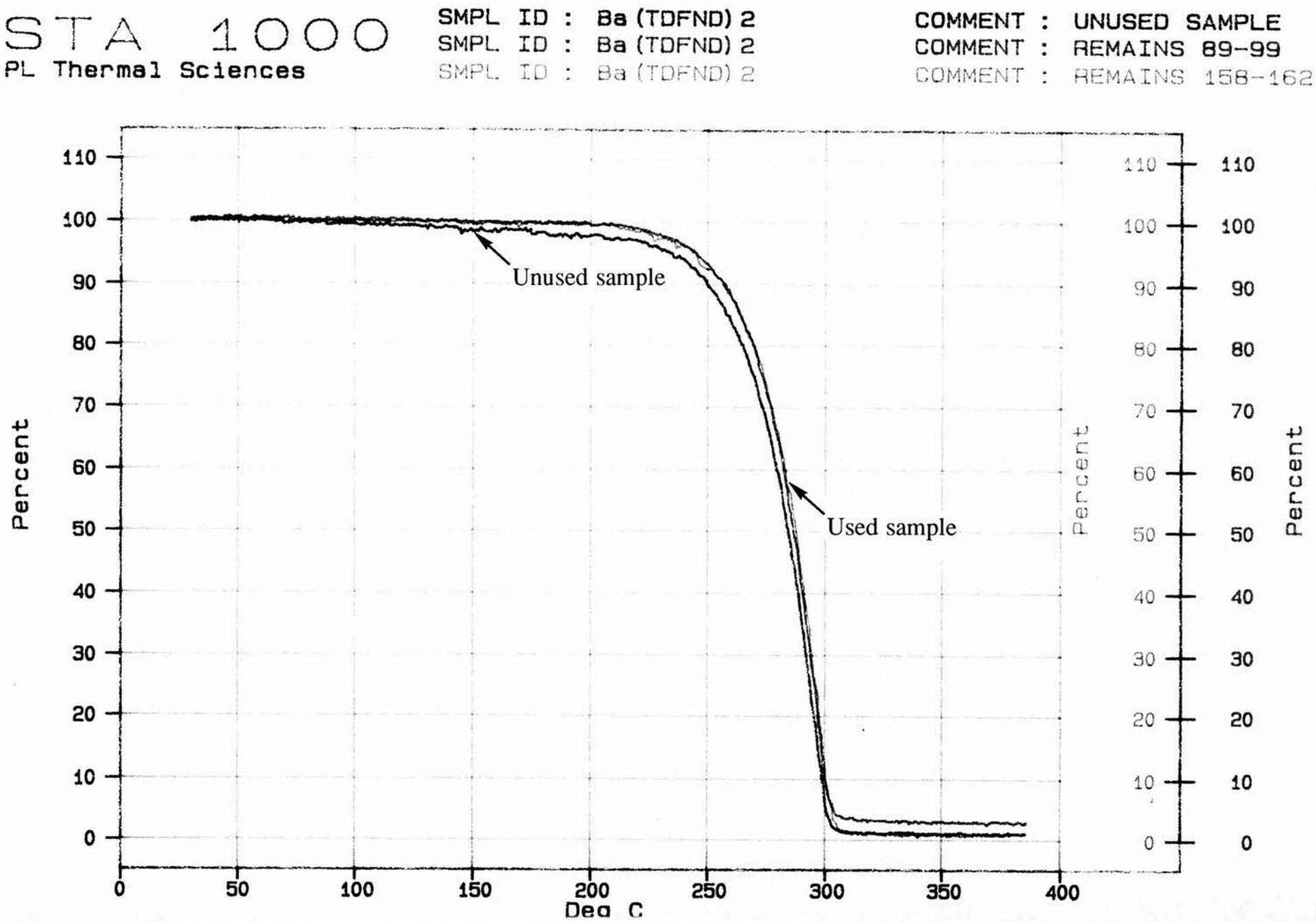

Figure 6.6; Weight loss comparison of used and un-used [$Ba(TDFND)_2$]

and -126.5 were identical to those in the un-used sample.

The IR peaks were as follows; 220(w), 240(w), 290(w), 315(w), 445(w), 525(m,br), 565(w), 670(w), 715(m), 770(w), 870(w), 915(m), 935(m), 955(m), 1050(m), 1110(s), 1135(m), 1175(s), 1220(s), 1275(m), 1450(s), 1505(s), 1645(s) cm^{-1}.

The major difference between this spectrum and that of the unused complex is the absence of a peak in the 3000-3600 cm^{-1} region which provides further confirmation that the sample has been dehydrated.

On the basis of the analytical evidence we were able to conclude that the sample was, at worst, only undergoing slight decomposition. The loss of volatility of the complex must therefore be attributed to the loss of water from the complex. However, we know that water is lost quite readily so how can the continued reduction in volatility as a series of deposition runs be explained? We believe that as water is lost from the complex a gradual rearrangement in the molecular structure takes place. This is most marked during the loss of water which leads to some oligomerisation and reduces the volatility. As the complex is heated for a longer time this oligomerisation continues at an increasingly slower rate until the prefered anhydrous structure is attained. The net effect of this gradual structural rearrangement can be observed in Figure 6.4.

6.4.4; Calcium;

Investigations have thus far been limited to the $[Ca(DFHD)_2]$ complex. This has been volatilised in the range 120-130°C but was found to suffer severe decomposition. The deposited films were found

by XRD to be calcium (II) fluoride (CaF_2). They were of poor quality and suffered from major cracking and poor adhesion. This was probably due to a mismatch of the thermal expansion between the film and the silicon wafer on which it was deposited.

6.4.5; Strontium;

As was the case for calcium, investigations have been limited to the DFHD complex.This required a far higher source temperature in the range 180-185°C to facilitate deposition. Once again, the complex underwent severe decomposition. The films produced were, however, of good quality and were found, by XRD, to be highly orientated strontium (II) fluroide (SrF_2).

CHAPTER 7

EXPERIMENTAL SECTION;
THE PREPARATION OF ESTABLISHED PRECURSORS

7.1; PREPARTION AND ANALYSIS OF COPPER β-DIKETONATES:

As we intimated in earlier chapters, $[Cu(ACAC)_2]$ and $[Cu(DPM)_2]$ have adequate volatility for use as CVD precursors and, consequently, our work has concentrated upon these two complexes. Whilst these compounds are now commercially available, we have synthesised both of them. $[Cu(ACAC)_2]$ was prepared by the method described by Peacock[81] whilst we based the preparation of $[Cu(DPM)_2]$ upon that which we had developed for the β−diketonates of other metals.

7.1.1; Preparation and analysis of $[Cu(ACAC)_2]$;

H(ACAC) (12.82 g, 0.13 mol) was dissolved in the minimum volume of dilute ammonia in order to give a homogeneous solution. This was added slowly to a solution of copper (II) sulphate pentahydrate (16.00g, 0.064 mol) in water (250 cm^3). The resultant pale blue precipitate was collected, washed with water (200 cm^3) and then ether (50 cm^3) and recrystallised from methanol to give dark blue needles.

The analysis of this, and other, copper β-diketonates cannot be undertaken using NMR techniques due to the paramagnetic nature of the complexes. However, the $[Cu(ACAC)_2]$ and $[Cu(DPM)_2]$ complexes are easily identified by other analytical techniques.

Aldrich reports that $[Cu(ACAC)_2]$ decomposes without melting. We confirmed this and observed decomposition, accompanied by some sublimation, under atmospheric pressure at 250°C.

We were able to compare our IR spectrum with that of Duval[82] and obtained a close match between our peaks and their reported

findings.

IR peaks; 215(s), 235(w), 255(w), 280(m), 420(w), 445(s), 620(m), 660(m), 690(m), 790(s), 945(m), 1030(s), 1195(w), 1270(m), 1350(m), 1520(s), 1540(m), 1575(s) cm^{-1}.

The 1575 cm^{-1} band can be assigned to the chelated carbonyl whilst that at 1520 cm^{-1} is due to the perturbed carbon-carbon double bond. The absence of the band in the 3000-3600 cm^{-1} region indicates that the complex is anhydrous. The strong bands in the 200 cm^{-1}-500 cm^{-1} region represent M-O vibrations.

7.1.2; Preparation and analysis of $[Cu(DPM)_2]$;

H(DPM) (5.52g, 0.03 mol) was dissolved in aqueous ethanol ($30cm^3$, 90%). NaOH (1.2g, 0.03 mol), also dissolved in aqueous ethanol ($30cm^3$, 50%), was slowly added to the stirred solution. The resultant solution was added to a stirred solution of copper (II) sulphate pentahydrate dissolved in aqueous ethanol ($50cm^3$, 50%). The reaction flask was evacuated and maintained under active vacuum until the volume of liquid had reduced by 25%. Water ($50cm^3$) was then added and the flask was again put under vacuum until the product precipitated. The purple solid was removed by filtration, washed with water ($50cm^3$) then dried in vacuo.

The melting point of the product was close to that reported by Aldrich (literature 198°C, found 196°C) and the purple colour of the complex was also as expected.

The IR peaks were; 220(w), 240(w), 275(m), 285(m), 320(w), 390(w), 615(w), 640(m), 745(w), 770(w), 800(m), 825(w), 875(m), 935(w), 960(w), 1020(w), 1150(m), 1180(m), 1225(m), 1245(w), 1360(m), 1400(s), 1500(s), 1535(m), 1550(s), 1565(m), 1590(m) cm^{-1}.

The assignment of the key peaks outlined in the discussion of the IR analysis of $[Cu(ACAC)_2]$ holds for this complex also. The peak at 1590 cm^{-1} is representative of the chelated carbonyl. The peak at 1565 cm^{-1} can be assigned to the perturbed carbon-carbon double bond. The absence of any peaks in the 3000-3600 cm^{-1} region confirms that this is an anhydrous species. There are several bands between 220 and 390 cm^{-1} which represent Cu-O vibrations.

7.2; PREPARATION AND ANALYSIS OF $[Y(DPM)_3]$;

This was based upon the method outlined by Eisentraut and Sievers[43]. H(DPM) (11.06g, 0.60 mol) was dissolved in ethanol (30 cm^3, 95%) in a flask with a vacuum connection. Sodium hydroxide (2.4 g, 0.60 mol) dissolved in ethanol (50 cm^3, 50%) was added. The stirred solution was then reacted with yttrium (III) nitrate pentahydrate (7.3 g, 0.20 mol) dissolved in aqueous ethanol (50 cm^3, 50%). The flask was immediately evacuated and the reactants were stirred for two hours. The volume was reduced by 50% and water (350 cm^3) was added. The product was then separated by filtration and purified by sublimation at around 180°C under vacuum.

The ^1H NMR was taken in $CDCl_3$. It was seen to have just two peaks for the product at δ 1.1 and δ 5.75 in the ratio 18.1:1 which clearly represent the tertiary butyl and methyne group hydrogens respectively.

The gas phase structure of the complex was assessed by electron impact mass spectroscopy. This clearly indicates that the complex is monomeric in the gas phase. The major peaks and their assignments are;

57	$[Bu^t]^+$
455	$[Y(DPM)_2]^+$
581	$[M\text{-}Bu^t]^+$
638	$[Y(DPM)_3]^+$

The IR peaks were; 215(s), 235(s), 305(w), 340(m), 470(s), 600(m), 750(m), 760(m), 790(m), 830(w), 865(s), 925(w), 965(w), 1015(w), 1120(s), 1175(m), 1215(s), 1240(m), 1280(m), 1350(s), 1495(s), 1530-50(m), 1565(s), 1590(m), 3000-3500(s) cm^{-1}.

It can be seen from the position of these peaks that this spectrum is closely related to that of the $[Cu(DPM)_2]$. The peaks at 1590 cm^{-1} and 1565 cm^{-1} represent the chelated carbonyl and perturbed carbon-carbon double bond respectively. The major differences are to be found below 500 cm^{-1} and above 3000 cm^{-1}. The broad peak in the 3000-3500 cm^{-1} region probably indicates the presence of water in the complex. The peaks below 500 cm^{-1} represent Y-O vibration bands which would be expected to differ from those seen in the IR of $[Cu(DPM)_2]$.

The melting point was recorded as 166-170°C which is slightly below that reported by Eisentraut and Sievers[43] (169-172.5°C)

The microanalysis result, shown overleaf, is close to the theoretical value and is within experimental error.

$C_{33}H_{57}O_6Y$ requires C 62.07%, H 8.93%.

found C 62.35%, H 9.30%.

7.2.1; The STA of [$Y(DPM)_3$];

This STA (Figure 7.1) represents in most respects the ideal which one would hope for from a CVD precursor. There is no evidence of any exotherms below the temperature at which most of the complex has sublimed and there is only a small percentage of residue (4.0%) remaining. Taking the worst case, that is all of the residue being [Y_2O_3], we still have 84% of the precusor volatilising intact. In reality the residue probably has a more complex structure and may contain some impurities so a greater proportion of the product than 84% will have volatilised.

Taking the individual events in turn we can obtain a clearer picture of the volatilisation of the complex. The first major trough is at 100°C and is accompanied by a 2.4% reduction in the weight loss curve. This reduction represents a loss of a unit with a molecular weight of 15.3. The closeness of this to 18 and the temperature involved leads us to the conclusion that this event is the loss of a mole of water.

The deep trough at approximately 170°C accompanied with only a tiny reduction in weight is clearly the fusion temperature of the complex. This correlates closely with the melting point which we had already measured.

The trough which deepens gradually in the region 200-250°C and the corresponding major and rapid weight loss indicates that the sample is vapourising. As has already been stated, there are no exotherms in this region so it appesrs that the sublimation is clean and occurs with little decomposition.

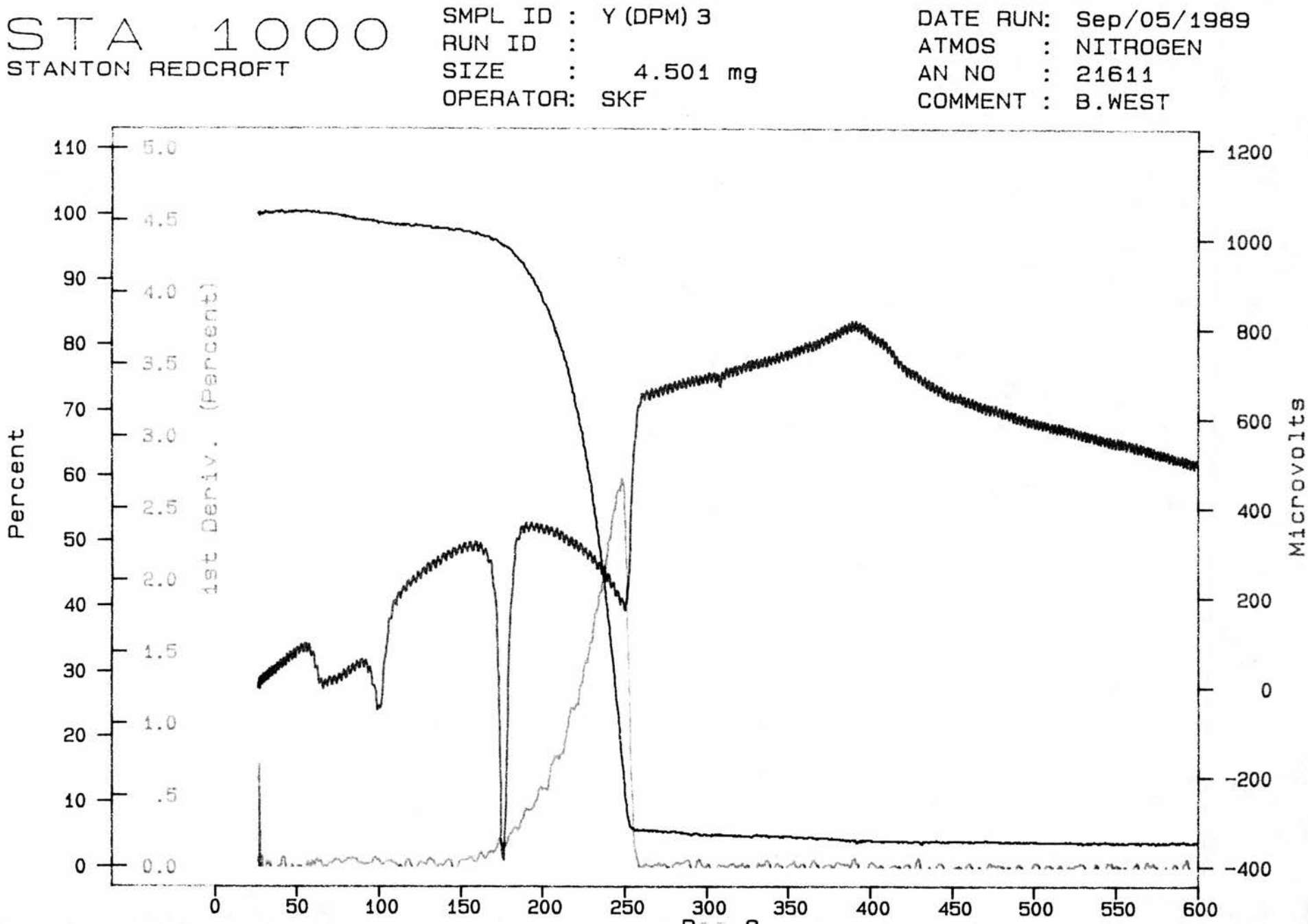

Figure 7.1; The STA of [Y(DPM)3]

7.3; THE PREPARATION AND ANALYSIS OF [$Ba(DPM)_2$] AND [$Ba(HFOD)_2$];

The preparation of the chelates were undertaken using the method described by Berg and Herrera[42]. However, we encountered difficulties with the excessive volume of ammonia solution which was required to carry out the reactions. As a consequence we decided to change the base to sodium hydroxide, which we had used effectively in the preparation of the [$Y(DPM)_3$]. As the nitrate, the metal salt we had used for the [$Y(DPM)_3$] synthesis, is only slightly soluble in water or ethanol we elected to use the bromide(the most soluble of the halides).

7.3.1; The preparation and analysis of [$Ba(DPM)_2$];

The H(DPM) (1.84 g, 0.01 mol) was dissolved in aqueous ethanol (20 cm^3, 50%) and was reacted with sodium hydroxide (0.40 g, 0.01 mol) dissolved in aqueous ethanol (30 cm^3, 50%). To this stirred solution was added barium (II) bromide dihydrate (1.67 g, 0.005 mol) dissolved in aqueous ethanol (25 cm^3, 50%). The solution was stirred for an hour and then reduced to 66% of its volume under vacuum. Water (30 cm^3) was then added to the solution to ensure the precipitation of all of the product. The precipitate was then collected and dried in vacuo.

IR peaks; 200-300(m), 330(w), 390(m), 470(s), 585(s), 750(w), 785(m), 795(m), 860(s), 930(w), 950(m), 1015(w), 1120(s), 1180(m), 1210(s), 1235(m), 1265(m), 1350(m), 1405(s), 1490(s), 1520(m), 1560(s), 1580(s), 3000-3600(s) cm^{-1}.

The peak assignment is very much the same as for the copper and barium complexes with this ligand. The peak at 1580 cm^{-1} is that of the chelated carbonyl and the peak at 1560 cm^{-1} is representative of the perturbed carbon-carbon double bond. The broad peak at 3000-3600 cm^{-1} probably indicates the presence of water in the complex, whilst the peaks below 500 cm^{-1} are again distinctive and markedly different from those of the copper and yttrium complex.

The ^1H NMR was taken in $CDCl_3$ and shows that the hydrated complex has been obtained in high purity. The three peaks in the spectrum were at δ1.0, δ4.25 and δ5.5 and had an integral ratio of 18.38:1.25:1. These clearly represent the tertiarybutyl group, water and the intermediate hydrogen respectively. The presence of water in the complex confirms the result of the IR analysis.

The microanalysis result was as follows;

Found C 51.46%, H 8.24%
$C_{22}H_{38}BaO_4$ requires C 52.48%, H 7.55%
$C_{22}H_{40}BaO_5$ requires C 50.67%, H 7.68%

This result seems to confirm our contention from the other analyses that we have prepared the hydrated species

7.3.2; The preparation and analysis of $[Ba(HFOD)_2]$;

$[Ba(HFOD)_2$ was prepared by the method already described for $[Ba(DPM)_2]$.

The $[Ba(HFOD)_2]$ complex was found to be soluble in chloroform, so the ^1H NMR was carried out in this deuterated solvent. This had the added advantage of removing the hydroxyl hydrogen peak

which would be present if deuterated alcohol had been used as the solvent. With the removal of this peak it is possible to determine the amount of water in the complex more accurately.

The ^1H NMR had 2 singlet peaks at δ1.0 and δ5.65 with an integral ratio of 30:1 and a broad peak at δ4.0-4.3 with a relative integral of 1.25. Despite the size of the integral for the peak at δ1.0 being somewhat anomalous, the peak assignment is otherwise relatively straightforward. Briefly, the peak at δ5.65 represents the methyne hydrogen atom, the peak at δ1.0 represents the tertiarybutyl group and the broad peak shows the presence of approximately one mole of water. However, it was important that other analytical techniques were pursued to check the anomalous size of the integral of the δ1.0 peak.

IR peaks; 200(m), 215(m), 240(m), 260(w), 290(w), 330(w), 370(m), 470(s), 525(s), 580(m), 620(m), 685(m), 695(w), 735(m), 750(m), 785(m), 830(m), 905(m), 930(m), 955(s), 1015(m), 1065(s), 1110(s), 1140(s), 1155(s), 1175(s), 1215(s), 1255(m), 1270(m), 1345(s), 1470-1510(s), 1570(m), 1625(s), 3100-3600(s) cm^{-1}.

Strong carbon-fluorine bands are evident in this spectrum in the 1000-1300 cm^{-1} region. The band at 1625 cm^{-1} represents the chelated carbonyl and that at 1570 cm^{-1} the perturbed carbon-carbon double bond. The broad peak at 3100-3600 cm^{-1} probably shows that water is present in the complex.

Microanalysis;

The following microanalysis is close to that which would be expected for the hydrated complex.

Found	C 31.55%, H 2.81%
$C_{20}H_{20}BaF_{14}O_4$ requires	C 34.93%, H 2.91%
$C_{20}H_{22}BaF_{14}O_5$ requires	C 32.21%, H 2.95%

CHAPTER 8;

CONCLUSION

8.1; INTRODUCTION;

The devolpment of suitable precursors for the CVD of high temperture superconductors has been rapid. A variety of methods have been employed to develop complexes which are of adequate volatility in their own right or to enhance the volatility of otherwise less volatile and less thermally stable complexes.

There is no easy answer to the question as to which is the best precursor for a particular metal for use in CVD. If we take the case of barium, it is clear that $[Ba(HFOD)_2]$ is the most established precursor and is capable of producing some reproducability with a good deposition rate. Our own complex, $[Ba(TDFND)_2]$, is more volatile and provides a much enhanced initial deposition rate when compared to $[Ba(HFOD)_2]$. However, more work is required to maintain this high flow rate during subsequent runs. The most volatile precursor is $[Ba(DPM)_2]$ when enhanced by amine vapour. However the neccessity to use this vapour introduces a complication into the system and a complex of equal volatility not requiring the addition of this vapour stream would be advantageous.

The most important discoveries described in this thesis are now summarised.

8.2; $[Ba(DPM)_2(tetraglyme)]$;

We believe this complex to be the most volatile non-fluorinated barium precursor so far developed. It could be of particular importance where there is a necessity to ensure that the as-deposited film is free of fluorine. It may be possible further to enhance the volatility of this complex by introducing tetraglyme into the carrier gas stream. There

may also be advantages in changing the polyether from tetraglyme to others such as triglyme or crown ethers, although it has been reported by Norman and Pez[47] that 18-crown-6 was lost on heating and that this complex proved, therefore, to be an ineffective precursor.

8.3; $[Cu(TDFND)_2(EtOH)]$;

The structural determination of this complex showed what we believe to be the only complex with ethanol bound directly to the copper atom. This complex also provided a valuable insight into the structure of the TDFND ligand and enabled us to draw some definite conclusions as to the cause of the enhanced volatility of the Group 2 complexes of this ligand. Confirmation of our view based on analytical techniques that this was due to the steric bulk of the fluoroalkyl chains was provided by this structural determination.

8.4; Other TDFND and DFHD complexes;

These new complexes for elememts of group 2 and for yttrium are amongst the most volatile and thermally stable so far produced. The thermal analyses show that they can be volatilised at acceptable temperatures and that the amount of decomposition is often negligible. Whilst the CVD testing of the barium complex has failed to show consistent flow rates throughout a series of runs, we do believe that this is due to the complex dehydrating and a consequent conversion to a less volatile oligomeric structure. If the dehydration of this complex can be controlled and the volatilisation optimised this complex should be a very useful CVD precursor.

8.5; Future developments;

The scope for further developments of the β-diketonate ligands is limited. Slight improvements to the performance of existing ligands might be possible, for example adjusting the carrier gas stream of $[Ba(TDFND)_2]$ to prevent the loss of water from the complex. Probably the only β-diketonate alternative to this would be the use of ligands with branched side chains with as high a proportion of fluorine as possible. The synthesis of such complexes would, however, be more lengthy and difficult than any syntheses so far employed.

The new nitrogen-containg ligands developed by Norman et al[37, 38] provide the most likely way of improving upon the β-diketonates. As we described in Section 2.3.1, these ligands have an extra alkyl group bound to the nitrogen atom close to the central metal atom. The presence of this group increases the steric crowding in this region and should help to reduce intermolecular interactions and so enhance the volatility of the complex. Furthermore, the presence of the nitrogen atom replacing one of the oxygen atoms means that there are less lone pairs for bonding to adjacent molecules. Up to the present time only copper derivatives have been prepared and these are likely to be the complexes which benefit the least from this steric crowding (we have already explained at some length that $[Cu(DPM)_2]$ has sufficient steric crowding and the addition of heavier ligands decreases the volatility of the molecule by increasing the molecular weight of an already monomeric species).

In the case of barium, however, this type of ligand could certainly produce a new range of volatile complexes. It would be of particular interest to prepare highly fluorinated complexes. If it proved possible to prepare analogues of TDFND we believe that the resulting

complexes might exhibit the enhanced volatility of the [Ba(TDFND)$_2$] without the problem of dehydration. This problem would be most unlikely to exist because the presence of the added group close to the barium would be likely to prevent the binding of water to the complex.

There is still a large amount of research to be done involving ether addition to β-diketonates. On the one hand the ethers so far used could be extended to other crown ethers or polyethers, whilst on the other there are a large number of β-diketonates to which these ethers have not yet been added. This might be another method of increasing the volatility of our highly fluorinated ligands.

We described a further alternative in Chapter 5. This would be to develop fluorinated derivatives of the methoxy alcohols. Whilst it is unlikely that these complexes would have weaker intermolecular interactions than the β-diketonates, there is a possibility that the reduced molecular weight of these complexes relative to the fluorinated β-diketonates might lead to increased volatility.

There are further possible ligands types which might produce volatile precursors and which have not so far been investigated.

Schiff base ligands (Figure 8.1) are well known and readily bind to transition metal ions in a chelate form after deprotonation. Anionic ligands capable of chelation to form 5-membered rings by coordination of a suitably placed amino group are also worthy of consideration (Figure 8.2).

The final option which we believe to be feasible is to design a ligand incorporating several of the features identified as improving volatility. It is clear that optimum volatility of a β-diketonate complex can be attained if at least one side chain is a heptafluoropropyl group. It is also the case that it is necessary to try to block additional sites on the central metal atom by binding, for example, water or tetraglyme. If the

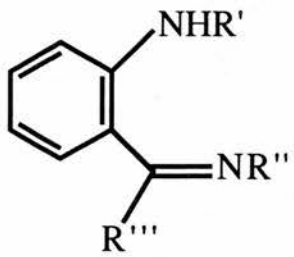

Figure 8.1; Schiff base ligand

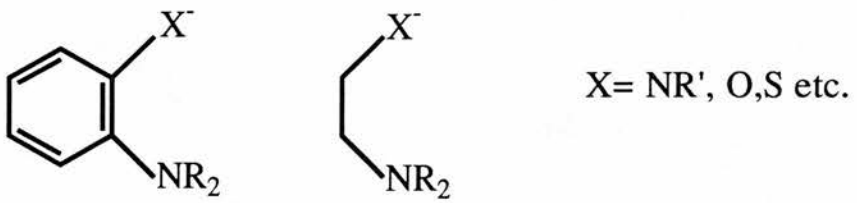

Figure 8.2; ligands containing a suitably placed amino group

other side chain on the β-diketonate were modelled upon the methoxy ethanol ligand (Figure 8.3) it might be possible for the oxygen on this side chain to bind to the central metal atom and produce (for a group 2 metal) a 6-coordinate complex (Figure 8.4).

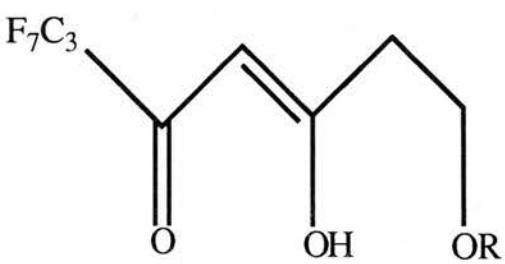

Figure 8.3; β–diketone ligand modelled upon methoxy ethanol

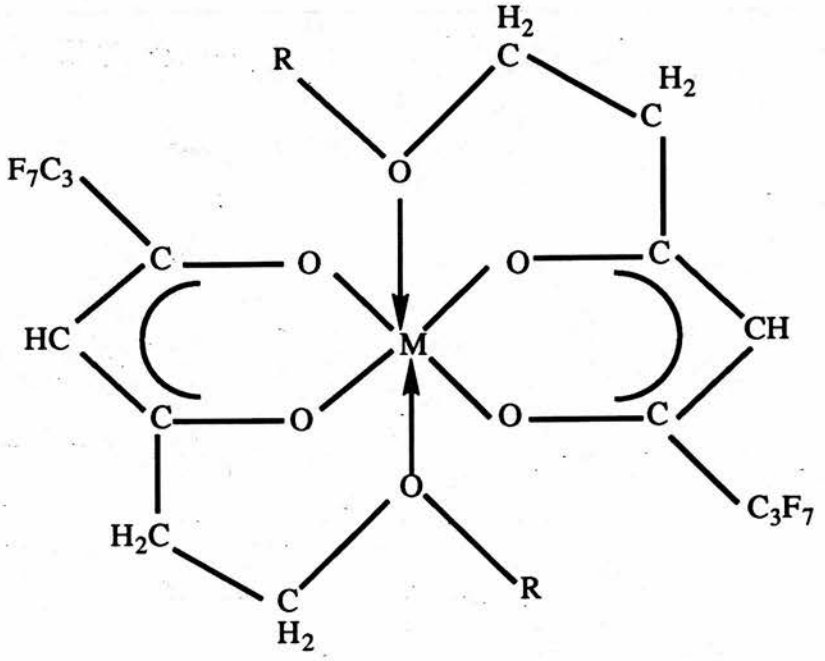

Figure 8.4; 6-coordinate complex

APPENDIX;

ANALYTICAL EQUIPMENT

NMR Spectroscopy;

^{1}H NMR were recorded on a Bruker AM300 Spectrometer (300 MHz), a Bruker WP80 Spectrometer (80 MHz) and a Varian EM 360 Spectrometer (60 MHz). ^{13}C NMR were recorded on the Bruker AM300 Spectrometer and ^{19}F NMR on the Bruker WP80 Spectrometer. The chemical shifts quoted for ^{1}H and ^{13}C are relative to internal tetramethylsilane (TMS) and those for ^{19}F are relative to fluorotrichloromethane.

IR Spectroscopy;

This was carried out on nujol mulls of solids and thin films of liquids between caesium iodide plates on a Perkin-Elmer 1330 Infra-Red Spectrometer.

EI Mass Spectrometry;

This was undertaken using an AEI MS50 Electron Impact Mass Spectrometer.

FAB Mass Spectrometry;

This was undertaken by the SERC Mass Spectrometry Service.

Simultaneous Thermal Analysis;

This was undertaken at Associated Octel using a Stanton Redcroft STA 1000 Simultaneous Thermal Analyser

Microanalysis;

This was carried out by the University of St. Andrews microanalytical service

REFERENCES

QUOTED REFERENCES

1) K. Onnes, Leiden Comm. Suppl. 1913 (34).

2) B. T. Matthias, T. H. Gaballe, S. Geller, E. Corenzwit. Phys. Rev., 1954 (95) p.1435.

3) J. G. Bednorz, K. A. Muller. Z. Phys., 1986 (B64), P.189.

4) M. K. Wu, J. R. Ashburn, C. J. Torng, P. H. Hor, R. L. Meng, L. Gao, Z. J. Huang, Y. Q. Wang and C. W. Chu. Phys. Rev. Lett., 1987 (58), P.908.

5) H. Maeda, Y. Tamaka, M. Fufutoni and T. Asano. Jpn. J. of Appl. Phys., 1988 (27), P.L209.

6) Z. Z. Sheng and A. M. Hermann. Nature, 1988 (332), P. 138-9.

7) K. Watanabe, H. Yamane, H. Kurosawa, T. Hirai, N. Kobayashi, H. Iwasaki, K. Noto and Y. Muto. Appl. Phys. Lett., 1989 (54), P.575.

8) W. Meissner and R. Ochsenfeld. Naturwissenschaften, 1933 (21), P. 787.

9) B. D. Josephson. Phys. Lett., 1962 (1), P. 251.

10) B. Vasilev. New Scientist, 23.9.89., P.33.

11) H. Jaeger. Advanced Materials, 1990 (2.1) P.16-22.

12) R. W. Simon, J. F. Burch, K. P. Daly, W. D. Dozier, R. Hu, A. E. Lee, J. A. Luine, J. M. Murduck, T. P. Neal, C. E. Platt, M. S. Wire and M. J. Zani. Paper presented to conference on the Science and Technology of Thin Film Superconductors, Denver, Colorado (30.4-4.5.1990).

13) K. Wasa, H. Adachi, Y. Ichikawa, K. Hirochi, A. Enokihara and K. Setsune. Paper presented to conference on the Science and Technology of Thin Film Superconductors, Denver, Colorado (30.4-4.5.1990).

14) L. Schultz. Paper presented to conference on the Science and Technology of Thin Film Superconductors, Denver, Colorado (30.4-4.5.1990).

15) A. D. Berry, D. K. Gaskill, R. T. Holm, E. J. Cukauskas, R. Kaplan and R. L.Henry. Appl. Phys. Lett., 1988 (52:20), P. 1743-1745.

16) K. Shinohara, F. Munakata and M. Yamanaka. Jap. J. of Appl. Phys., 1988 (27), P.L1265.

17) A. J. Panson, R. G. Charles, D. N. Schmidt, J. R. Szedon, J. Machikog and A. I. Braginski. Appl. Phys. Lett., 1988 (53), P.1756.

18) J. Zhao, K.-H. Dahmen, H. O. Marcey, L. M. Tonge, T. J. Marks, B. W. Wessels and C. R. Kannewurf. Appl. Phys. Lett., 1988 (53) P.1750.

19) D. W. Noh, B. Gallois, Y. Q. Li, C. Chern, B. Kear, G. S. Tompa, P. Norris and P. Zawadzki. Paper presented to the American Materials Research Society's autumn conference, 1989.

20) J. Zhao, D. W. Noh, C. Chern, Y. Q. Li, P. Norris, B. Gallois, and B. Kear. Paper presented to conference on the Science and Technology of Thin Film Superconductors, Denver, Colorado (30.4-4.5.1990).

21) D. C. Bradley. Chem. Rev., 1989 (89), P.1317.

22) E. W. Berg and J. J. C. Acosta. Anal. Chim. Acta, 1968 (40), P. 101-113.

23) J. O. Williams. Private communication.

24) R. E. Sievers and J. E. Sadlowski. Science, 1978 (201), P.217.

25) Z. A. Starikova and E. A. Shugham. Zh. Strukt. Khim., 1969 (10), P.290.

26) P. C. Lebrun, W. D. Lyon and H. A. Kuska. J. Cryst. Spectroscop., 1986 (16), P.889-93.

27) F. A. Cotton and J. J. Wise. Inorg. Chem, 1966 (5), P. 1200.

28) F. A. Cotton and J. J. Wise. Inorg. Chem, 1967 (6) P.917.

29) S. Oda, H. Zama, T. Ohtsuka, K. Sugiyama and T. Hattori. Jap. J. of Appl. Phys., 1989 (28), P.L427.

30) H. Yamane, H. Masumoto, T. Hirai, H. Iwasaki, K. Watanabe, N. Kobayashi, Y. Muto and H. Kurosawa. Appl. Phys. Lett., 1988 (53), P. 1548-53.

31) T. Nakamori, H. Ake, T. Kanamori, and S. Shibata. Jap. J. of Appl. Phys. 1988 (27), P.L1265.

32) H. Abe, T. Tsuruoka and T. Nakamari. Jap. J. of Appl. Phys. 1988 (27), P. 1473.

33) K. Zhang, B. S. Kwak, E. P. Boyd, A. C. Wright and A. Erbil. Appl.Phys. Lett., 1989 (54), P.380.

34) T. Tsuda, T. Hashimoto and T. Saegusa. J. Am. Chem. Soc., 1972 (94), P. 658-9.

35) T. Greiser and E. Weiss. Chem. Ber., 1976 (109), P. 3142-6.

36) P. M. Jeffries and G. S. Girolami. Chem. of Materials, 1989 (1), P. 8.

37) S. M. Fine, P. N. Dyer, J. A. T. Norman, B. A. Muratore and R. L. Iampietro. Mat. Res. Soc. Symp. Proc., 1991 (204), P. 415-420.

38) J. A. T. Norman. U. S. Patent No. 4, 950, 790, 21.8.90.

39) D. B. Beach, F. K. LeGoues and Chau-kun Hu. Chem. Materials, 1990 (2), P.216-219.

40) M. J. Hampden-Smith, T. T. Kodas, M. Paffett, J. D. Farr and H.-K. Shin. Chem. Materials, 1990 (2), P. 636-639.

41) H.-K. Shin, K.-M. Chi, M.J. Hampden-Smith, T. T. Kodas, J. D. Farr and M. Paffett. Advanced Materials, 1991 (3), P. 246-248.

42) E. W. Berg and N. M. Herrera. Anal. Chim. Acta, 1972 (60), P.117-125.

43) K. J. Eisentraut and R. E. Seivers. J. Amer. Chem. Soc., 1965 (87:22), P.5254-6.

44) R. Belcher, C. R. Cranley, J. R. Majer, W. I. Stephen and P. C. Uden. Anal. Chim. Acta, 1972 (60), P.109-116.

45) T. J. Marks. International patent, No. WO 89 / 07666.

46) K. Timmer, C. I. M. A. Spee, A. Mackor and H. A. Meinema, Eur. Pat. Appl., 1991, 405, 634, A2.

H. A. Meinema, K. Timmer, E. A. van der Zouwen-Assink, C. I. M. A. Spee, P. van der Sluis and A. L. Spek. XXVIIIth Int. Conf. on Coordination Chem., Gera, DDR, August 1990, Abstr. 6-82.

47) J. A. T. Norman and G. P. Pez. J. Chem. Soc. Chem. Commun., 1991, P. 971-2.

48) A. R. Barron. The Strem Chemiker, Oct. 1990 (13:1).

49) S. Matsuno, F. Uchikawa and K. Yoshizaki. Jap. J. of Appl. Phys., 1990 (29:6), P.L947-8.

50) J. Zhang, J. Zhao, H. O. Marcy, L. M. Tonge, T. J. Marks, B. W. Wessels and C. R. Kannewurf. Appl. Phys. Lett., 1989 (54), P.1166.

51) A. P. Purdy, A. D. Berry, R. T. Holm, M. Fatemi and D. K. Gaskill. Inorg. Chem., 1989 (28), P.2799.

52) J. M. Zhang, B. W. Wessels, D. S. Richeson, T. J. Marks, D. C. DeGroot and C. R. Kannewurf. J. Appl. Phys., 1991 (69), P.2743-5.

53) L. G. Hubert-Pfalzgraf, M.-C. Massiani, R. Papiernik and J.-C. Daran. Polyhedron, 1991 (10:4/5), P.437-445.

54) D. S. Richeson, L. M. Tonge, J. Zhao, J. Zhang, H. O. Marcy, T. J. Marks, B. W. Wessels and C. R. Kannewurf. Appl. Phys. Lett., 1989 (54), P. 2154.

55) K. Zhang, E. P. Boyd, B. S. Kwak, A. C. Wright, and A. Erbil. Appl. Phys. Lett., 1989 (55), P.1258.

56) A. D. Berry, R. T. Holm, R. L. Mowery, N. H. Turner and M. Fatemi. Chem. Materials, 1991 (3) P.72-77.

57) Z. Jablonski, T. Wasag, S. Millo. Rocz. Chem., 1976 (50:9), P. 1467-72.

58) C. Reichert, J. Westmore. Can. J. Chem., 1970 (48:20), P. 3213-22.

59) T. Sekine, R. Murai, M. Niitsu, M. Iharo. J. Inorg. Nucl. Chem., 1974 (36), P. 2569-74.

60) K.J. Eisentraut and R. E. Sievers. J. Inorg. Nucl. Chem., 1967 (29), P. 1937-45.

61) H. F. Holtzclaw and J. P. Collmann. J. Amer. Chem. Soc., 1957 (79), P. 3318-22.

62) K. Nakamoto, Infrared and Raman Spectra of Inorganic and Coordination Compounds (3rd Edition). John Wiley and sons.

62a) S. B. Turnispeed, R. M. Barkley and R. E. Sievers. Inorg. Chem., 1991 (30), P. 1164-1170.

63) M. F. Farona, D. C. Perry and H. A. Kuska. Inorg. Chem., 1968 (7), P. 2415-2418.

64) W. G. Scribner. J. Org. Chem., 1970 (35), P. 1696-1698.

65) S. V. Volkov, G. M. Larin, V. Ya Zub, E. A. Mazurenko. Koord. Khim., 1983(9:1), P. 26-30.

66) M. Brookhart and M. L. H. Green. J. of Organometallic Chem., 1983(250), P. 395-408.

67) Annual reports on NMR Spetroscopy. Editor G. A. Webb

(Academic Press), vol. 14 (1983).

68) M. J. Van Hamme and D. J. Burton. J. of Organometallic Chem., 1979(169), P. 123.

69) See B. J. Hathaway in 'Comprehensive Coordination Chemistry', Eds. G. Wilkinson, R. D. Gillard and J. A. McCleverty (Pergamon, Oxford), 1987, Vol. 5, P. 594-619.

70) B. Morosin. Acta Crystallogr., Sect. B, 1969(25), P. 19.

71) G. M. Sheldrick, SHELXS86. Program for crystal structure determination. University of Gottingen, Germany (1986).

72) G. M. Sheldrick, SHELX76. Program for structure determination. University of Cambridge, England (1976).

73) P. Roberts and G. M. Sheldrick, XANADU. Program for molecular geometry calculations. University of Cambridge, England (1975).

74) W. D. S. Motherwell and W. Clegg, PLUTO. Program for plotting molecular crystal structures. University of Cambridge, England (1978).

75) K. G. Caulton, M. H. Chisholm, S. R. Drake and K Folting. J. Chem Soc., Chem. Commun., 1990, P. 1349-51.

76) K. G. Caulton, M. H. Chisholm, S. R. Drake and J. C. Huffman. Chem. Commun., 1990, P. 1498-1499.

77) L. G. Hubert-Pfalzgraf, O. Poncelot, J. C. Daran and R. J. Astier. J. Chem. Soc. Chem. Commun. 1989, P.1846.

78) M. L. Hitchman, D. D. Gilliland, D. J. Cole-Hamilton and S. C. Thompson. Paper presented at Int. Conf. on New Materials and their Applications, Univ. of Warwick, 1990.

79) K. G. Caulton, M. H. Chisholm, S. R. Drake and W. E. Streib. Angew. Chem. Int. Ed. Engl., 1990(29), No. 12, P. 1483-5.

80) D. H. Williams and I. Fleming, Spectroscopic methods in Organic

Chemistry (3rd Edition). McGraw-Hill.

81) D. D. Peacock. J. Chem. Ed., 1971 (48:2), P. 133-4.

82) C. Duval, R. Freymann and J. Lecompte. Bull. Soc. Chim. France, 1952, P.106-13.

GENERAL REFERENCES

i) H. Jaeger. Advanced Materials. 1990 (2.1) P.16-22.

ii) M. Strongin, D. O. Welch and J. W. Davenport. Nature, 1987(325), P. 664.

iii) J. Robbins. Materials Edge, 16.11.87.

iv) P. Campbell. Nature, 1987(330), P.21.

v) Superconductivity (Methuen). E. A. Lynton, 1st Edition, 1962.

vi) Superconductivity (Science Paperback). E. A. Lynton, 3rd Edition, 1971.

vii) Superconducting materials (Plenum Press). E. M. Savitskii, V. V. Baron, Yu. V. Efimov, M. I. Bychkova and L. F. Myzenkova, 1973.

viii) Superconductivity (Mills and Boon). I. M. Firth, 1972.